

**Metabolic Network Activity Characterization  
Using Mass Spectrometric Methods**

**Dissertation**

**Zur Erlangung des Grades**

**Des Doktors der Naturwissenschaften**

**Der Naturwissenschaftlich-Technischen Fakultät III**

**Chemie, Pharmazie, Bio-und Werkstoffwissenschaften**

**Der Universität des Saarlandes**

**von**

**Yongbo Yuan**

**Saarbrücken, Germany**

**2010**

# Acknowledgements

First of all, I would like to express my deep sense of respect and sincere gratitude to Prof. Dr. Elmar Heinzle for providing me a Ph.D. position and for his valuable guidance, stimulating discussion, and constant supports throughout the course of this work. I especially would like to thank him for giving me brilliant directions and his continuous help in solving problems.

I would like to express my appreciation to Prof. Dr. Dietrich Volmer for his kind review of this thesis.

My great thanks go to Dr. Taehoon Yang for his fruitful discussion on metabolic flux analysis and his XFLUXGATE program which are extremely critical to my project.

I especially want to express gratitude to my colleagues. Without the generous help of you all, this thesis would not have been possible. Many thanks to Michel Fritz and Dr. Klaus Hollemeyer for their most valuable assistance of GC-MS, HPLC and MALDI-TOF MS analysis, as well as very useful suggestions. Thank Dr. Susanne Kohring, Robert Schmidt and Veronika Witte for their valuable support. I would like to thank Dr. Fozia Noor for her English correction of my thesis and advices for my work. I thank Verena Schütz for her kind help on my living here in Saarbrücken and fruitful discussions on my project. Thanks to Alexander Stigun for the thesis abstract translation to German. I am sincerely grateful to Konstantin Schneider, Susanne Peifer, Andreas Neuner, Jens Niklas, Simone Beckers and all others for valuable discussions and never ending personal support throughout the years.

I gratefully acknowledge financial support from German Research Foundation DFG under the project, “European Postgraduate School of Physical Methods for the Structural Investigation of New Materials” (GRK-532) and special thanks to Dr. Markus Eheses for his support.

Finally, I thank my beloved wife Kuiying, my family and all my friends for their encouragement and support during this Ph.D. work.

## Abbreviations

### Symbols:

<b>CDW</b>	Cell dry weight;
<b>CTAB</b>	Cetyl trimethylammonium bromide;
<b>TE</b>	Toluene-ethanol mixture;
<b>MALDI-TOF MS</b>	Matrix-assisted laser desorption/ionization time-of –flight mass spectrometry;
<b>[U-<sup>13</sup>C<sub>6</sub>] G6P</b>	[U- <sup>13</sup> C <sub>6</sub> ] Glucose-6-phosphate;
<b>EP</b>	Eppendorf tube;
<b>DHB</b>	2, 5-dihydroxybenzoic acid;
<b>CHCA</b>	$\alpha$ -Cyano-4-hydroxycinnamic acid;
<b>GC-C-IRMS</b>	Gas chromatography combustion isotope ratio mass spectrometry;
<b>GC-MS</b>	Gas chromatography mass spectrometry;
<b>MFA</b>	Metabolic flux analysis;
<b>KIE</b>	Kinetic isotope effect;
<b>9AA</b>	9-aminoacridine;
<b>PPP</b>	Pentose phosphate pathway;
<b>TCA</b>	Tricarboxylic acid;
<b>MBDSTFA</b>	N-methyl-N- <i>t</i> -butyldimethylsilyl-trifluoroacetamide;

### Metabolites:

<b>G6P</b>	Glucose-6-phosphate;
<b>NADP</b>	Nicotinamide adenine dinucleotide phosphate;
<b>NADPH</b>	Nicotinamide adenine dinucleotide phosphate reduced form;
<b>F6P</b>	Fructose-6-phosphate;
<b>F16BP</b>	Fructose-1, 6-biphosphate;
<b>DHAP</b>	Dihydroxyacetone phosphate;
<b>GADP</b>	Glyceraldehydes 3-phosphate;
<b>3PG</b>	3-phosphoglycerate;
<b>2PG</b>	2-phosphoglycerate;
<b>PEP</b>	Phosphoenolpyruvate;

## Abbreviations

---

<b>PYR</b>	Pyruvate;
<b>6PG</b>	6-phosphogluconate;
<b>P5P</b>	Ribulose 5-phosphate/Ribose 5-phosphate/Xylulose 5-phosphate;
<b>S7P</b>	Sedoheptulose 7-phosphate;
<b>13BP</b>	1, 3-bisphosphoglycerate;
<b>E4P</b>	Erythrose 4-phosphate;
<b>ATP</b>	Adenosine-5'-triphosphate;
<b>ADP</b>	Adenosine diphosphate;
<b>OAA</b>	Oxaloacetate;

## Enzymes :

<b>G6PDH</b>	Glucose-6-phosphate dehydrogenase;
<b>IDH</b>	Isocitrate dehydrogenase;
<b>ME</b>	Malic enzyme;
<b>PGI</b>	Glucose-6-phosphate isomerase;
<b>6PGDH</b>	6-phosphogluconate dehydrogenase;
<b>HK</b>	Hexokinase;

# Contents

Acknowledgements.....	1
List of Abbreviations.....	2
Abstract .....	6
Abstract (German version) .....	7
<b>Chapter 1</b>	
General introduction .....	8
1.1 Metabolic flux analysis.....	8
1.1.1 GC-C-IRMS.....	9
1.1.2 Application of GC-C-IRMS to MFA.....	11
1.1.3 Kinetic isotope effect (KIE) .....	13
1.2 Kinetic modeling .....	13
1.2.1 Permeabilization for enzyme characterization.....	14
1.2.2 MALDI-TOF MS.....	16
1.2.3 Intracellular metabolites sampling and quantification.....	19
Aim and outline of this thesis.....	21
<b>Chapter 2</b>	
Analysis of <sup>13</sup> C Labeling Enrichment in Microbial Culture	
Applying Metabolic Tracer Experiments Using GC-C-IRMS .....	31
2.1 Introduction.....	32
2.2 Materials and methods.....	33
2.3 Theoretical background.....	36
2.4 Results and discussion.....	41
2.5 Conclusion.....	51
Appendix .....	56
<b>Chapter 3</b>	
<sup>13</sup> C Metabolic Flux Analysis for Larger-Scale Cultivation	
Using GC-C-IRMS.....	57
3.1 Introduction.....	58
3.2 Materials and methods.....	60
3.3 Results.....	62
3.4 Discussion.....	72
3.5 Conclusion.....	74
Appendix .....	79

# Contents

---

## Chapter 4

Permeabilization of *Corynebacterium glutamicum* for

NAD(P)H-dependent intracellular enzyme activity measurement.....	83
4.1 Introduction.....	84
4.2 Materials and methods.....	85
4.3 Results.....	87
4.4 Discussion.....	99
4.5 Conclusion.....	101

## Chapter 5

*In-situ* multi-enzyme network kinetics study using MALDI-TOF MS.....

105	
5.1 Introduction.....	106
5.2 Materials and methods.....	109
5.3 Results and discussion.....	113
5.4 Conclusion.....	125

## Chapter 6

Kinetic modeling of in-situ enzymatic system.....

129	
6.1 Introduction.....	130
6.2 Kinetic network simplification.....	130
6.3 Reactions in the network.....	131
6.4 Kinetic model formulation.....	132
6.5 results and conclusion.....	134
Appendix.....	139

## Chapter 7

Concluding Remarks.....

Summary.....

List of publications.....

Curriculum Vitae.....

## Abstract

Innovative methods were developed for metabolic network activity characterization using mass spectrometry. Metabolic flux analysis (MFA) and kinetics of metabolic networks were developed and applied to *Corynebacterium glutamicum*. A protocol to determine metabolic fluxes at low degree of labelling using gas chromatography-combustion-isotope ratio mass spectrometry (GC-C-IRMS) by the measurement of  $^{13}\text{C}$  enrichment in proteinogenic amino acid hydrolyzates was described. Kinetic isotope effects played an increasing role at low degree of labeling but could be corrected. From these corrected  $^{13}\text{C}$  enrichments *In vivo* fluxes in the central metabolism were determined by numerical optimization. The GC-C-IRMS-based method involving low labeling degree of expensive tracer substrate, e.g. 1%, is therefore promising for larger laboratory and industrial pilot scale fermentations.

Permeabilization of *Corynebacterium glutamicum* cells was investigated and optimized. Permeabilized cells are considered closer to the *in-vivo* situation than purified enzyme(s) for the study of kinetics. A novel strategy was developed for the determination of *in-situ* enzymatic network kinetics combining permeabilization and matrix-assisted laser desorption/ionization time-of-flight mass spectrometry (MALDI-TOF-MS) quantification. Quantification of small molecular mass metabolites in glycolysis and pentose-phosphate pathway using MALDI-TOF-MS with  $[\text{U-}^{13}\text{C}_6]$  glucose-6-phosphate as single internal standard was established. Signal suppression during MALDI analysis could be compensated by applying the standard addition method. Adding selected substrates and cofactors, kinetics of glycolysis and pentose-phosphate pathways were be characterized using this method.

### Abstract (German version)

Im Rahmen dieser Arbeit wurden neue Massenspektrometrie-basierte Methoden zur Charakterisierung der Aktivität metabolischer Netzwerke entwickelt, die zur Flussanalyse in metabolischen Netzwerken sowie zur Analyse der Kinetik metabolischer Netzwerke angewendet wurden.

Die Methode zur Bestimmung metabolischer Flüsse basiert auf der Messung der  $^{13}\text{C}$ -Anreicherung in Aminosäuren von Proteinhydrolysaten mit Hilfe von GC-C-IRMS (gas-chromatography-combustion-isotope ratio mass spectrometry). Der Vorteil dieser Methode besteht darin, dass die Bestimmung metabolischer Flüsse auch bei sehr geringen Mengen an  $^{13}\text{C}$ -markiertem Substrat möglich ist. Durch Messung der  $^{13}\text{C}$ -Anreicherung in Aminosäuren und Korrektur von Isotopen-Effekten sowie durch Anpassung der korrigierten Daten mit Hilfe numerischer Optimierungen, konnten *in vivo* Flussverteilungen im Zentralstoffwechsel bestimmt werden. Da bei der GC-C-IRMS basierten Methode nur sehr geringe Mengen an relativ teurem  $^{13}\text{C}$  markiertem Substrat benötigt werden (~1%), ist diese Methodik insbesondere für die Anwendung in größerem Maßstab geeignet.

Des Weiteren wurden Techniken zur Permeabilisierung von *Corynebacterium glutamicum* untersucht und optimiert. Generell sind permeabilisierte Zellen zur Bestimmung von *in vivo* Enzymkinetiken besser geeignet als isolierte und gereinigte Enzyme. Zur *in situ* Bestimmung von Kinetiken in enzymatischen Netzwerken wurde in dieser Arbeit eine Methode entwickelt, bei der die Enzymaktivität in permeabilisierten Zellen bestimmt wird und des Weiteren eine MALDI-TOF-MS-basierte Quantifizierung von intrazellulären Metaboliten erfolgt. Die Quantifizierung von Metaboliten der Glykolyse und des Pentosephosphat-Wegs mittels MALDI-TOF-MS erfolgte mit Hilfe von [U- $^{13}\text{C}_6$ ] Glukose-6-Phosphat als internem Standard. Die bei der MALDI-Messung auftretenden Signal-Unterdrückungen konnten durch Zugabe des Standards korrigiert werden. Durch Messung der entsprechenden Metabolite sowie durch Bestimmung von intrazellulären Enzymaktivitäten mit Hilfe geeigneter Substrate und Kofaktoren, konnten die Kinetiken von Glykolyse sowie des Pentose-Phosphatweg erfolgreich charakterisiert werden.

# Chapter 1

## General Introduction

Biotechnology has been greatly developed in the last decades and is applied for the production of many useful compounds in industry (Becker et al. 2008a; Biwer et al. 2005; Kromer et al. 2005). Cost-effectiveness and environmental concerns are major reasons for the development and the application of bioprocesses. Besides primary metabolites, fine chemicals, organic acids, vitamins, food additives and alcohols, some secondary metabolites as pharmaceuticals are also produced by fermentations. The increasing demand in industry requires powerful techniques that can improve the performance of the producing strains. Metabolic engineering, which was used to optimize industrial microorganisms in a rational way, is now playing an ever increasing role for the development of biotechnological production processes (Iwatani et al. 2008; Liebermeister and Klipp 2006a; Liebermeister and Klipp 2006b; Sauer 2006; Wittmann 2007; Zamboni et al. 2009; Zamboni and Sauer 2009).

### **Metabolic networks**

A metabolic network is the set and topology of metabolic biochemical reactions within a cell (Grüning et al. 2010). A metabolic network comprises both chemical reactions of metabolism and the regulatory interactions that control these reactions. Newly developed metabolic engineering processes allow the reconstruction of the network to improve the desired characteristics of biochemical systems (Schomburg 2009; Stelling et al. 2002). Since *in vivo* metabolic flux analysis and *in situ* network kinetic modeling are regarded as critical techniques for quantitative studies of metabolic networks, these were investigated in detail in this study.

### **1.1 Metabolic flux analysis**

For rational engineering of a strain it is critical to quantify intracellular reaction rates in a metabolic network. A method termed metabolic flux analysis (MFA) is applied for quantitative analyze of carbon fluxes *in-vivo*. Therefore, MFA is the core of metabolic engineering attracting great interest from biologists (Iwatani et al. 2008; Sauer 2006; Wittmann 2007).

Conventional metabolic flux analysis contains only mass balances which are constructed based on data from extracellular measurements such as specific substrate uptake and production formation rates (Vallino and Stephanopoulos 1993). This mass balance-based approach provides only limited information of the intracellular network, and it was further developed by introducing  $^{13}\text{C}$  labeling information for the calculation of intracellular fluxes. Labeling pattern information from proteinogenic amino acids at steady state can be provided by nuclear magnetic resonance (NMR), gas chromatography mass spectrometry (GC-MS) (Bolten et al. 2009; Michael Dauner 2000) and MALDI-TOF MS (Hollemeier et al. 2007; Wittmann and Heinzle 2001a). Compared to NMR method, GC-MS method was more widely used for flux analysis owing to its much lower amount of the sample requirement and higher sensitivity. Conventional mass balance combining with data from GC-MS labeling measurement has been regarded as a key technique in biotechnology (Wittmann 2007).

### **1.1.1 Gas chromatography combustion isotope ratio mass spectrometry (GC-C-IRMS)**

Gas chromatography combustion isotope ratio mass spectrometry (GC-C-IRMS) is an analytical mass spectroscopic technique used for the determination of the relative ratio of stable isotopes of carbon ( $^{13}\text{C}/^{12}\text{C}$ ), hydrogen ( $^2\text{H}/^1\text{H}$ ), nitrogen ( $^{15}\text{N}/^{14}\text{N}$ ) or oxygen ( $^{18}\text{O}/^{16}\text{O}$ ) in individual compounds separated from complex samples (Meier-Augenstein 1999a). Different from radioactive tracers which are harmful, these above mentioned stable isotopes do not cause any adverse physiological effects (Koletzko et al. 1997). Isotopic fractionation during physical, chemical and biological processes causes the relative ratio of isotopes in natural materials to vary slightly. Thus, relative isotopic ratios of specific compounds can be applied for diagnosis of special environmental processes. Furthermore, utilization of artificially synthesized isotope labeled substrates can help in the understanding of some highly complex and obscure biogeochemical pathways. Like GC-MS, the primary prerequisite of GC-C-IRMS is that the sample mixture is amenable to GC, i.e. it is suitably volatile and thermally stable. Therefore, chemical modification (derivatization) is necessary for polar compounds. This requires to account for stable isotope ratio of the derivatization agent in the analysis (Godin et al. 2007b).

## General Introduction

---

Figure 1 depicts the scheme of a typical GC-C-IRMS instrument (based on a ThermoElectron Delta XP instrument). The IRMS instrument is coupled to a gas chromatography (GC) via a combustion interface (C). Generally, the GC is equipped with an auto sampler and all sample solutions are automatically injected into the GC inlet following a pre-set program. Samples are then vaporized and swept onto a chromatographic column by the carrier gas (usually helium). Compounds in a sample are separated according to various chemical properties causing different retention times in the whole column. Compounds then pass through a combustion reactor (alumina tube containing Ni/Cu/Pt wires maintained at 980 °C) and combusted to e.g. CO<sub>2</sub>. A reduction reactor (an alumina tube containing three Cu wires maintained at 640 °C) is followed to reduce any nitrogen oxides to nitrogen. Water is then removed in a water separator by passing the gas stream through a tube constructed from a water permeable nafion membrane. The gas stream containing the combustion products then flows into the MS by an open split interface for analysis.

Mass spectrometry identifies compounds by the mass of the analyte molecule. Ionization of the analyte gases (CO<sub>2</sub>, H<sub>2</sub>, N<sub>2</sub> or CO) is achieved using electron impact ionization (EI), the principle is the same as has already been described elsewhere (Wittmann and Heinzle 1999b). An array of Faraday cups, e.g. CO<sub>2</sub> can be set to *m/z* 44, 45 and 46 to detect separated ionized gases and used to calculate the final stable isotope ratio. Reference CO<sub>2</sub> of known isotopic composition is introduced directly into the ion source at the beginning and at the end of every run. <sup>13</sup>C/<sup>12</sup>C values are calculated by integrating the *m/z* 44, 45, and 46 ion currents. The compound-specific isotope values (δ<sup>13</sup>C) are calculated as follows:

$$\delta^{13}\text{C} = \left( \frac{R_A - R_S}{R_S} \right) \times 1000 \quad [\text{‰}]$$

$$R_A = \frac{\delta^{13}\text{C} \cdot R_S}{1000} + R_S$$

Where  $R_A$  is the ratio of <sup>13</sup>C/<sup>12</sup>C in the sample and  $R_S$  is the corresponding ratio measured for the used international standard (For carbon,  $R_S = 0.0112372$ ). For metabolic investigation, the atom fraction, namely atom percent (AP or A %), is used as described in the following formula:

## General Introduction

$$AP = \left[ \frac{100 \times R_A \times ((\delta^{13}C/1000) + 1)}{1 + R_A \times ((\delta^{13}C/1000) + 1)} \right]$$

The APE is another general variable calculated which is defined as an absolute measurement of the isotopic enrichment.

$$APE = AP_{(\text{sample})} - AP_{(\text{background})}$$

APE can be then transformed in molar percent excess (MPE) using following formula:

$$MPE = APE \times (C_{\text{total}} / C_{\text{labeled}})$$

Where  $C_{\text{total}}$  is the total number of carbon in the molecule and  $C_{\text{labeled}}$  is the number of labeled carbon in the molecule.

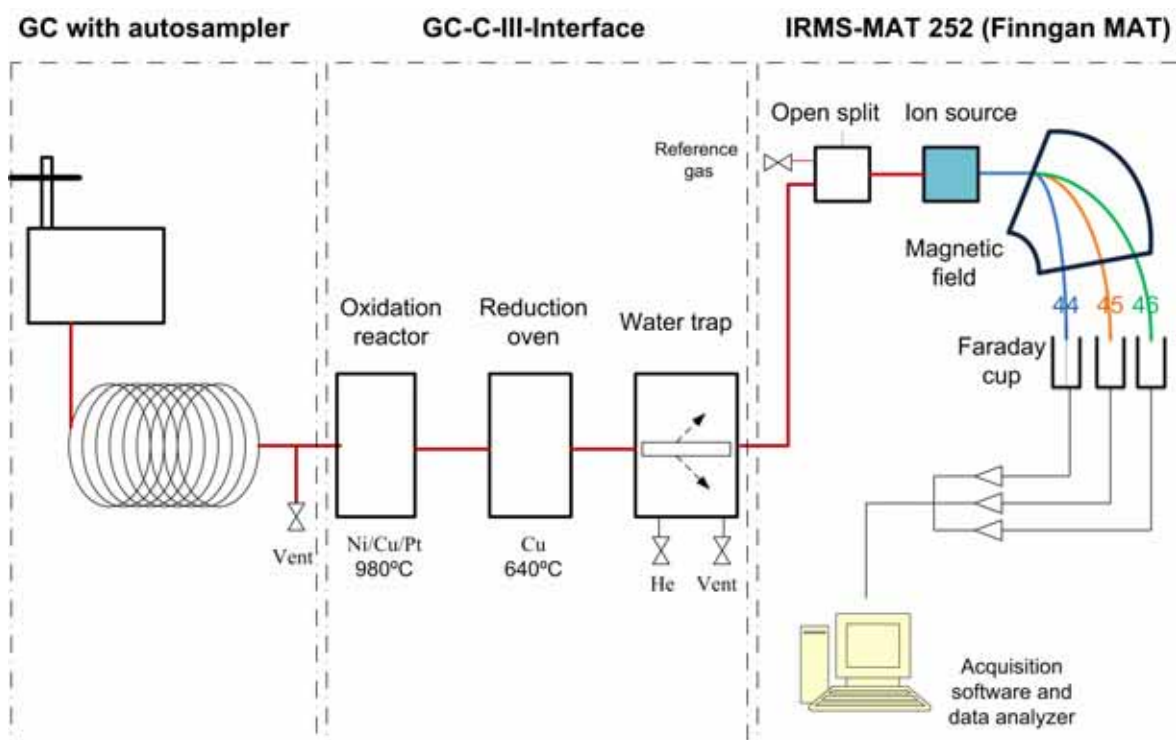


**Figure 1.** Scheme of a typical GC-C-IRMS instrument.

### 1.1.2 Application of GC-C-IRMS to metabolic flux analysis

Techniques combining  $^{13}C$  tracer experiments and GC-MS analysis have been developed to high standards and successfully applied to metabolic flux analysis for recent years (Wittmann and Heinzle 1999b; Zamboni et al. 2009). But this strategy can not be used for

## General Introduction

---

all cases especially for those where isotope enrichment is lower than 0.5 atom % excess (APE) due to the limited accuracy and precision of isotope ratio measurement by GC-MS even in the SIM mode (Preston and Slater 1994; Rennie et al. 1996). In contrast, GC-C-IRMS has the ability to measure samples with very low isotope enrichment close to the natural abundance level. Therefore, it has potential to be applied to these cases (Corr et al. 2007; Meier-Augenstein 1999b).

A state-of-art metabolic flux analysis using GC-C-IRMS can be performed in three steps: tracer experiment, GC-C-IRMS analysis and final flux computational estimation (Figure 2). First, specially labeled substrates, mostly  $^{13}\text{C}$  labeled, should be carefully designed based not only on the metabolic network of the organism of interest but also on the spectrum of active paths and their approximative activities. Different from the GC-MS method, the position of the labeled stable isotope is not important for GC-C-IRMS-based metabolic flux analysis because all of compounds separated from GC are burnt to  $\text{CO}_2$ . Therefore, only the mass isotopomers of  $\text{CO}_2$  will be obtained from MS subsequently.  $\text{CO}_2$  has only one carbon atom, and then corresponding mass isotopomer fractions are referred to only  $m$  and  $m+1$ . Therefore, the final results can not reflect carbon positional transition information of the intermediates. The procedure of tracer experiment for microorganism cultivation and sampling is the same as with the GC-MS based experiment. But the derivatization procedure for GC-C-IRMS measurement is more restricting, e.g. agents involved must be extremely water-free, to ensure a subsequent good separation by GC due to the lack of MS spectrum for each compound.

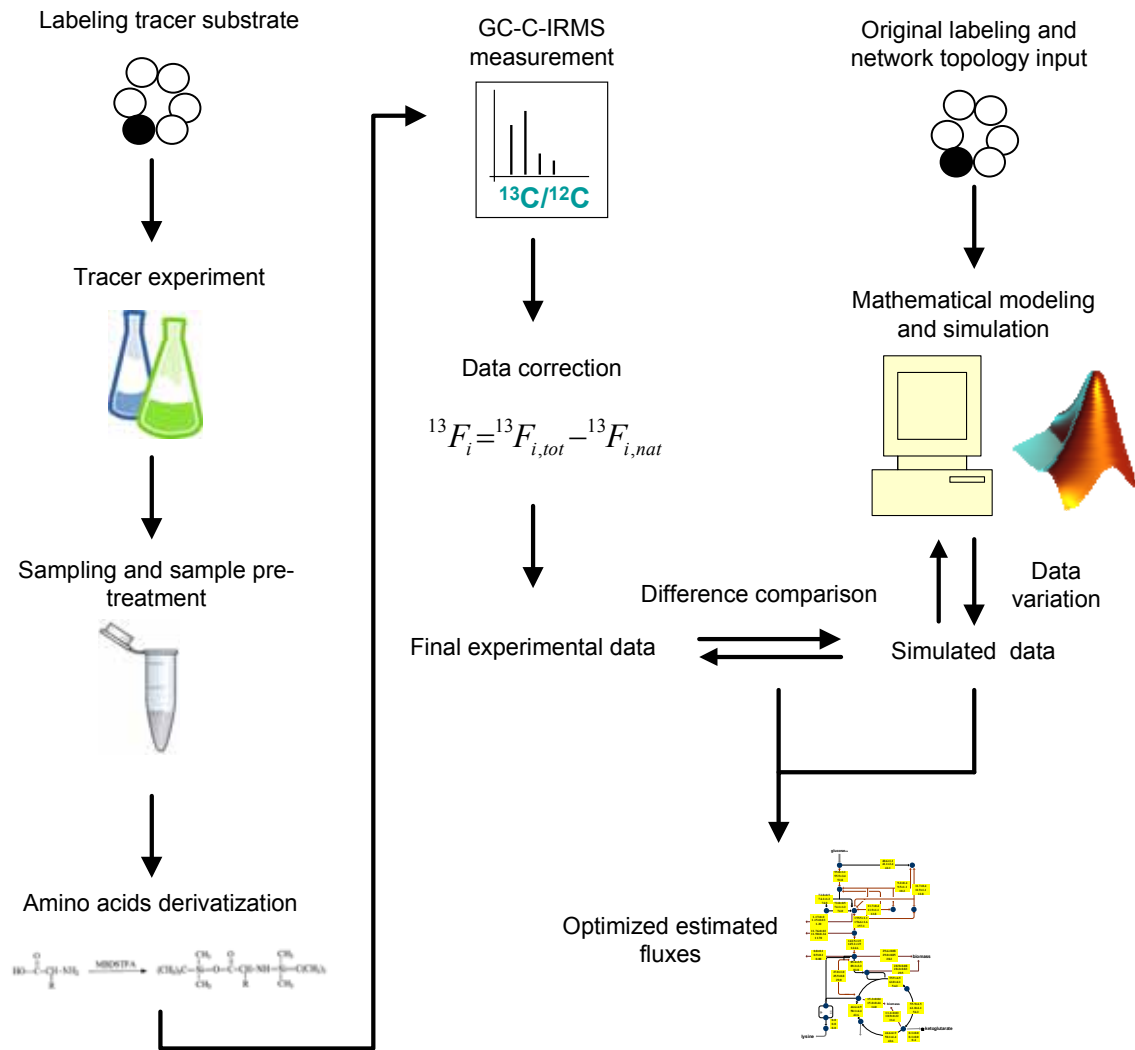


**Figure 2.** Schematic of strategy for GC-C-IRMS based metabolic flux analysis.

### 1.1.3 Kinetic isotope effect (KIE)

KIE is a variation in the reaction rate of a chemical reaction when an atom in one of the reactants is replaced by one of its isotopes. It is also called "isotope fractionation" and can be represented as:

$$KIE = \frac{K_{light}}{K_{heavy}}$$

Where  $K_{light}$  is reaction rate constant of the light atom and  $K_{heavy}$  is the reaction rate constant of the heavy isotope. Primary isotope effect and secondary isotope effect are two

## General Introduction

---

main types of KIE. The former is caused by the isotopic replacement which happens in a chemical bond breaking or forming in a rate limiting step (Rieley 1994). The later is caused in cases that isotopic substitution is remote from the bond being broken. KIE can be utilized for some enzyme mechanisms study (Adams et al. 1990; Anderson et al. 1994; Axelsson et al. 1992), but causes reaction rate variation and makes the metabolic flux calculation more complex.  $^{13}\text{C}$  labeled substrates are the major labeling used for metabolic study. By the measurement of both the rapidly removed product and the conversion to an isotopically stable form, as well as isotope ratio analysis, the isotope effect on hydration and dehydration is  $k_{12}/k_{13} = 1.0069 \pm 0.0003$  and  $1.0147 \pm 0.0007$ , respectively (Marlier and Oleary 1984). For GC-MS based tracer experiments which normally use high degree of labeling e.g. 100% [ $^{13}\text{C}$ ] glucose (generally 1% impurity), the involved  $^{12}\text{C}$  is about only 1%, therefore the kinetic isotope effect is very small and can be neglected. However, for cases using low degree of labeling e.g. 1% [ $1\text{-}^{13}\text{C}$ ] glucose which is very close to natural abundance level, KIE should be considered and corrected while designing the experiment (Corr et al. 2007).

### 1.2 Kinetic modeling

Kinetic network models describe the complete dynamics of the network or usually only sub-networks of a cell, and have been proven useful for optimization and control over the network. The complexity of this task increases with the size of the network considered, and the estimation of parameters is critical for the creation of a reliable kinetic model (Domingues et al. 2010; Hadlich et al. 2009; Theobald et al. 1997; Visser et al. 2004). Generally, the construction of a mathematical model comprises three steps: (1) participating metabolites identification by experimental measurement, (2) assignment of rate laws, (3) parameter estimation (Drager et al. 2009). In this study, the focus is on the first two steps. Instead of using directly the complex *in vivo* system, the *in situ* system is very promising for this kinetic study owe to its ease of experimental operation and the similarity to *in vivo*. For identification and quantification of low molecular mass metabolites, MALDI-TOF MS has the potential to be applied for measurement of a large number of samples.

#### 1.2.1 Permeabilization for enzyme characterization

## General Introduction

---

Enzymes have been applied in industry for the production of chemicals and drugs for more than one century. The increasing interests force a deep understanding of potentially applicable enzymes. For a long time purified enzymes and cell extracts are utilized for characterizing enzymes *in vitro*. Unfortunately, obtained parameters from *in-vitro* condition can not entirely explain how enzymes fulfill their functions in a living cell due to the difference between an artificial reaction condition and original environment (Minton 2006). Permeabilized cells has been shown to be a better material for enzyme characterization (Felix 1982; Miranda et al. 2006; Serrano et al. 1973). The process of permeabilization of cells is relative easy and rapid. Some physical methods or chemical detergents or drugs can gently penetrate the cell membrane and make pores to allow low molecular weight compounds or metabolites diffuse into and out of the cell and keep big molecular weight proteins inside the cell. Figure 3 shows the pictures of stained cells before and after permeabilization. Before permeabilization the dye molecules are not able to enter the cells, in contrast, after permeabilization the cells are completely stained. Since enzymes are still at their original positions in the cell, this *in-situ* condition is regarded closer to *in-vivo* than the *in-vitro*. Permeabilized cells combine the original nature of experiments *in-vivo* with much of the control possibility in experiments *in-vitro*. Because of its suitability for enzyme study, different approaches have been tested and applied for a number of organism permeabilization. Chemicals and drugs such as DMSO (Mowshowitz 1976), ethanol (Somkuti et al. 1998), Triton X-100 (Christova et al. 1996; Galabova et al. 1996), toluene and ethanol mixture (TE) (Chelico and Khachatourians 2003; Sorol et al. 2001), cetyl-trimethyl ammonium bromide (CTAB) (Bindu et al. 1998), digitonin (Cordeiro and Freire 1995; Martins et al. 2001c), and chloroform/SDS mixture (Griffith and Wolf 2002) were mostly utilized agents. Recently, rather than chemical methods, other approaches were also developed. A *lpp* gene (encoding Braun's lipoprotein) deletion was tested for permeabilization (Kiefer et al. 2007). Pulsed electric field was also tested to permeate *Corynebacterium glutamicum* and the results are satisfying (Tryfona and Bustard 2008a). It seems permeabilization has a wide application range on various organisms, not only on a number of bacteria, but also on baker's yeast (Abraham and Bhat 2008), fungal conidia on surfaces (Filion et al. 2009), Red blood cells (Schneiker et al. 2007) etc.

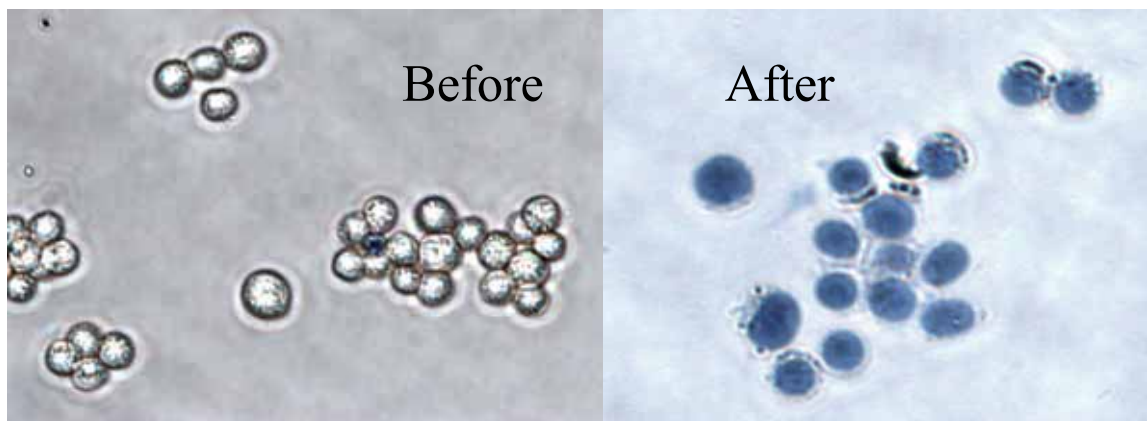


**Figure 3.** Staining of cells with methylene blue before and after Triton X-100 permeabilization.

### 1.2.2 MALDI-TOF MS

MALDI-TOF MS was firstly introduced by Karas et al. (Karas et al. 1987; Karas and Hillenkamp 1988). Instead of conventional ionization methods, it allows the soft ionization and sensitive analysis of biomolecules (biopolymers such as proteins, peptides and sugars) and large organic molecules (such as polymers and other macromolecules). A scheme of a MALDI-TOF MS instrument is shown in Figure 4. A matrix material (normally an organic solvent) is mixed with the sample to form absorbs applying laser light and then produces charged ionic species and a crystalline lattice with the surface molecules of the analyte. This crystalline lattice facilitates desorption and ionization of the analytes. The analyte ions are accelerated by a high voltage (15-25 KV) and then travel in a field-free flight tube. The ions with the lower mass to charge ratio ( $m/z$ ) will travel at a greater velocity and reach the detector faster than the larger  $m/z$  ions. Analyte ions are separated and detected as an electrical signal by MS. Several specific advantages, including simplicity of sample preparation, high mass measurement range, high sensitivity, little sample consumption and fast measurement, make MALDI-TOF MS an excellent analysis technique for enzyme activity screening and dynamic study.

An appropriate matrix is essential for MALDI-TOF MS analysis. It must be dissolvable in the solvent together with analytes to get a proper molar ratio, and should not react with analytes. 2, 5-dihydroxybenzoic acid (DHB) and  $\alpha$ -cyano-4-hydroxycinnamic acid (CHCA) are very common matrices for protein or peptide analysis (Lasaosa et al. 2009a; Lasaosa et

## General Introduction

---

al. 2009b; Zabet-Moghaddam et al. 2004b). Recently, MALDI-TOF MS was also applied to quantify some low molecular weight compounds. This new approach was applied for enzyme activity measurement (Bungert et al. 2004a; Bungert et al. 2004b) and metabolic flux analysis (Hollemeier et al. 2007; Wittmann and Heinzle 2001a). New matrices, namely 9-aminoacridine (9AA) and DMAN (1,8-bis(dimethylamino)naphthalene) were successfully employed for low molecular mass metabolites measurement. They were proven to be suitable for low mass weight molecule measurement with little noisy background (Edwards and Kennedy 2005; Rachal L. Vermillion-Salsbury 2002; Rohit and Alescaron 2009; Shroff et al. 2007; Shroff et al. 2009; Vaidyanathan and Goodacre 2007). The structures of these two compounds are shown in Figure 5.

For a long time, MALDI-TOF MS was applied only for identification of large biomolecules. Generally the sample is ionized and then directly analyzed by MS without any additional separation. A problem limiting quantification is signal suppression. Some analytes, especially having similar structures, can interfere with each other (Sojo et al. 2003; Wu et al. 2004). Nowadays, with the development of more powerful MALDI instrument as well as the application of internal standards (Duncan et al. 2008), these limitations can be mostly overcome. In this study, the investigation of MALDI-TOF MS focuses on small molecular mass metabolites quantification. The detailed introduction and the application of the matrix 9 AA are described in Chapter 5.

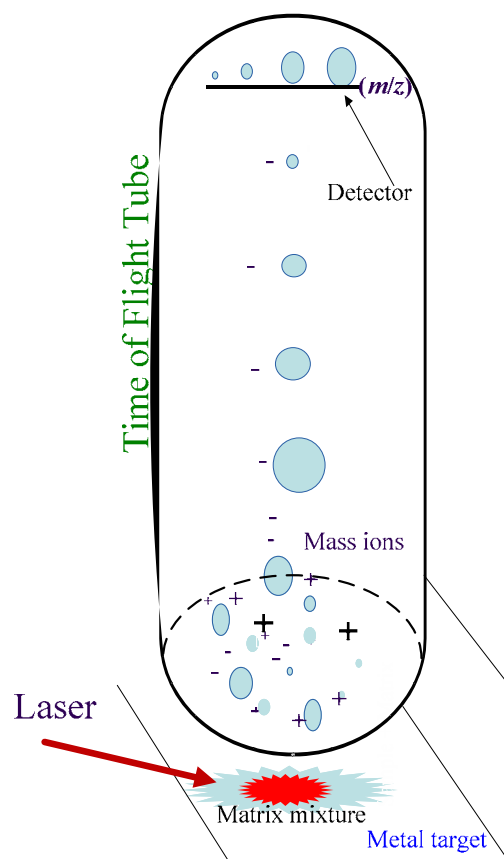


**Figure 4.** Representation of the principle of MALDI-TOF MS operating in the negative mode. The smaller ions (low  $m/z$  ratio) will travel faster than the larger masses (high  $m/z$  ratios).

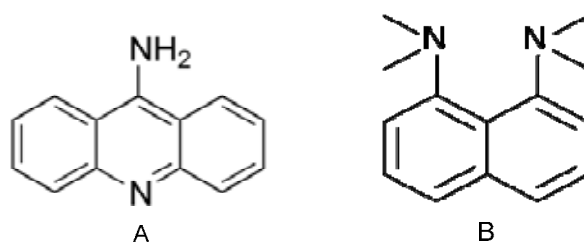


**Figure 5.** Chemical structures of two newly developed matrices: 9-aminoacridine (A) (Rachal L. Vermillion-Salsbury 2002) and 1,8-bis(dimethylamino)naphthalene (B) (Shroff et al. 2009).

### 1.2.3 Intracellular metabolites sampling and quantification

An appropriate sampling is essential for intracellular metabolism study. This is due to the extremely small size of the intermediate pools and short turnover time of intermediates. Sampling in a microbial experiment is so far a big challenge and limiting step. Quenching of the cells in the sub second time scale to stop all the reactions in living cells is generally employed and proved an effective method for yeast (Bolten and Wittmann 2008; Canelas et al. 2008) as well as different bacteria (Bolten et al. 2007; Moritz et al. 2000a; Zhu and Shimizu 2004). A method applicable for both yeast and bacteria was also reported (Spura et al. 2009). Generally, samples are directly put into cold methanol/water mixture which is pre-cold and kept in a dry ice/acetone mixture (-80 °C), followed by a centrifugation with pre-cooled centrifugator (-20 °C). The temperature is kept always lower than -20 °C during the whole procedure. Quenching method is performed under the assumption that all metabolites are kept in the cell over the whole process, but in practice, metabolites can leak from the cells to some extent and result in an underestimation of intracellular metabolites. Canelas et al. developed a leakage-free method for yeast (Canelas et al. 2008), but for bacteria this leakage is still a problem. A new strategy is highly desirable to improve this quenching method or avoid using quenching method for metabolism study in bacteria.

The next task following sampling and sample preparation is intracellular metabolites identification and quantification. Enzymatic assay (Schaefer et al. 1999) and NMR (Neves et al. 1999) methods have been in the forefront of this task but limited by the requirement of big sample volume. Recently, quantitative measurement based on LC-ESI-MS (Mashego et al. 2004; van Dam et al. 2002; Wunschel et al. 1997) and GC-MS (Kramer et al. 2006; Kromer et al. 2005) were described. Some limitations of LC-MS and GC-MS methods were also reported. For the LC-ESI-MS method, *e.g.*, non linear response caused by the ion suppression of electrospray ionization (Shi 2003) and the influence of the sample matrix from various microbial cultures (Mashego et al. 2004) were reported. GC-MS method is usually applied for metabolites that are volatile or that can be modified to be volatile by an additional derivatization step. However, this derivatization can truly impede quantification. Some special instruments were developed which allow an automatic derivatization to decrease this influence on quantification. In general, by the use of internal standard, above drawbacks can be fully or partly overcome (Mashego et al. 2004).

Quantification of small molecular mass metabolites was also investigated using MALDI-TOF MS (Szajli et al. 2008). Some preliminary efforts have been done on amino acids (Rohit Shroff 2007; Vaidyanathan and Goodacre 2007; Wittmann and Heinzle 2001a; Wittmann and Heinzle 2001c), cyanobacterial toxins (Howard et al. 2006) and bile acids (Mims and Hercules 2004; Simion et al. 1983). In this thesis, some details about small molecule metabolite quantification were investigated.

### **Aim and outline of this thesis**

The aim of this thesis is to develop and apply novel experimental and analytical tools for metabolic network characterization. The developed tools are expected to be useful for engineering of applicable microbial or mammalian strains.

Metabolic flux analysis is a critical tool in metabolic engineering. Isotope labeled substrates, normally  $^{13}\text{C}$  labeled, are applied in MFA and the isotope mass distributions of the metabolites can be observed by GC-MS measurement. Generally, high degrees of labeled substrates are used for a tracer experiment in order to obtain satisfactory isotopic enrichment that can be detected by GC-MS. The high cost of isotopic traces has however restricted this MFA to laboratory scales. Unfortunately, small-scale fermentation can not be directly scaled up to a large-scale industrial fermentation. Therefore, a method performing MFA in large-scale fermentation is urgently needed. In Chapter 2, GC-C-IRMS was investigated in depth for the measurement of extremely low isotopic

## General Introduction

---

enrichments of amino acids. The high precision of this analysis allows the use of low degree of labeled substrates for trace experiments. Kinetic isotope effect plays a role in metabolic reactions using low degree of labeling. A simple and effective method was developed and applied to correct for the KIE. In chapter 3, a novel strategy was successfully developed combining a low labeling tracer experiment and GC-C-IRMS analysis for metabolic flux analysis.

Enzyme activity plays a major role in metabolic networks. Enzyme kinetics are mainly studied experimentally using purified enzymes or cell extracts which are so called *in-vitro* conditions. But identified parameters are proved not fully applicable in a living cell because of differences between *in-vitro* and *in-vivo* conditions. The permeabilized cell *in-situ*, is regarded as closer to *in-vivo* condition and a better material for the enzyme kinetic study. In chapter 4, permeabilization in *Corynebacterium glutamicum* was attentively studied to obtain optimized conditions. Enzyme properties of *in-vitro* and *in-situ* conditions were compared. Quantification of intracellular metabolites is critical in metabolic system study. Enzymatic assays need relatively large volumes and are limited to certain metabolites and reactions. Nowadays, LC-MS and GC-MS methods are mostly applied for intracellular metabolites quantification but have limited sensitivity and are time-consuming. In metabolic system experiments, due to the extremely low concentrations of the metabolites and large number of samples, a new method with higher sensitivity and much shorter analysis time is desirable. In chapter 5, a novel strategy combining permeabilization and MALDI-TOF MS analysis was developed to meet this requirement. The successful quantification of metabolites makes it possible to obtain kinetics of glycolysis and the pentose-phosphate pathway. A scheme of this new strategy is demonstrated in Figure 6.

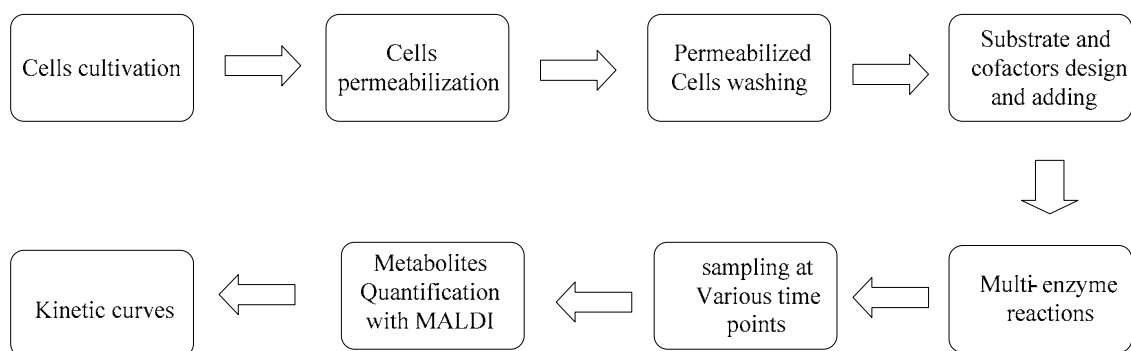


Figure 6. Schematic of strategy for MALDI-TOF MS quantification based kinetic study.

## General Introduction

---

At the end, chapter 7 discusses the challenges and outlook of these developed strategies in metabolic system analysis.

Chapter 2 has been published as : Heinzle E\*, Yuan Y, Kumar S, Wittmann C, Gehre M, Richnow HH, Wehrung P, Adam P, Albrecht P. 2008. Analysis of C-13 labeling enrichment in microbial culture applying metabolic tracer experiments using gas chromatography-combustion-isotope ratio mass spectrometry. *Analytical Biochemistry* 380(2):202-210.

Chapter 3 has been published as : Yuan Y, Yang TH, Heinzle E. 2010. C-13 metabolic flux analysis for larger scale cultivation using gas chromatography-combustion-isotope ratio mass spectrometry. *Metabolic Engineering* 12(4):392-400.

Chapter 4 has been published as : Yuan Y, Heinzle E. 2009. Permeabilization of *Corynebacterium glutamicum* for NAD(P)H-dependent intracellular enzyme activity measurement. *Comptes Rendus Chimie* 12(10-11):1154-1162.

Chapter 5 has been submitted as : Yuan Y, Heinzle E. 2010. *in-situ* multi-enzyme network kinetics study using MALDI-TOF MS. submitted to *Analytical Biochemistry*.

Chapter 6 is under preparation as : Yuan Y, Heinzle E. 2010. Kinetic modeling of *in-situ* enzymatic system.

### References:

- Abraham J, Bhat SG. 2008. Permeabilization of baker's yeast with N-lauroyl sarcosine. *Journal of Industrial Microbiology & Biotechnology* 35(8):799-804.
- Adams KAH, Chung SH, Klivanov AM. 1990. Kinetic Isotope Effect Investigation of Enzyme Mechanism in Organic-Solvents. *Journal of the American Chemical Society* 112(25):9418-9419.
- Anderson SR, Anderson VE, Knowles JR. 1994. Primary and Secondary Kinetic Isotope Effects as Probes of the Mechanism of Yeast Enolase. *Biochemistry* 33(34):10545-10555.
- Axelsson BS, Bjurling P, Matsson O, Langstrom B. 1992. C-11/C-14 Kinetic Isotope Effects in Enzyme Mechanism Studies - C-11/C-14 Kinetic Isotope Effect of the Tyrosine Phenol-Lyase Catalyzed Alpha,Beta-Elimination of L-Tyrosine. *Journal of the American Chemical Society* 114(4):1502-1503.
- Becker J, Klopprogge C, Wittmann C. 2008. Metabolic responses to pyruvate kinase deletion in lysine producing *Corynebacterium glutamicum*. *Microbial Cell Factories* 7:-.
- Bindu S, Somashekar D, Joseph R. 1998. A comparative study on permeabilization treatments for in situ determination of phytase of *Rhodotorula gracilis*. *Letters in Applied Microbiology* 27(6):336-340.
- Biwer AP, Zuber PT, Zelic B, Gerharz T, Bellmann KJ, Heinzle E. 2005. Modeling and analysis of a new process for pyruvate production. *Industrial & Engineering Chemistry Research* 44(9):3124-3133.
- Bolten CJ, Heinzle E, Muller R, Wittmann C. 2009. Investigation of the Central Carbon Metabolism of *Sorangium cellulosum*: Metabolic Network Reconstruction and Quantification of Pathway Fluxes. *Journal of Microbiology and Biotechnology* 19(1):23-36.
- Bolten CJ, Kiefer P, Letisse F, Portais J-C, Wittmann C. 2007. Sampling for Metabolome Analysis of Microorganisms. *Analytical Chemistry* 79(10):3843-3849.
- Bolten CJ, Wittmann C. 2008. Appropriate sampling for intracellular amino acid analysis in five phylogenetically different yeasts. *Biotechnology Letters* 30(11):1993-2000.

## General Introduction

---

- Bungert D, Bastian S, Heckmann-Pohl DM, Giffhorn F, Heinzle E, Tholey A. 2004a. Screening of sugar converting enzymes using quantitative MALDI-ToF mass spectrometry. *Biotechnology Letters* 26(13):1025-1030.
- Bungert D, Heinzle E, Tholey A. 2004b. Quantitative matrix-assisted laser desorption/ionization mass spectrometry for the determination of enzyme activities. *Analytical Biochemistry* 326(2):167-175.
- Canelas AB, Ras C, ten Pierick A, van Dam JC, Heijnen JJ, Van Gulik WM. 2008. Leakage-free rapid quenching technique for yeast metabolomics. *Metabolomics* 4(3):226-239.
- Chelico L, Khachatourians GG. 2003. Permeabilization of *Beauveria bassiana* blastospores for in situ enzymatic assays. *Mycologia* 95(5):976-981.
- Christova N, Tuleva B, Galabova D. 1996. Dependence of yeast permeabilization with triton X-100 on the cell age. *Biotechnology Techniques* 10(2):77-78.
- Cordeiro C, Freire AP. 1995. Digitonin permeabilization of *Saccharomyces cerevisiae* cells for in situ enzyme assay. *Anal Biochem* 229(1):145-8.
- Corr LT, Berstan R, Evershed RP. 2007. Optimisation of derivatisation procedures for the determination of delta C-13 values of amino acids by gas chromatography/combustion/isotope ratio mass spectrometry. *Rapid Communications in Mass Spectrometry* 21(23):3759-3771.
- Domingues A, Vinga S, Lemos J. 2010. Optimization strategies for metabolic networks. *BMC Systems Biology* 4(1):113.
- Drager A, Kronfeld M, Ziller MJ, Supper J, Planatscher H, Magnus JB, Oldiges M, Kohlbacher O, Zell A. 2009. Modeling metabolic networks in *C. glutamicum*: a comparison of rate laws in combination with various parameter optimization strategies. *BMC Syst Biol* 3:5.
- Duncan MW, Roder H, Hunsucker SW. 2008. Quantitative matrix-assisted laser desorption/ionization mass spectrometry. *Brief Funct Genomic Proteomic* 7(5):355-370.
- Edwards JL, Kennedy RT. 2005. Metabolomic analysis of eukaryotic tissue and prokaryotes using negative mode MALDI time-of-flight mass spectrometry. *Anal Chem* 77(7):2201-9.
- Felix H. 1982. Permeabilized cells. *Anal Biochem* 120(2):211-34.

## General Introduction

---

- Filion G, Laflamme C, Turgeon N, Ho J, Duchaine C. 2009. Permeabilization and hybridization protocols for rapid detection of *Bacillus* spores using fluorescence in situ hybridization. *Journal of Microbiological Methods* 77(1):29-36.
- Galabova D, Tuleva B, Spasova D. 1996. Permeabilization of *Yarrowia lipolytica* cells by Triton X-100. *Enzyme and Microbial Technology* 18(1):18-22.
- Godin JP, Faure M, Breuille D, Hopfgartner G, Fay LB. 2007. Determination of C-13 isotopic enrichment of valine and threonine by GC-C-IRMS after formation of the N(O,S)-ethoxycarbonyl ethyl ester derivatives of the amino acids. *Analytical and Bioanalytical Chemistry* 388(4):909-918.
- Griffith KL, Wolf RE, Jr. 2002. Measuring beta-galactosidase activity in bacteria: cell growth, permeabilization, and enzyme assays in 96-well arrays. *Biochem Biophys Res Commun* 290(1):397-402.
- Grüning N-M, Lehrach H, Ralser M. 2010. Regulatory crosstalk of the metabolic network. *Trends in Biochemical Sciences* 35(4):220-227.
- Hollemeyer K, Velagapudi VR, Wittmann C, Heinzle E. 2007. Matrix-assisted laser desorption/ionization time-of-flight mass spectrometry for metabolic flux analyses using isotope-labeled ethanol. *Rapid Communications in Mass Spectrometry* 21(3):336-342.
- Howard M, Twamley J, Wittmann C, Gaebel T, Jelezko F, Wrachtrup J. 2006. Quantum process tomography and Linblad estimation of a solid-state qubit. *New Journal of Physics* 8:1-21.
- Iwatani S, Yamada Y, Usuda Y. 2008. Metabolic flux analysis in biotechnology processes. *Biotechnology Letters* 30(5):791-799.
- Karas M, Bachmann D, Bahr U, Hillenkamp F. 1987. Matrix-Assisted Ultraviolet-Laser Desorption of Nonvolatile Compounds. *International Journal of Mass Spectrometry and Ion Processes* 78:53-68.
- Karas M, Hillenkamp F. 1988. Laser Desorption Ionization of Proteins with Molecular Masses Exceeding 10000 Daltons. *Analytical Chemistry* 60(20):2299-2301.
- Kiefer P, Nicolas C, Letisse F, Portais JC. 2007. Determination of carbon labeling distribution of intracellular metabolites from single fragment ions by ion chromatography tandem mass spectrometry. *Anal Biochem* 360(2):182-8.
- Koletzko B, Sauerwald T, Demmelmair H. 1997. Safety of stable isotope use. *European Journal of Pediatrics* 156:S12-S17.

## General Introduction

---

- Kramer JO, Heinzle E, Wittmann C. 2006. Quantification of S-adenosyl methionine in microbial cell extracts. *Biotechnology Letters* 28(2):69-71.
- Kromer JO, Fritz M, Heinzle E, Wittmann C. 2005. In vivo quantification of intracellular amino acids and intermediates of the methionine pathway in *Corynebacterium glutamicum*. *Analytical Biochemistry* 340(1):171-173.
- Lasaosa M, Delmotte N, Huber CG, Melchior K, Heinzle E, Tholey A. 2009a. A 2D reversed-phase x ion-pair reversed-phase HPLC-MALDI TOF/TOF-MS approach for shotgun proteome analysis. *Analytical and Bioanalytical Chemistry* 393(4):1245-1256.
- Lasaosa M, Jakoby T, Delmotte N, Huber CG, Heinzle E, Tholey A. 2009b. Rapid selection of peptide containing fractions in off-line 2-D HPLC in shotgun proteome analysis by screening with MALDI TOF MS. *Proteomics* 9(19):4577-4581.
- Liebermeister W, Klipp E. 2006a. Bringing metabolic networks to life: convenience rate law and thermodynamic constraints. *Theor Biol Med Model* 3:41.
- Liebermeister W, Klipp E. 2006b. Bringing metabolic networks to life: integration of kinetic, metabolic, and proteomic data. *Theor Biol Med Model* 3:42.
- Marlier JF, Oleary MH. 1984. Carbon Kinetic Isotope Effects on the Hydration of Carbon-Dioxide and the Dehydration of Bicarbonate Ion. *Journal of the American Chemical Society* 106(18):5054-5057.
- Martins AMTBS, Cordeiro CAA, Freire AMJP. 2001. In situ analysis of methylglyoxal metabolism in *Saccharomyces cerevisiae*. *Febs Letters* 499(1-2):41-44.
- Mashego MR, Wu L, Van Dam JC, Ras C, Vinke JL, Van Winden WA, Van Gulik WM, Heijnen JJ. 2004. MIRACLE: mass isotopomer ratio analysis of U-13C-labeled extracts. A new method for accurate quantification of changes in concentrations of intracellular metabolites. *Biotechnol Bioeng* 85(6):620-8.
- Meier-Augenstein W. 1999a. Applied gas chromatography coupled to isotope ratio mass spectrometry. *Journal of Chromatography A* 842(1-2):351-371.
- Meier-Augenstein W. 1999b. Use of gas chromatography-combustion-isotope ratio mass spectrometry in nutrition and metabolic research. *Curr Opin Clin Nutr Metab Care* 2(6):465-70.
- Michael Dauner US. 2000. GC-MS Analysis of Amino Acids Rapidly Provides Rich Information for Isotopomer Balancing. *Biotechnology Progress* 16(4):642-649.
- Mims D, Hercules D. 2004. Quantification of bile acids directly from plasma by MALDI-TOF-MS. *Analytical and Bioanalytical Chemistry* 378(5):1322-1326.

## General Introduction

---

- Minton AP. 2006. How can biochemical reactions within cells differ from those in test tubes? *J Cell Sci* 119(14):2863-2869.
- Miranda HV, Ferreira AE, Cordeiro C, Freire AP. 2006. Kinetic assay for measurement of enzyme concentration in situ. *Anal Biochem* 354(1):148-50.
- Moritz B, Striegel K, de Graaf AA, Sahm H. 2000. Kinetic properties of the glucose-6-phosphate and 6-phosphogluconate dehydrogenases from *Corynebacterium glutamicum* and their application for predicting pentose phosphate pathway flux in vivo. *European Journal of Biochemistry* 267(12):3442-3452.
- Mowshowitz DB. 1976. Permeabilization of yeast for enzyme assays: an extremely simple method for small samples. *Anal Biochem* 70(1):94-9.
- Neves AR, Ramos A, Nunes MC, Kleerebezem M, Hugenholtz J, de Vos WM, Almeida J, Santos H. 1999. In vivo nuclear magnetic resonance studies of glycolytic kinetics in *Lactococcus lactis*. *Biotechnol Bioeng* 64(2):200-12.
- Preston T, Slater C. 1994. Mass-Spectrometric Analysis of Stable-Isotope-Labeled Amino-Acid Tracers. *Proceedings of the Nutrition Society* 53(2):363-372.
- Rachal L, Vermillion-Salsbury DMH. 2002. 9-Aminoacridine as a matrix for negative mode matrix-assisted laser desorption/ionization. *Rapid Communications in Mass Spectrometry* 16(16):1575-1581.
- Rennie MJ, MeierAugenstein W, Watt PW, Patel A, Begley IS, Scrimgeour CM. 1996. Use of continuous-flow combustion MS in studies of human metabolism. *Biochemical Society Transactions* 24(3):927-932.
- Rieley G. 1994. Derivatization of Organic-Compounds Prior to Gas-Chromatographic Combustion-Isotope Ratio Mass-Spectrometric Analysis - Identification of Isotope Fractionation Processes. *Analyst* 119(5):915-919.
- Rohit S, Alescaron S. 2009. 1,8-Bis(dimethylamino)naphthalene: a novel superbasic matrix for matrix-assisted laser desorption/ionization time-of-flight mass spectrometric analysis of fatty acids. *Rapid Communications in Mass Spectrometry* 23(15):2380-2382.
- Rohit Shroff AMAS. 2007. Analysis of low molecular weight acids by negative mode matrix-assisted laser desorption/ionization time-of-flight mass spectrometry. *Rapid Communications in Mass Spectrometry* 21(20):3295-3300.
- Schaefer U, Boos W, Takors R, Weuster-Botz D. 1999. Automated sampling device for monitoring intracellular metabolite dynamics. *Anal Biochem* 270(1):88-96.

## General Introduction

---

- Schneiker S, Perlova O, Kaiser O, Gerth K, Alici A, Altmeyer MO, Bartels D, Bekel T, Beyer S, Bode E and others. 2007. Complete genome sequence of the myxobacterium *Sorangium cellulosum*. *Nature Biotechnology* 25(11):1281-1289.
- Schomburg D. 2009. A metabolic network described in absolute terms. *Nat Chem Biol* 5(8):535-536.
- Serrano R, Gancedo JM, Gancedo C. 1973. Assay of yeast enzymes in situ. A potential tool in regulation studies. *Eur J Biochem* 34(3):479-82.
- Shi GE. 2003. Application of co-eluting structural analog internal standards for expanded linear dynamic range in liquid chromatography/electrospray mass spectrometry. *Rapid Communications in Mass Spectrometry* 17(3):202-206.
- Shroff R, Muck A, Svatos A. 2007. Analysis of low molecular weight acids by negative mode matrix-assisted laser desorption/ionization time-of-flight mass spectrometry. *Rapid Communications in Mass Spectrometry* 21(20):3295-3300.
- Shroff R, Rulisek L, Doubsky J, Svatos A. 2009. Acid-base-driven matrix-assisted mass spectrometry for targeted metabolomics. *Proceedings of the National Academy of Sciences of the United States of America* 106(25):10092-10096.
- Simion FA, Tanner RD, Crooke PS, Heinzle E. 1983. Criteria for Determining the Direction of the Sustained Oscillation Trajectory in the Cell-Substrate Phase Plane Describing Continuous Fermentation Systems. *Biotechnology and Bioengineering*:257-264.
- Sojo LE, Lum G, Chee P. 2003. Internal standard signal suppression by co-eluting analyte in isotope dilution LC-ESI-MS. *Analyst* 128(1):51-4.
- Somkuti GA, Dominiecki ME, Steinberg DH. 1998. Permeabilization of *Streptococcus thermophilus* and *Lactobacillus delbrueckii* subsp. *bulgaricus* with ethanol. *Curr Microbiol* 36(4):202-6.
- Sorol MR, Pereyra E, Mizyrycki C, Rossi S, Moreno S. 2001. Protein kinase A activity in permeabilized cells as an approximation to in vivo activity. *Experimental Cell Research* 271(2):337-343.
- Spura J, Reimer LC, Wieloch P, Schreiber K, Buchinger S, Schomburg D. 2009. A method for enzyme quenching in microbial metabolome analysis successfully applied to gram-positive and gram-negative bacteria and yeast. *Analytical Biochemistry* 394(2):192-201.

## General Introduction

---

- Stelling J, Klamt S, Bettenbrock K, Schuster S, Gilles ED. 2002. Metabolic network structure determines key aspects of functionality and regulation. *Nature* 420(6912):190-193.
- Szajli E, Feher T, Medzihradzky KF. 2008. Investigating the Quantitative Nature of MALDI-TOF MS. *Mol Cell Proteomics* 7(12):2410-2418.
- Tryfona T, Bustard MT. 2008. Impact of pulsed electric fields on *Corynebacterium glutamicum* cell membrane permeabilization. *Journal of Bioscience and Bioengineering* 105(4):375-382.
- Vaidyanathan S, Goodacre R. 2007. Quantitative detection of metabolites using matrix-assisted laser desorption/ionization mass spectrometry with 9-aminoacridine as the matrix. *Rapid Commun Mass Spectrom* 21(13):2072-8.
- Vallino JJ, Stephanopoulos G. 1993. Metabolic Flux Distributions in *Corynebacterium-Glutamicum* during Growth and Lysine Overproduction. *Biotechnology and Bioengineering* 41(6):633-646.
- van Dam JC, Eman MR, Frank J, Lange HC, van Dedem GWK, Heijnen SJ. 2002. Analysis of glycolytic intermediates in *Saccharomyces cerevisiae* using anion exchange chromatography and electrospray ionization with tandem mass spectrometric detection. *Analytica Chimica Acta* 460(2):209-218.
- van der Werf MJ, Takors R, Smedsgaard J, Nielsen J, Ferenci T, Portais JC, Wittmann C, Hooks M, Tomassini A, Oldiges M and others. 2007. Standard reporting requirements for biological samples in metabolomics experiments: microbial and in vitro biology experiments. *Metabolomics* 3(3):189-194.
- Wittmann C. 2007. Fluxome analysis using GC-MS. *Microbial Cell Factories* 6:-.
- Wittmann C, Heinzle E. 1999. Mass spectrometry for metabolic flux analysis. *Biotechnology and Bioengineering* 62(6):739-750.
- Wittmann C, Heinzle E. 2001. Application of MALDI-TOF MS to lysine-producing *Corynebacterium glutamicum* - A novel approach for metabolic flux analysis. *European Journal of Biochemistry* 268(8):2441-2455.
- Wittmann C, Heinzle E. 2001b. Application of MALDI-TOF MS to lysine-producing *Corynebacterium glutamicum*: a novel approach for metabolic flux analysis. *Eur J Biochem* 268(8):2441-55.
- Wittmann C, Heinzle E. 2001c. MALDI-TOF MS for quantification of substrates and products in cultivations of *Corynebacterium glutamicum*. *Biotechnology and Bioengineering* 72(6):642-647.

- Wu L, Wang W, van Winden WA, van Gulik WM, Heijnen JJ. 2004. A new framework for the estimation of control parameters in metabolic pathways using lin-log kinetics. *Eur J Biochem* 271(16):3348-59.
- Wunschel DS, Fox KF, Fox A, Nagpal ML, Kim K, Stewart GC, Shahgholi M. 1997. Quantitative analysis of neutral and acidic sugars in whole bacterial cell hydrolysates using high-performance anion-exchange liquid chromatography electrospray ionization tandem mass spectrometry. *Journal of Chromatography A* 776(2):205-219.
- Zabet-Moghaddam M, Kruger R, Heinzle E, Tholey A. 2004. Matrix-assisted laser desorption/ionization mass spectrometry for the characterization of ionic liquids and the analysis of amino acids, peptides and proteins in ionic liquids. *Journal of Mass Spectrometry* 39(12):1494-1505.
- Zamboni N, Fendt S-M, Ruhl M, Sauer U. 2009. <sup>13</sup>C-based metabolic flux analysis. *Nat. Protocols* 4(6):878-892.
- Zamboni N, Sauer U. 2009. Novel biological insights through metabolomics and <sup>13</sup>C-flux analysis. *Current Opinion in Microbiology* 12(5):553-558.
- Zhu J, Shimizu K. 2004. The effect of pfl gene knockout on the metabolism for optically pure D-lactate production by *Escherichia coli*. *Applied Microbiology and Biotechnology* 64(3):367-375.

## Chapter 2

# Analysis of $^{13}\text{C}$ Labeling Enrichment in Microbial Culture Applying Metabolic Tracer Experiments Using GC-C-IRMS

### Abstract

The applicability of isotope ratio monitoring gas chromatography-mass spectrometry (GC-C-IRMS) for the quantification of  $^{13}\text{C}$  enrichment of proteinogenic amino acids in metabolic tracer experiments was evaluated. Measurement of the  $^{13}\text{C}$  enrichment of proteinogenic amino acids from cell hydrolysates of *Corynebacterium glutamicum* growing on different mixtures containing between 0.5 % and 10 % [ $1\text{-}^{13}\text{C}$ ] glucose shows the significance of kinetic isotope effects in metabolic flux studies at low degree of labeling. Assuming that only reacting carbon atoms are subjected to kinetic isotope effects, we developed a method to calculate the  $^{13}\text{C}$  enrichment. The approach to correct for these effects in metabolic flux studies using  $\delta^{13}\text{C}$  measurement by GC-C-IRMS uses two parallel experiments applying substrate with natural abundance and  $^{13}\text{C}$  enriched tracer substrate, respectively. The fractional enrichment obtained in natural substrate is subtracted from that of the enriched one. Tracer studies with *C. glutamicum* resulted in a statistically identical relative fractional enrichment of  $^{13}\text{C}$  in proteinogenic amino acids over the whole range of applied concentrations of [ $1\text{-}^{13}\text{C}$ ] glucose. The present findings indicate a great potential of GC-C-IRMS for labeling quantification in  $^{13}\text{C}$  metabolic flux analysis with low labeling degree of tracer substrate directly in larger scale bioreactors.

This chapter has been published as : Heinzle E\*, Yuan Y, Kumar S, Wittmann C, Gehre M, Richnow HH, Wehrung P, Adam P, Albrecht P. 2008. Analysis of C-13 labeling enrichment in microbial culture applying metabolic tracer experiments using gas chromatography-combustion-isotope ratio mass spectrometry. Analytical Biochemistry 380(2):202-210.

## 2.1 Introduction

In recent years,  $^{13}\text{C}$  metabolic flux analysis has gained momentum as a powerful tool for quantitative studies of *in vivo* activities of pathways (G.N.Stephanopoulos 1998; Wittmann 2002). It is based on the use of  $^{13}\text{C}$ -labeled compounds as tracer for biological system studies. In such tracer studies the labeled carbon atoms are distributed among the metabolic network. After reaching an isotopic steady-state, the isotopic enrichment in different intracellular or extracellular metabolite pools can be measured by NMR (Maaheimo et al. 2001; Sauer et al. 1997), GC-MS (Christensen and Nielsen 1999; Michael Dauner 2000; Wittmann and Heinzle 2002b) or MALDI-TOF MS (Wittmann and Heinzle 2001a). The calculation of metabolic fluxes from the  $^{13}\text{C}$  labeling data is then based on the network topology of the studied system including knowledge on carbon transfer in the underlying reactions. Often amino acids contained in the cell protein are analyzed for this purpose, because they provide valuable information for the calculation of metabolic fluxes (Christensen and Nielsen 1999; Michael Dauner 2000). Resulting mass isotopomer ratios or fractional carbon labeling can be directly used for metabolic flux calculation (Wittmann and Heinzle 1999b; Yang et al. 2008).

Typically, isotopic tracer substrates are applied at high  $^{13}\text{C}$  enrichment such as 100 % [1- $^{13}\text{C}$ ] glucose, mixtures of [1- $^{13}\text{C}$ ] glucose and glucose with a natural carbon isotope abundance (50:50), or mixtures of [ $^{13}\text{C}_6$ ] glucose and glucose with a natural carbon isotope abundance (90:10, 80:20, and 60:40), respectively, to get an isotopic enrichment in the metabolites of interest that can be satisfactorily detected with standard MS or NMR methods (Kelleher 2001) In few cases, such as medium demanding chemostat cultivations, a lower  $^{13}\text{C}$  enrichment of the substrate is applied, which however results in a loss in accuracy (Fiaux et al. 2003). The high  $^{13}\text{C}$  enrichment required and the high costs of isotopic tracer substrates have restricted  $^{13}\text{C}$  metabolic flux analysis to small scale (Kumar et al. 2004). Studies at larger-scale bioreactors have therefore not been realized (Wittmann C 2008). Investigations at large scale are inevitable since it is well known that conditions in small-scale often cannot accurately predict the events in the large-scale fermentation and in many cases scale-up is a major bottleneck in bioprocess development (Bourne et al. 1992; K. van't Riet 1991; S. Aiba 1973). Recent approaches to assess metabolic flux at large scale rely on identical performance of the large scale reactor to be characterized and a small scale reactor run in parallel for the  $^{13}\text{C}$ -based metabolic flux analysis and are

limited by high experimental effort and highly sophisticated instrumentation to integrate, control and run the two processes in parallel (El Massaoudi et al. 2003). Therefore, solutions for direct metabolic flux analysis of large-scale biotechnological processes are highly desirable. In this context GC-C-IRMS exhibits a high-precision (0.0002 atom %) and accuracy for measurement of low isotopic enrichment compared to GC-MS (0.05 atom %) (Brand 1996; Godin et al. 2007c; Meier-Augenstein 1999a). It therefore appears interesting to be used in the field of metabolic flux analysis by overcoming the limitations of present approaches at large scale. GC-C-IRMS has been applied for stable isotope analysis in archaeology (Stott and Evershed 1996), environmental chemistry (Ishiwatari et al.; Schmidt et al. 2004), geochemistry (Behrens et al. 2000; Derrien et al. 2003), nutrition and medically oriented metabolic research (Aguilera et al. 2000; Meier-Augenstein 1999b). Biological studies included the determination the incorporation of  $^{13}\text{C}$  into glutamine by infusion of  $^{13}\text{C}$  labeled acetate in humans (Menand et al. 1997) or of  $[1-^{13}\text{C}]$  valine into muscle protein in piglets (Reijngoud et al. 1998b) or of  $^{13}\text{C}$  into fatty acid of human retinoblastoma cells (Huang et al. 2000). However, GC-C-IRMS has not yet been considered for  $^{13}\text{C}$  metabolic flux analysis.

Here, we present an experimental protocol to measure  $^{13}\text{C}$  fractional enrichment in proteinogenic amino acids by GC-C-IRMS. The applicability of GC-C-IRMS for metabolic flux analysis is investigated by different tracer substrates employing low levels of  $^{13}\text{C}$ -labeled substrate. The experiments are based on biosynthetically directed fractional  $^{13}\text{C}$  labeling of the proteinogenic amino acids, which is achieved by feeding a mixture of  $[1-^{13}\text{C}]$  glucose and glucose with a natural carbon isotope abundance and subsequent measurement of  $^{13}\text{C}$  fractional enrichment by GC-C-IRMS. The studied microorganism *Corynebacterium glutamicum* is intensively used for the industrial production of amino acids such as glutamate and lysine (P.A. Lessard 1999; Wittmann and Becker 2007b) and thus is a potential candidate for metabolic flux analysis at large scale.

## 2.2 Materials and methods

### Reagents

$[1-^{13}\text{C}]$  glucose (99 % atom  $^{13}\text{C}$ ) was purchased from Cambridge Isotope Laboratories Inc. (Andover, USA). L-  $[1-^{13}\text{C}]$  alanine (99 % atom  $^{13}\text{C}$ ) was purchased from Euriso-top (Gif-sur-Yvette, France). Yeast extract and tryptone used for LB5G medium were from Difco Laboratories (Becton Dickinson, France S.A., France). All other chemicals were from

## Analysis of $^{13}\text{C}$ enrichment using GC-C-IRMS

---

Sigma-Aldrich (St. Louis, USA). For all experiments the same batch of chemicals was used.

### **Growth and labeling of *C. glutamicum***

Stock cultures of *C. glutamicum* ATCC 13032 were stored at  $-70\text{ }^{\circ}\text{C}$  in complex LB5G medium supplemented with 10 % (v/v) glycerol (Vallino and Stephanopoulos 1993). For cultivation a mineral medium containing 110 mM glucose as carbon source was applied (Yang et al. 2003). For first pre-cultivation, a single colony was inoculated from a 2 day grown LB5G agar plate into 50 mL LB5G medium in a 500 mL baffled shake flask and incubated for 12 hours on a rotary shaker at 250 rpm (Multitron; Infors AG, Bottmingen, Switzerland). For second pre-cultivation, cells were transferred into mineral medium with a starting cell concentration ( $\text{OD}_{660}$ ) of 0.05, and grown overnight as described above. Subsequently, cells were washed twice with mineral medium by centrifugation at 10,000 g (Biofuge® fresco; Heraeus, Kendro Laboratory Products, Hanau, Germany) and used as inoculum for the main cultures. Tracer experiments were carried out in 25 ml baffled shake flasks containing 5 ml mineral medium. Hereby mixtures of (i) 0.5 % (w/w) [ $1\text{-}^{13}\text{C}$ ] glucose and 99.5 % (w/w) glucose with a natural carbon isotope abundance, (ii) 1.0 % (w/w) [ $1\text{-}^{13}\text{C}$ ] glucose and 99.0 % (w/w) glucose with a natural carbon isotope abundance, (iii) 2.0 % (w/w) [ $1\text{-}^{13}\text{C}$ ] glucose and 98.0 % (w/w) glucose with a natural carbon isotope abundance and (iv) 10.0 % (w/w) [ $1\text{-}^{13}\text{C}$ ] glucose and 90.0 % (w/w) glucose with a natural carbon isotope abundance were applied, respectively.

All flasks were incubated in parallel at  $30\text{ }^{\circ}\text{C}$  and 250 rpm on a rotary shaker (Multitron; Infors AG, Bottmingen, Switzerland). It can be expected that cellular components will reach an isotopic steady state during the balanced exponential growth. Growth was monitored by measurement of optical density. At the mid of exponential phase, samples were taken from all the five flasks. Cell concentration ( $\text{OD}_{660}$ ) was determined and biomass and supernatant was collected for purpose of analysis.

### **Sample preparation for labeling analysis**

For GC-C-IRMS analysis of proteinogenic amino acids, mid exponential culture biomass (2 mg) was harvested. The pellet was washed twice with deionized water, mixed with 0.5 ml of 6 M HCl and incubated for 24 h at  $110\text{ }^{\circ}\text{C}$  for hydrolysis. The hydrolysis was complete after 24 hours of reaction and is not associated with measurable isotope effects

## Analysis of $^{13}\text{C}$ enrichment using GC-C-IRMS

---

on the  $\delta^{13}\text{C}$  isotope composition of amino acids (Jim et al. 2003). After cooling down to room temperature, the hydrolyzate was filtered through a 0.22  $\mu\text{m}$  membrane (Ultrafree®, Millipore, USA). 50  $\mu\text{l}$  of the hydrolyzate was lyophilized. The amino acids in the lyophilisate were converted into *t*-butyl-dimethylsilyl (*t*-BDMS) derivatives by addition of 100  $\mu\text{l}$  of N-methyl-N-*t*-butyldimethylsilyl-trifluoroacetamide (MBDSTFA, Macherey-Nagel GmbH & Co., Düren, Germany). This corresponds to more than 200-fold molar excess of MBDSTFA ensuring complete conversion of the amino acids. The mixture was allowed to react for 60 min at 80 °C. After cooling down to room temperature, derivatized samples were filtered through 0.22  $\mu\text{m}$  membranes (Ultrafree®, Millipore, USA) and then directly used for GC-C-IRMS analysis.

### Analytical procedures for GC-C-IRMS analysis

$^{13}\text{C}$ -labeling measurements were performed on an GC-C-IRMS instrument comprising a HP6890 gas chromatograph (Agilent 6890; Agilent Technologies, Palo Alto, USA), a standard GC/C III interface with a Ni/Cu/Pt combustion reactor set at 940 °C (Thermo Fisher Scientific, Bremen, Germany) and a MAT 253 gas isotope mass spectrometer (Thermo Fisher Scientific MAT, Bremen, Germany). Electron ionization voltage was 77 eV, electron current was 1.5 mA and three Faraday cup collectors for  $m/z$  44, 45 and 46 were used for detection of  $\text{CO}_2$ . The GC was equipped with a split/splitless injector and a DB-1 column (60 m x 0.25 mm, 0.1  $\mu\text{m}$  film thickness, J&W). Helium was used as carrier gas with a constant flow of 1.5 ml/min.  $\text{H}_2\text{O}$  generated in the combustion interface was removed by passage of the combustion products through a water trap cooled to 3 °C. (Nafion: 50 cm x 0.3 mm i.d.; 15 ml  $\text{min}^{-1}$  helium flow rate).  $\delta^{13}\text{C}$  determinations were carried out with the faraday cup set to measure  $m/z$  44, 45 and 46. Isotope ratios were calculated from the relative abundances of these mass traces. For analysis 1  $\mu\text{l}$  of sample was injected in split mode (split 1:10) using an autosampler (CTC Combipal, Chromtech, Idstein, Germany). The split/splitless injector was set to 270 °C. The GC temperature parameters were set as follows. The initial temperature of 120 °C was kept for 5 minutes. Subsequently the temperature was increased by 5 °C/min to 280 °C and then by 20 °C/min to 310 °C and kept isotherm for 5 min. Isotope ratios were calibrated against reference  $\text{CO}_2$  of known isotopic composition introduced directly into the ion source three times at the beginning and at the end of every run.  $\delta^{13}\text{C}$  values were calculated by integrating the  $m/z$  44, 45, and 46 ion currents. The compound-specific isotope values ( $\delta^{13}\text{C}$ ) were calculated relative to calibrated reference gas ( $\text{CO}_2$ ). The reference gas was calibrated

against Vienna Pee Dee Belemnite (VPDB) scale (Coplen et al. 2006). Each measurement was performed at least in triplicate.

## 2.3 Theoretical background

**Calculation of fractional  $^{13}\text{C}$  enrichment.** The  $^{13}\text{C}$  enrichment, expressed as  $\delta^{13}\text{C}$  in units of ‰, is defined as the relative difference between a sample isotope ratio and the isotope ratio of the standard PDB (Eq. 1).  $\delta$  units are therefore relative units and not a measure of absolute isotope concentration (Slater et al. 2001).

$$\delta^{13}\text{C} = \left( \frac{R_A - R_S}{R_S} \right) \times 1000 \quad [\text{‰}] \quad (1)$$

Hereby,  $R_A$  is the measured isotope ratio ( $^{13}\text{C}/^{12}\text{C}$ ) of the sample analyte.  $R_S$  is the known isotope ratio for the PDB international standard (0.0112372) respectively. This results in:

$$R_A = \frac{\delta^{13}\text{C} \cdot R_S}{1000} + R_S \quad (2)$$

Neglecting  $^{14}\text{C}$  atoms, the  $^{13}\text{C}$  fraction is calculated as

$${}^{13}\text{F}_A = \frac{[{}^{13}\text{C}]}{[{}^{12}\text{C}] + [{}^{13}\text{C}]} = \frac{R_A}{1 + R_A} \quad (3)$$

where

$$R_A = \frac{[{}^{13}\text{C}]}{[{}^{12}\text{C}]} \quad (4)$$

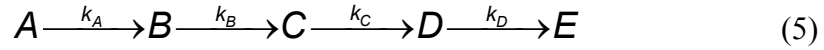
### Correction for kinetic isotope effects

Kinetic isotope effects are the result from the lower activation energies needed to break chemical bonds formed by light (e.g.  $^{16}\text{O}$ ,  $^{12}\text{C}$ ,  $^1\text{H}$ ) compared to heavy (e.g.  $^{18}\text{O}$ ,  $^{13}\text{C}$ ,  $^2\text{H}$ ) isotopes. Light isotopes form weaker bonds and thus react faster than the heavy isotopes, leading to depletion in the product and an enrichment of heavy isotopes in the not yet degraded residual fraction. Thus, the reactive center of the reacting molecule is mostly

## Analysis of $^{13}\text{C}$ enrichment using GC-C-IRMS

---

responsible whereas more remote atoms are less contributing to this effect. If we assume as a first approximation that isotope effects are only concerned with the reacting carbon atom, we can directly calculate the expected effect for this single carbon atom. For doing that we look at a simple linear reaction network



If we assume that the concentration of A is constant and that B and C are at metabolic steady-state, the corresponding material balances for B and C are

$$\begin{aligned} 0 &= k_A C_A - k_B C_B \\ 0 &= k_B C_B - k_C C_C \\ 0 &= k_C C_C - k_D C_D \end{aligned} \quad (6)$$

where  $k_i$  are reaction rate constants and  $C_i$  are concentrations. Then we directly get,

$$k_A C_A = k_D C_D \quad (7)$$

and for the labeled species with modified rate constants

$$k_A^* C_A^* = k_D^* C_D^* \quad (8)$$

If we calculate the fractional labeling of D as function of the fractional labeling of A for carbon atom j of the product reacting along path i we obtain,

$$\frac{C_{D,j}^*}{C_D} = {}^{13}F_{D,j} = \frac{k_D k_{A,j}^* C_A^*}{k_{D,j}^* k_A C_A} = k'_{i,j} \frac{C_A^*}{C_A} = k'_{i,j} {}^{13}F_A \quad (9)$$

We can see that the resulting labeling ratio of this carbon atom is always proportional to the input labeling. At a given set of flux distribution, each carbon atom of the substrate applied will statistically have its characteristic path and therefore its corresponding  $k'$  value as defined in equation (9). We can now sum all possible paths,  $m$ , of one substrate carbon atom ending up in any of  $n$  product carbon atoms

$$\frac{\sum_{j=1}^n C_{D,j}^*}{C_D} = {}^{13}F_D = \frac{\sum_{i=1}^m \sum_{j=1}^n \frac{k_{A,i}^*}{k_{D,j}^*} C_A^*}{\frac{k_A}{k_D} C_A} = k' \frac{C_A^*}{C_A} = k' {}^{13}F_A \quad (10)$$

Similarly this can be done for all naturally labeled carbon atoms with the exception of the labeled one. We can define,

$$\frac{C_{D,r}^*}{C_D} = F_{D,r} = \frac{k_D k_{A,r}^* C_{A,r}^*}{k_{D,r}^* k_A C_A} = k_r' \frac{C_{A,r}^*}{C_A} = k_r' F_{A,r} \quad (11)$$

here r indicates the residual carbon atoms. Now the total fractional labeling of a metabolite measured will be the sum of the traced atom and all others yielding

$${}^{13}F_{D,tot} = {}^{13}F_D + {}^{13}F_{D,r} = k' {}^{13}F_A + k_r' {}^{13}F_{A,r} \quad (12)$$

Here *tot* indicates the total labeling as measured by GC-C-IRMS. Plotting the fractional enrichment  ${}^{13}F_{D,tot}$  versus the applied fractional enrichment  ${}^{13}F_A$ , i.e. the fraction of applied labeled glucose, should yield a straight line which generally has an intercept different from zero. The values of  $k'$  and  $k_r'$  are different for each carbon atom and each path this carbon atom has experienced during metabolism. However, at identical flux distributions these parameters should remain constant. If we compare the measured fractional labeling of two metabolites at identical carbon paths and metabolic flux distributions we get,

$$\frac{{}^{13}F_{D,tot,1}}{{}^{13}F_{D,tot,2}} = \frac{k_1' {}^{13}F_A + k_{r,1}' {}^{13}F_{A,r}}{k_2' {}^{13}F_A + k_{r,2}' {}^{13}F_{A,r}} \quad (13)$$

If  $k_{r,i}' {}^{13}F_{A,r} \ll k_i' {}^{13}F_A$ , the measured ratio  ${}^{13}F_{D,tot,1}/{}^{13}F_{D,tot,2}$  should be constant with varying substrate labeling  ${}^{13}F_A$ . However, if we want to apply substrate labeling comparable to natural labeling, this will not be the case. If we now subtract the residual labeling,  ${}^{13}F_{D,r}$  as

## Analysis of $^{13}\text{C}$ enrichment using GC-C-IRMS

---

measured in an experiment with only naturally labeled substrate, from the measured total labeling,  $^{13}\text{F}_{D,tot}$  we get the labeling originating from the labeled carbon atom.

$$^{13}\text{F}_D = k' ^{13}\text{F}_A + k'_r ^{13}\text{F}_{A,r} - ^{13}\text{F}_{D,r} \quad (14)$$

Using equation (14) we can compare the fractional labeling of two metabolites calculating their ratio.

$$\frac{^{13}\text{F}_{D,1}}{^{13}\text{F}_{D,2}} = \frac{k'_1 ^{13}\text{F}_A + k'_{r,1} ^{13}\text{F}_{A,r} - ^{13}\text{F}_{D,r,1}}{k'_2 ^{13}\text{F}_A + k'_{r,2} ^{13}\text{F}_{A,r} - ^{13}\text{F}_{D,r,2}} \quad (15)$$

If added substrate labeling  $^{13}\text{F}_A$  approaches zero in equation (12), we get  $^{13}\text{F}_{D,tot} = ^{13}\text{F}_{D,r} = k'_r ^{13}\text{F}_{A,r}$ , therefore the difference  $^{13}\text{F}_{A,r} - ^{13}\text{F}_{D,r} = 0$ . This further means that the ratio  $^{13}\text{F}_{D,1}/^{13}\text{F}_{D,2}$  should be constant at constant flux distributions but varying degree of substrate labeling.

In the present work this approach was applied to the correction of kinetic isotope effects in metabolic tracer studies. In the case of growing *Corynebacterium glutamicum*, the corrected  $^{13}\text{C}$  enrichment of the analyte A was defined as

$$^{13}\text{F}_i = ^{13}\text{F}_{i,tot} - ^{13}\text{F}_{i,nat} \quad (16)$$

Where  $^{13}\text{F}_{i,nat}$  is the observed fractional abundance of  $^{13}\text{C}$  of component 'i' in the sample that was grown on naturally labeled carbon source and serves as reference.  $^{13}\text{F}_{i,tot}$  is the measured fractional abundance of the sample that was grown on labeled carbon source.  $^{13}\text{F}_i$  can be converted into atom percent excess, APE ( $\text{APE} = 100 \times ^{13}\text{F}_i$ ). If kinetic isotope effects are identical in both samples, this effect is corrected for by equation (16). If kinetic effects are more complex, e.g. in multiple labeled substrates, corresponding errors will remain. If the labeling degree is very small,  $^{13}\text{F}_i$  will have a large error because both,  $^{13}\text{F}_{i,tot}$  and  $^{13}\text{F}_{i,nat}$ , are corrupted with errors and these errors will be amplified while calculating the difference, since

$$\sigma_{^{13}F_i} = \sqrt{\sigma_{^{13}F_{i,tot}}^2 + \sigma_{^{13}F_{i,nat}}^2} \quad (17)$$

Using equation (15) and (16), we define a ratio of true corrected  $^{13}\text{C}$  fractional enrichment of two compounds 'i' and 'j' as mentioned in equation (18). We can expect that this ratio of two compounds, e.g., amino acids, will be identical in cultures grown under identical conditions but with different concentrations of labeled substrate applied.

$$^{13}F_{i,j} = \frac{^{13}F_{i,tot} - ^{13}F_{i,nat}}{^{13}F_{j,tot} - ^{13}F_{j,nat}} \quad (18)$$

The magnitude of error amplification is estimated by Gaussian law of error propagation using equation (19)

$$\sigma_{F_{i,j}} = \sqrt{\left(\sigma_{^{13}F_{i,tot}}^2 + \sigma_{^{13}F_{i,nat}}^2\right) \cdot \left(\frac{1}{^{13}F_{i,tot} - ^{13}F_{i,nat}}\right)^2 + \left(\sigma_{^{13}F_{j,tot}}^2 + \sigma_{^{13}F_{j,nat}}^2\right) \cdot \left(\frac{^{13}F_{i,tot} - ^{13}F_{i,nat}}{\left(^{13}F_{j,tot} - ^{13}F_{j,nat}\right)^2}\right)^2} \quad (19)$$

## Correction of the data for contribution of $^{13}\text{C}$ from derivatization agent

The derivatization has an effect on the  $^{13}\text{C}$  content in the entire analyte. The contribution of derivative carbon must therefore be taken into account when only the fractional  $^{13}\text{C}$  value of the analyte is required (Docherty et al. 2001). Additional  $^{13}\text{C}$  fraction from carbon atoms introduced during the derivatization reaction can be corrected by using a correction factor. This factor can be determined by measuring the  $\delta^{13}\text{C}$  value of an underivatized molecule and of the same molecule after derivatization by GC-C-IRMS, respectively. Kinetic effects caused by the analyte can be neglected because it is completely converted. This is not the case for the derivative agent, which is supplied in large excess. However, as the silylation reaction does not involve any direct carbon bond formation, it does not lead to any primary kinetic isotope effect, which may occur with other derivatization agents (Rieley 1994). Due to this, the contribution of  $^{13}\text{C}$  from the derivatization agent can be corrected by using simple mass balance (Brenna et al. 1997).

$$N_{LCar}^{DA} = N_{LCar}^A + N_{LCar}^D \quad (20)$$

$N_{LCar}^{DA}$  - Number of labeled carbon atoms in derivatized analyte;  $N_{LCar}^A$  - Number of labeled carbon atoms in analyte;  $N_{LCar}^D$  - Number of labeled carbon atoms in derivatization agent.

Hereby we assumed in a first approximation that the  $^{13}\text{C}$  contribution from the derivatization reagent is natural with an abundance of 0.011078 (K.J.R. Rosman 1997). Corrections were made by using equation (21)

$$^{13}F_A = \frac{R(N_{Car}^A + N_{Car}^D) - N_{Car}^D \ ^{13}F_D (1+R)}{N_{Car}^A (1+R)} \quad (21)$$

where,  $^{13}F_A$  -  $^{13}\text{C}$  fraction of the analyte originating from labeled substrate; R- Measured  $^{13}\text{C}/^{12}\text{C}$  ratio of the sample;  $N_{Car}^A$  - Number of carbon atoms in analyte;  $N_{Car}^D$  - Number of carbon atoms in derivatization agent and  $^{13}F_D$  -  $^{13}\text{C}$  fraction of the derivatization agent. If  $^{13}F_A$  and  $^{13}F_D$  -values are further used for calculation of  $E_A$ , the term containing  $^{13}F_D$  cancels out. For an exact determination of  $^{13}F_A$ ,  $^{13}F_D$  has to be measured experimentally.

## 2.4 Results and discussion

### $^{13}\text{C}$ Labeling analysis of amino acids by GC-C-IRMS

GC-C-IRMS chromatograms of a synthetic amino acid mixture and a protein hydrolysate from *C. glutamicum* culture are shown in Figure 1. The  $^{13}\text{C}$  fraction of 16 proteinogenic amino acids could be determined. Note that during the hydrolysis procedure cysteine and tryptophan are destroyed. Asparagine and glutamine are converted into aspartic acid and glutamic acid, respectively. The upper part of each chromatogram (Figure. 1 A, C) shows the  $m/z$  45/44 ratios, and the lower part of each chromatogram (Figure. 1 B, D) depicts the  $m/z$  44 ion current. It can be seen from the chromatogram that the developed method allowed baseline resolution of amino acids and subsequent  $\delta^{13}\text{C}$  measurement of amino acids in standard amino acid mixture and proteinogenic amino acids from crude biomass hydrolysate. High chromatographic resolution, high precision of determination and accurate calibration of isotope abundances ( $\delta$  values) as well as adequate correction for background carbon dioxide are the most important requirements for achieving this. All

# Analysis of $^{13}\text{C}$ enrichment using GC-C-IRMS

amino acids present in the standard mixture were found satisfactorily separated without any co-eluting peaks (Figure. 1 A, B). The  $m/z$  45/44 ratio tracer

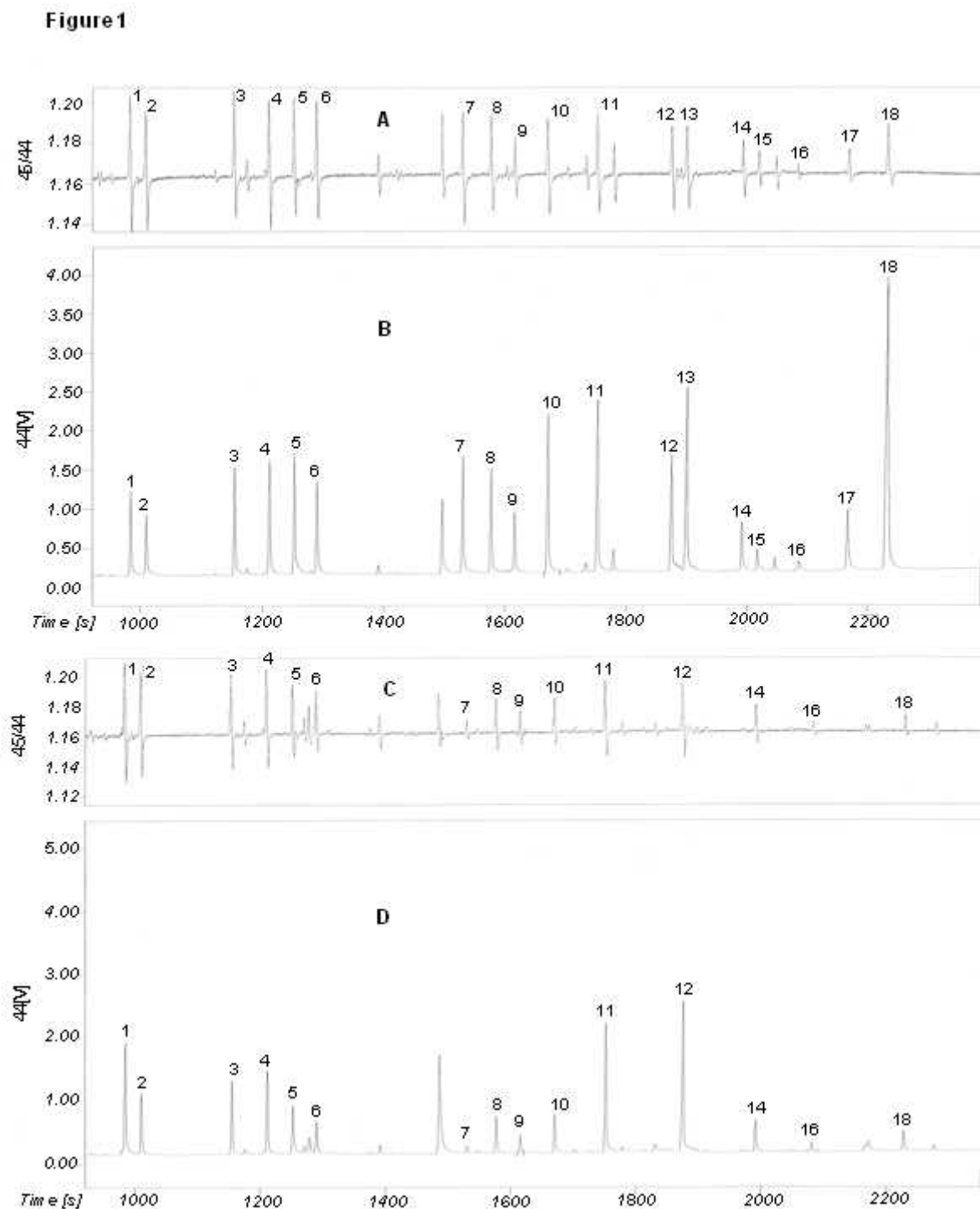


**Figure 1:** GC-C-IRMS chromatogram of the  $\delta^{13}\text{C}$  analysis of *t*-butyl-dimethylsilyl (*t*-BDMS) derivatives of amino acids. **A, B:** Standard amino acid mixture (Sigma-Aldrich);

## Analysis of $^{13}\text{C}$ enrichment using GC-C-IRMS

---

**C, D:** proteinogenic amino acids from biomass hydrolyzate of *C. glutamicum*. **B** and **D** show the  $m/z$  44 ion current while **A** and **C** depicts the  $m/z$  45/44 ratio traces of the analyte. Peak identities: 1-alanine; 2-glycine; 3-valine; 4-leucine; 5-isoleucine; 6-proline; 7-methionine; 8-serine; 9-threonine; 10-phenylalanine; 11-aspartic acid; 12-glutamic acid; 13-asparagine; 14-lysine; 15-glutamine; 16-arginine; 17-histidine; 18-tyrosine. The amino acids cysteine, tryptophan are oxidized during the hydrolysis process, whereas asparagine and glutamine are deaminated to yield aspartic acid and glutamic acid. The latter peaks are therefore the sum of the acid and its corresponding amide.

also clearly did not show any background noise. Another prerequisite for the development of a robust analytical method is the efficient separation of the amino acids in crude biomass hydrolyzate. As can be seen in the Figure. 1 (C, D) the  $m/z$  44 and the  $m/z$  45/44 ratio traces did not exhibit any interfering peaks. Excellent sensitivity of the method was observed considering that the peak signals yielded from 2 C-nmol of sample injected into the GC-C-IRMS reflect the proteinogenic amino acids from only 50 ng of biomass.

The precision of the measured  $\delta^{13}\text{C}$  values from GC-C-IRMS for proteinogenic amino acids is shown in Table 2. These errors include also biological variation using two parallel cell shake-flask cultures. This relative variation in  $^{13}\text{C}$  fraction can be considered in the simulation model for calculating the fluxes.

**Linearity and measurement range.** For the intended application of GC-C-IRMS measurements to metabolic flux analysis it is important to characterize the measurement range and to check the linearity because they are directly influencing the required degree of substrate labelling, the most dominant factor for the cost of such experiments. Linearity and measurement range were investigated using different mixtures of [ $1-^{13}\text{C}$ ] alanine and alanine with natural isotope abundance (range: 0 to 0.05 % [ $1-^{13}\text{C}$ ] alanine). An enrichment as low as 0.0001 atom % excess could be detected in the measured  $\text{CO}_2$ . Figure 2 displays the observed relation between the theoretical and the measured enrichment in  $\text{CO}_2$  resulting from the combustion of alanine. The linear regression analysis of the calibration curve indicated a statistically significant linear relationship ( $R^2=0.9995$ ) over the whole range tested.

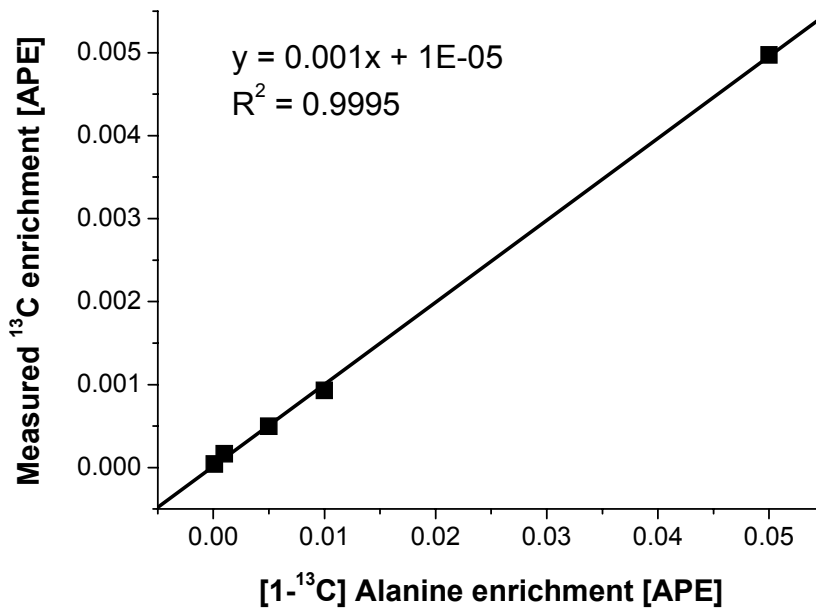


**Figure 2:** Measurement of  $^{13}\text{C}$  fraction of alanine measured by GC-C-IRMS as function of  $[1-^{13}\text{C}]$  alanine fraction applied.

$^{13}\text{C}$  analysis of biomass hydrolyzate from tracer studies with varied  $^{13}\text{C}$  enrichment of tracer substrate. *Corynebacterium glutamicum* was cultivated in parallel with different fractions of  $[1-^{13}\text{C}]$  glucose and glucose with natural carbon isotope abundance (range: 0.5 % to 10 %  $[1-^{13}\text{C}]$  glucose). The average initial cell concentration ( $\text{OD}_{660}$ ) of all the six flasks was  $0.14 \pm 0.01$ . Identical growth was observed in all the flasks with a specific growth rate of  $0.42 \text{ h}^{-1}$ . Protein hydrolyzates from each flask were derivatized and analyzed by GC-C-IRMS.

## Analysis of $^{13}\text{C}$ enrichment using GC-C-IRMS

**Table 1:** Experimental  $\delta$  values of different proteinogenic amino acids from a *C. glutamicum* culture grown on glucose with a natural carbon isotope abundance, its corrections for the contribution of carbon atoms from derivatization reagent and final corrected fractional  $^{13}\text{C}$  of the analyte.

Amino Acid	$\delta$ (‰) <sup>a</sup>	$R_A$ <sup>b</sup>	$^{13}F_{i,nat}$ <sup>c</sup> (Uncorrected)	$N_{Car}^A$ <sup>d</sup>	$N_{Car}^D$ <sup>e</sup>	$^{13}F_{i,nat}$ <sup>f</sup> (Corrected)
<b>Alanine</b>	-25.92	0.01095	0.01083	3	12	0.00983
<b>Glycine</b>	-27.86	0.01092	0.01081	2	12	0.00917
<b>Valine</b>	-25.31	0.01095	0.01083	5	12	0.01025
<b>Leucine</b>	-23.65	0.01097	0.01085	6	12	0.01040
<b>Isoleucine</b>	-22.64	0.01098	0.01086	6	12	0.01043
<b>Proline</b>	-22.06	0.01099	0.01087	5	12	0.01037
<b>Methionine</b>	-25.07	0.01096	0.01084	5	12	0.01026
<b>Serine</b>	-25.21	0.01095	0.01084	3	18	0.00938
<b>Threonine</b>	-25.45	0.01095	0.01083	4	18	0.00973
<b>Phenylalanine</b>	-22.82	0.01098	0.01086	9	12	0.01057
<b>Aspartic acid</b>	-25.66	0.01095	0.01083	4	18	0.00972
<b>Glutamic acid</b>	-24.89	0.01096	0.01084	5	18	0.01000
<b>Lysine</b>	-25.16	0.01095	0.01084	6	18	0.01011
<b>Arginine</b>	-27.31	0.01093	0.01081	6	18	0.01002
<b>Histidine</b>	-21.67	0.01099	0.01087	6	18	0.01026
<b>Tyrosine</b>	-24.80	0.01096	0.01084	9	18	0.01036

<sup>a</sup> Experimental  $\delta$  values obtained from the measurements

<sup>b</sup> Calculated  $^{13}\text{C}/^{12}\text{C}$  ratio from the experimental  $\delta$  values

<sup>c</sup> Uncorrected  $^{13}\text{C}$  fraction of the analyte

<sup>d</sup> Number of carbon atoms in the amino acid

<sup>e</sup> Number of carbon atoms from the derivatization agent

<sup>f</sup> Corrected  $^{13}\text{C}$  fraction of the analyte

**Table 2:**  $^{13}\text{C}$  fractional enrichment and standard deviation of selected proteinogenic amino acids after correction of carbon contribution from derivatization reagent at different fractions of  $[1-^{13}\text{C}]$  glucose used. Measured  $\delta^{13}\text{C}$  values are listed in Table A1.

[1- $^{13}\text{C}$ ] glucose fraction (%) <sup>a</sup>	0 <sup>b</sup>		0.49 <sup>a</sup>		0.99 <sup>a</sup>		1.98 <sup>a</sup>		9.85 <sup>a</sup>	
	mean	sdev	mean	sdev	Mean	sdev	mean	sdev	mean	sdev
Alanine	0.983%	5.75E-05	1.090%	3.89E-07	1.180%	1.01E-05	1.400%	1.63E-04	3.150%	2.31E-03
Glycine	0.918%	9.31E-06	0.924%	3.45E-05	0.936%	4.95E-05	0.962%	7.75E-05	1.060%	2.17E-04
Serine	0.938%	2.34E-05	1.010%	4.09E-05	1.070%	2.94E-06	1.210%	9.97E-05	2.300%	1.24E-03
Phenylalanine	1.060%	2.24E-05	1.110%	3.23E-05	1.150%	1.01E-05	1.260%	8.74E-05	2.040%	8.63E-04
Aspartic acid/Asparagine	0.972%	3.32E-05	1.060%	2.79E-05	1.130%	6.79E-06	1.310%	1.33E-04	2.680%	1.47E-03
Glutamic acid/Glutamine	0.998%	4.32E-05	1.090%	3.04E-05	1.170%	9.22E-06	1.360%	1.41E-04	2.850%	1.62E-03

<sup>a</sup>  $[1-^{13}\text{C}]$  glucose used for cultivation; <sup>b</sup> Culture grown with naturally labeled carbon source.

**Table 3:**  $^{13}\text{C}$  enrichment of selected proteinogenic amino acids and standard deviation at different fractions of  $[1-^{13}\text{C}]$  glucose used after subtraction of carbon enrichment of glucose with a natural carbon isotope abundance using equation (16). Standard deviations were calculated using equation (17)

$[1-^{13}\text{C}]$ glucose fraction (%) <sup>a</sup>	0.49		0.99		1.98		9.85	
	Mean (APE)	sdev						
Alanine	0.1050	5.75E-05	0.1980	5.84E-05	0.4160	1.73E-04	2.1700	2.31E-03
Glycine	0.0067	3.57E-05	0.0184	5.03E-05	0.0443	7.81E-05	0.1380	2.18E-04
Serine	0.0700	4.71E-05	0.1300	2.36E-05	0.2680	1.02E-04	1.3600	1.24E-03
Phenylalanine	0.0499	3.93E-05	0.0951	2.46E-05	0.1980	9.02E-05	0.9870	8.64E-04
Aspartic acid/Asparagine	0.0854	4.34E-05	0.1630	3.39E-05	0.3370	1.37E-04	1.7000	1.47E-03
Glutamic acid/Glutamine	0.0929	5.28E-05	0.1770	4.42E-05	0.3660	1.47E-04	1.8500	1.62E-03

<sup>a</sup>  $[1-^{13}\text{C}]$  glucose used in the cultivation.

# Analysis of $^{13}\text{C}$ enrichment using GC-C-IRMS

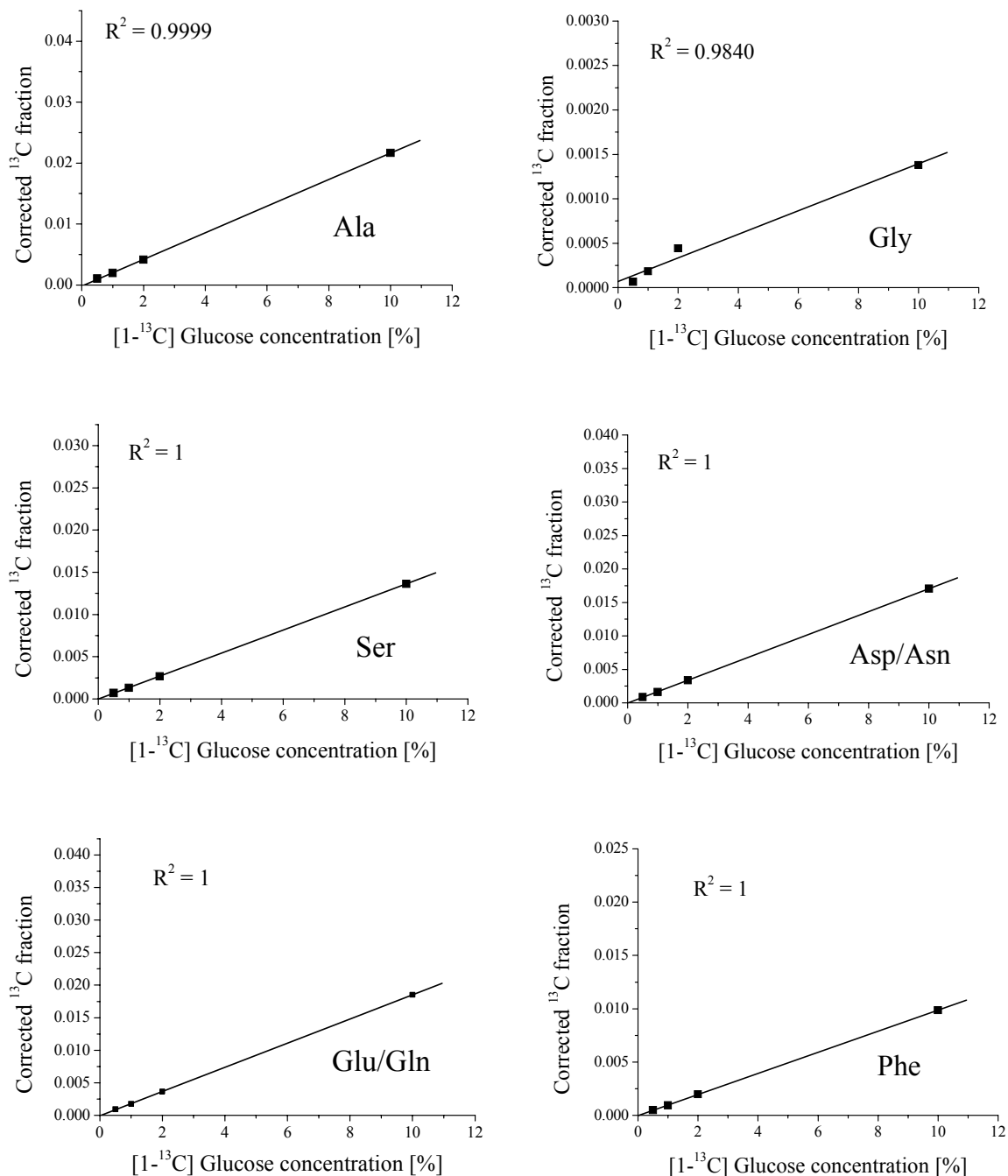


**Figure 3:** Regression analysis curves and its correlation coefficients of the corrected  $^{13}\text{C}$  enrichment ( $^{13}F_i = ^{13}F_{i,tot} - ^{13}F_{i,nat}$ ), of proteinogenic amino acid alanine, glycine, serine, phenylalanine, aspartic acid/asparagine and glutamic acid/glutamine, against fraction of applied  $[1-^{13}\text{C}]$  glucose. Measurements are from parallel cultures of *C. glutamicum* using identical inoculum.

## Analysis of $^{13}\text{C}$ enrichment using GC-C-IRMS

---

Table 1 shows experimental  $\delta^{13}\text{C}$  values and calculated enrichment values,  $^{13}\text{F}_{i, \text{nat}}$ , from a culture grown on glucose with a natural carbon isotope abundance. The bias introduced by the derivatization agent is corrected for as given in the rightmost column. The obtained values are significantly different for different amino acids, which are caused by kinetic isotopic effects in the enzymatic reaction of the different biosynthetic pathways.

For identifying the required minimum fraction of  $[1-^{13}\text{C}]$  glucose for metabolic flux analysis, experiments with 0.5 % to 10 % of the labeled glucose were compared. For this purpose, six amino acids were selected according to their information content for flux analysis. Table 2 lists the measured  $^{13}\text{C}$  fractions of selected amino acids at different fractions of tracer substrate corrected for the naturally labeled carbon introduced by derivatization. First, it can be seen from the table that the corrected fractional  $^{13}\text{C}$  content is increasing with increasing fractions of  $[1-^{13}\text{C}]$  glucose. Secondly, the amino acids have different  $^{13}\text{C}$  fractional enrichment values. The  $^{13}\text{C}$  fractional enrichment of the metabolites is a function of the network activity distribution and also of kinetic isotope effects in the metabolic network investigated. Therefore it is essential for later flux estimation to dissect these two effects.

After subtraction of the  $^{13}\text{C}$  fractional enrichment of the experiment with natural glucose from that of the labeling experiments using equation (16), mean values and standard deviations listed in Table 3 were obtained. From these results it is evident that statistical differences between the different proteinogenic amino acids can be observed. Figure 3 displays the dependency of these corrected mean values of  $^{13}\text{C}$  fractional enrichment on the fractions of  $[1-^{13}\text{C}]$  glucose in the glucose feed. Obviously a linear increase in measured fractional enrichment of various important amino acids with increase in fractions of  $[1-^{13}\text{C}]$  labeled carbon source resulted in curves running through the origin. The calculated correlation factor of the curves was 1 for serine, phenylalanine, aspartic acid/asparagine, glutamic acid/glutamine, 0.9999 for alanine and 0.9840 for glycine. Good reproducibility, repeatability and linearity were thus observed even at low fractions of tracer substrate used.

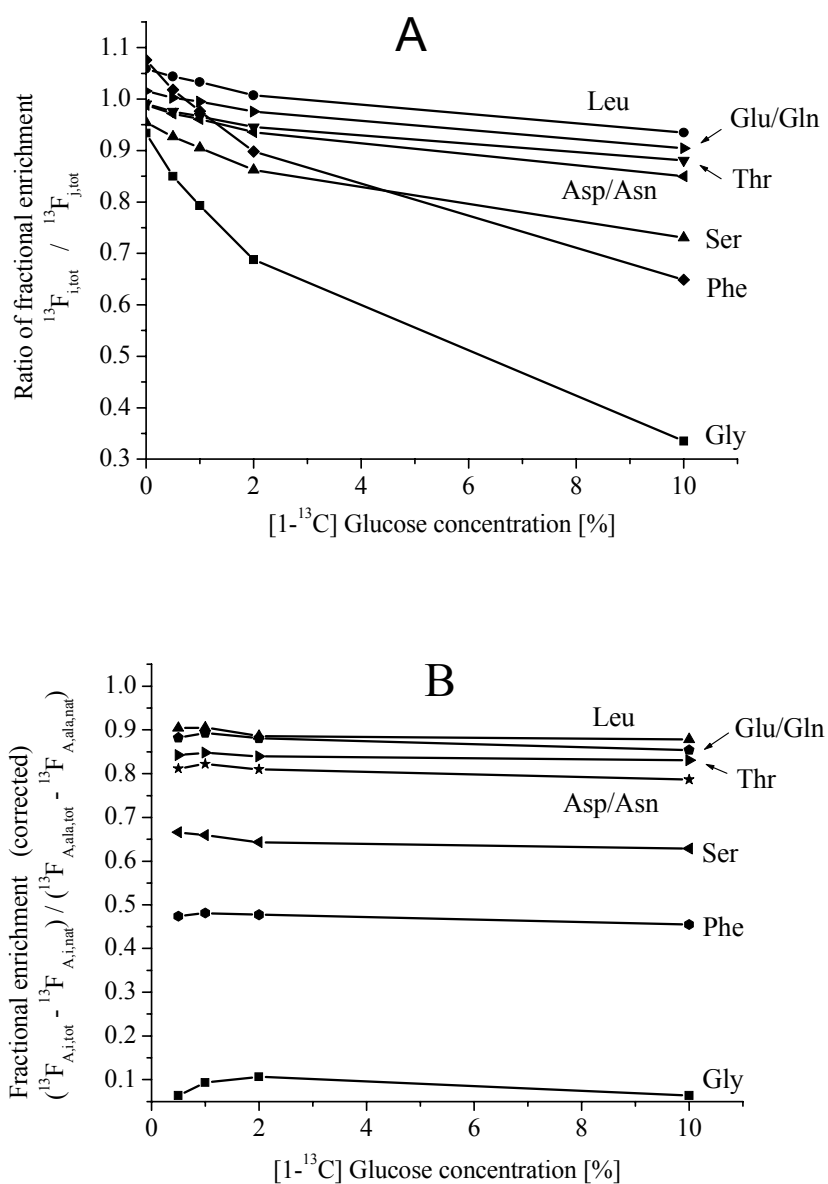


Figure 4: Ratio of fractional enrichments of proteinogenic amino acids as function of fraction of [1- $^{13}\text{C}$ ] glucose fed. A-ratios ( $\frac{{}^{13}\text{F}_{i,\text{tot}}}{{}^{13}\text{F}_{\text{ala,tot}}}$ ) of gly, ser, phe, asp/asn, leu, thr and glu/gln to that of ala, (uncorrected). B-ratios ( $\frac{({}^{13}\text{F}_{i,\text{tot}} - {}^{13}\text{F}_{i,\text{nat}})}{({}^{13}\text{F}_{\text{ala,tot}} - {}^{13}\text{F}_{\text{ala,nat}})}$ ) after subtraction of enrichment in sample where only glucose with a natural carbon isotope abundance was fed, (corrected).

## Analysis of $^{13}\text{C}$ enrichment using GC-C-IRMS

---

The importance of correcting for kinetic isotope is seen in Figure. 4A, where ratios of  $^{13}\text{C}$  enrichments for various amino acids to that of alanine are plotted. Increasing fractions of labeled glucose caused a significant variation of this ratio different for each amino acid. These results indicate that kinetic isotope effects exist certainly in experiments with fractional labeling below 10 % [ $1\text{-}^{13}\text{C}$ ] glucose fed. If similar ratios are calculated after subtraction of the  $^{13}\text{C}$  enrichments in natural glucose feeding experiments using equation (16), their values remain practically constant, irrespective of the applied [ $1\text{-}^{13}\text{C}$ ] glucose fraction in feed (Figure. 4B). Same results are obtained when plotting ratios to other amino acids. This is a good indication that under these conditions kinetic isotope effects from natural carbon atoms can be compensated for by subtracting the fractional enrichment values of the growth experiment with natural glucose from those obtained from a labeled culture using equation 16. This also indicates that only primary kinetic isotope effects as discussed above are relevant under these conditions.

### 2.5 Conclusion

The obtained results show that a combination of GC-C-IRMS and correction of kinetic isotope effects as presented here provide a sound basis for  $^{13}\text{C}$  metabolic flux analysis. The reliability and precision of this procedure allows the detection of low enrichment of  $^{13}\text{C}$  in various metabolites. Thus, the amount of the metabolic tracer can be decreased without affecting the precision of the results too much down to an application of about 0.5 % [ $1\text{-}^{13}\text{C}$ ] glucose in the cultivation of *Corynebacterium glutamicum*. Correction for kinetic isotope effects can be made based on the measurement of  $^{13}\text{C}$  fractional enrichment of detected proteinogenic amino acids obtained in experiments with natural glucose and those of the labeling experiments. The developed method can be implemented for stable isotope analysis of various amino acids as well as for important carbohydrates employing different derivatization procedures and respective gas chromatography parameters. The analysis is simple and has a high precision even at low labeling of tracer substrates. The method can detect enrichments that are 200-300 times lower than those routinely measured using conventional GC-MS. This cuts down the cost of tracer substrate used for experiments. The present developed methodology will be a novel technique for studying the metabolic fluxes of industrially relevant organisms directly at larger scale. Scale-up of fermentations is still very empirical and extrapolations to other scales

usually have a very low reliability. Uncertainties related to scale-up could be ruled out by conducting  $^{13}\text{C}$  metabolic flux analysis directly at the desired scale. In addition, this technique has a further potential application in fed-batch fermentations.

### References:

- Aguilera R, Chapman TE, Catlin DH. 2000. A rapid screening assay for measuring urinary androsterone and etiocholanolone  $\delta(13)\text{C}$  ( per thousand) values by gas chromatography/combustion/isotope ratio mass spectrometry. *Rapid Commun Mass Spectrom* 14(23):2294-9.
- Behrens A, Schaeffer P, Bernasconi S, Albrecht P. 2000. Mono- and bicyclic squalene derivatives as potential proxies for anaerobic photosynthesis in lacustrine sulfur-rich sediments. *Geochimica et Cosmochimica Acta* 64(19):3327-3336.
- Bourne JR, Zurita EP, Heinzle E. 1992. Bioreactor Scale-up for the Oxygen-Sensitive Culture *Bacillus-Subtilis* - the Influence of Stirrer Shaft Geometry. *Biotechnology Progress* 8(6):580-582.
- Brand WA. 1996. High precision isotope ratio monitoring techniques in mass spectrometry. *J Mass Spectrom* 31(3):225-35.
- Brenna JT, Corso TN, Tobias HJ, Caimi RJ. 1997. High-precision continuous-flow isotope ratio mass spectrometry. *Mass Spectrom Rev* 16(5):227-58.
- Christensen B, Nielsen J. 1999. Isotopomer analysis using GC-MS. *Metab Eng* 1(4):282-90.
- Coplen TB, Brand WA, Gehre M, Groning M, Meijer HA, Toman B, Verkouteren RM. 2006. After two decades a second anchor for the VPDB  $\delta 13\text{C}$  scale. *Rapid Commun Mass Spectrom* 20(21):3165-6.
- Derrien D, Balesdent J, Marol C, Santaella C. 2003. Measurement of the  $13\text{C}/12\text{C}$  ratio of soil-plant individual sugars by gas chromatography/combustion/isotope-ratio mass spectrometry of silylated derivatives. *Rapid Commun Mass Spectrom* 17(23):2626-31.

## Analysis of $^{13}\text{C}$ enrichment using GC-C-IRMS

---

- Docherty G, Jones V, Evershed RP. 2001. Practical and theoretical considerations in the gas chromatography/combustion/isotope ratio mass spectrometry  $\delta(13)\text{C}$  analysis of small polyfunctional compounds. *Rapid Commun Mass Spectrom* 15(9):730-8.
- El Massaoudi M, Spelthahn J, Drysch A, de Graaf A, Takors R. 2003. Production process monitoring by serial mapping of microbial carbon flux distributions using a novel sensor reactor approach: I--Sensor reactor system. *Metab Eng* 5(2):86-95.
- Fiaux J, Cakar ZP, Sonderegger M, Wuthrich K, Szyperski T, Sauer U. 2003. Metabolic-flux profiling of the yeasts *Saccharomyces cerevisiae* and *Pichia stipitis*. *Eukaryot Cell* 2(1):170-80.
- G.N.Stephanopoulos, A.A. Aristidou, Jens Høiriis Nielsen, Jens Nielsen. 1998. *Metabolic Engineering: Principles and Methodologies*. San Diego, CA, USA.
- Godin JP, Fay LB, Hopfgartner G. 2007. Liquid chromatography combined with mass spectrometry for  $^{13}\text{C}$  isotopic analysis in life science research. *Mass Spectrom Rev* 26(6):751-74.
- Huang MC, Muddana S, Horowitz EN, McCormick CC, Infante JP, Brenna JT. 2000. High-precision isotope ratio mass spectrometry and stable isotope precursors for tracer studies in cell culture. *Analytical Biochemistry* 287(1):80-86.
- Ishiwatari R, Uzaki M, Yamada K. Carbon isotope composition of individual n-alkanes in recent sediments. *Organic Geochemistry* 21(6-7):801-808.
- Jim S, Jones V, Copley MS, Ambrose SH, Evershed RP. 2003. Effects of hydrolysis on the  $\delta^{13}\text{C}$  values of individual amino acids derived from polypeptides and proteins. *Rapid Commun Mass Spectrom* 17(20):2283-9.
- K. van't Riet JT. 1991. *Basic Bioreactor Design*. New York: M. Dekker.
- K.J.R. Rosman PDPT. 1997. *Isotopic compositions of the elements: IUPAC*.
- Kelleher JK. 2001. Flux estimation using isotopic tracers: common ground for metabolic physiology and metabolic engineering. *Metab Eng* 3(2):100-10.
- Kumar S, Wittmann C, Heinzle E. 2004. Minibioreactors. *Biotechnology Letters* 26(1):1-10.
- Maaheimo H, Fiaux J, Cakar ZP, Bailey JE, Sauer U, Szyperski T. 2001. Central carbon metabolism of *Saccharomyces cerevisiae* explored by biosynthetic fractional C-13 labeling of common amino acids. *European Journal of Biochemistry* 268(8):2464-2479.
- Meier-Augenstein W. 1999a. Applied gas chromatography coupled to isotope ratio mass spectrometry. *Journal of Chromatography A* 842(1-2):351-371.

## Analysis of $^{13}\text{C}$ enrichment using GC-C-IRMS

---

- Meier-Augenstein W. 1999b. Use of gas chromatography-combustion-isotope ratio mass spectrometry in nutrition and metabolic research. *Curr Opin Clin Nutr Metab Care* 2(6):465-70.
- Menand C, Pouteau E, Marchini S, Maugere P, Krempf M, Darmaun D. 1997. Determination of low  $^{13}\text{C}$ -glutamine enrichments using gas chromatography-combustion-isotope ratio mass spectrometry. *J Mass Spectrom* 32(10):1094-9.
- Michael Dauner US. 2000. GC-MS Analysis of Amino Acids Rapidly Provides Rich Information for Isotopomer Balancing. *Biotechnology Progress* 16(4):642-649.
- P.A. Lessard SG, L.B. Willis, A.J. Sinskey. 1999. *Encyclopedia of Bioprocess Technology: Fermentation, Biocatalysis, and Bioseparation*. M.C. Flickinger SWD, editor. New York: John Wiley and Sons Inc. 729-740 p.
- Reijngoud DJ, Hellstern G, Elzinga H, de Sain-van der Velden MG, Okken A, Stellaard F. 1998. Determination of low isotopic enrichment of L-[1- $^{13}\text{C}$ ]valine by gas chromatography combustion isotope ratio mass spectrometry: a robust method for measuring protein fractional synthetic rates in vivo. *Journal of Mass Spectrometry* 33(7):621-626.
- Rieley G. 1994. Derivatization of Organic-Compounds Prior to Gas-Chromatographic Combustion-Isotope Ratio Mass-Spectrometric Analysis - Identification of Isotope Fractionation Processes. *Analyst* 119(5):915-919.
- S. Aiba, A.E. Humphrey, N.F. Millis. 1973. *Biochemical Engineering: Translation of Laboratory culture results to plant operation*. New York and London: Academic press. 218-237 p.
- Sauer U, Hatzimanikatis V, Bailey JE, Hochuli M, Szyperski T, Wuthrich K. 1997. Metabolic fluxes in riboflavin-producing *Bacillus subtilis*. *Nature Biotechnology* 15(5):448-452.
- Schmidt TC, Zwank L, Elsner M, Berg M, Meckenstock RU, Haderlein SB. 2004. Compound-specific stable isotope analysis of organic contaminants in natural environments: a critical review of the state of the art, prospects, and future challenges. *Anal Bioanal Chem* 378(2):283-300.
- Slater C, Preston T, Weaver LT. 2001. Stable isotopes and the international system of units. *Rapid Commun Mass Spectrom* 15(15):1270-3.
- Stott AW, Evershed RP. 1996.  $\delta^{13}\text{C}$  analysis of cholesterol preserved in archaeological bones and teeth. *Anal Chem* 68(24):4402-8.

## Analysis of $^{13}\text{C}$ enrichment using GC-C-IRMS

---

- Vallino JJ, Stephanopoulos G. 1993. Metabolic Flux Distributions in *Corynebacterium glutamicum* during Growth and Lysine Overproduction. *Biotechnology and Bioengineering* 41(6):633-646.
- Wittmann C. 2002. Metabolic Flux Analysis Using Mass Spectrometry. *Tools and Applications of Biochemical Engineering Science*. p 39-64.
- Wittmann C, Becker J. 2007. The L-Lysine Story: From Metabolic Pathways to Industrial Production. *Amino Acid Biosynthesis ~ Pathways, Regulation and Metabolic Engineering*. p 39-70.
- Wittmann C HE. 2008. Metabolic Network Analysis and Design in *Corynebacterium glutamicum*. In: *Corynebacteria. Genomics and Molecular Biology* (Ed. A. Burkovski) Caister. Norfolk UK: Academic Press. 79-112 p.
- Wittmann C, Heinzle E. 1999. Mass spectrometry for metabolic flux analysis. *Biotechnology and Bioengineering* 62(6):739-750.
- Wittmann C, Heinzle E. 2001. Application of MALDI-TOF MS to lysine-producing *Corynebacterium glutamicum* - A novel approach for metabolic flux analysis. *European Journal of Biochemistry* 268(8):2441-2455.
- Wittmann C, Heinzle E. 2002. Genealogy profiling through strain improvement by using metabolic network analysis: Metabolic flux genealogy of several generations of lysine-producing corynebacteria. *Applied and Environmental Microbiology* 68(12):5843-5859.
- Yang TH, Frick O, Heinzle E. 2008. Hybrid optimization for C-13 metabolic flux analysis using systems parametrized by compactification. *Bmc Systems Biology* 2:-.
- Yang TH, Wittmann C, Heinzle E. 2003. Dynamic calibration and dissolved gas analysis using membrane inlet mass spectrometry for the quantification of cell respiration. *Rapid Communications in Mass Spectrometry* 17(24):2721-2731.

## Appendix

Table A1. Measured  $\delta^{13}\text{C}$  of selected proteinogenic amino acids at different fractions of [ $1\text{-}^{13}\text{C}$ ] glucose used.

[ $1\text{-}^{13}\text{C}$ ] glucose fraction (%)	0 <sup>a</sup>	0.49 <sup>b</sup>	0.99 <sup>b</sup>	1.98 <sup>b</sup>	9.85 <sup>b</sup>
Alanine	-25.93	-6.78	10.05	49.75	370.10
Glycine	-27.86	-27.00	-25.47	-22.11	-9.95
Serine	-25.21	-16.10	-8.27	9.55	152.21
Phenylalanine	-22.82	-3.37	14.28	54.60	363.41
Aspartic acid/Asparagine	-25.66	-11.53	1.24	30.04	257.13
Glutamic acid/Glutamine	-24.89	-6.52	10.03	47.57	342.65

<sup>a</sup> [ $1\text{-}^{13}\text{C}$ ] glucose used for cultivation; <sup>b</sup> Culture grown with naturally labeled carbon source.

## Chapter 3

# <sup>13</sup>C Metabolic Flux Analysis for Larger-Scale Cultivation Using GC-C-IRMS

### Abstract

<sup>13</sup>C-based metabolic flux analysis (<sup>13</sup>CMFA) is limited to smaller scale experiments due to very high costs of labeled substrates. We measured <sup>13</sup>C enrichment in proteinogenic amino acid hydrolyzates using gas chromatography-combustion-isotope ratio mass spectrometry (GC-C-IRMS) from a series of parallel batch cultivations of *Corynebacterium glutamicum* utilizing mixtures of natural glucose and [1-<sup>13</sup>C] glucose, containing 0, 0.5, 1, 2, and 10% [1-<sup>13</sup>C] glucose. Decreasing the [1-<sup>13</sup>C] glucose content, kinetic isotope effects played an increasing role but could be corrected. From the corrected <sup>13</sup>C enrichments *in vivo* fluxes in the central metabolism were determined by numerical optimization. The obtained flux distribution was very similar to those obtained from parallel labeling experiments using conventional high labeling GC-MS method and to published results. The GC-C-IRMS-based method involving low labeling degree of expensive tracer substrate, e.g. 1%, is well suited for larger laboratory and industrial pilot scale fermentations.

This chapter has been published as : Yuan Y, Yang TH, Heinzle E. 2010. C-13 metabolic flux analysis for larger scale cultivation using gas chromatography-combustion-isotope ratio mass spectrometry. *Metabolic Engineering* 12(4):392-400.

## 3.1 Introduction

The quantitative analysis of *in vivo* carbon fluxes in a metabolic network is regarded a powerful tool for the optimization of industrial organisms (Bailey 1991; Nielsen and Jewett 2008). Developed from the previous methods using only metabolite balancing, flux estimation has been far advanced by supplementing the previous stoichiometry-based approach with isotopomer balances to overcome shortcomings of the previous method in many real-case situations (Antoniewicz et al. 2007; Iwatani et al. 2008; Schmidt et al. 1997; Schmidt et al. 1998; Wiechert 2001; Wiechert and de Graaf 1996; Wittmann and Heinzle 2008).

Theoretically, the most complete information would be obtained by the analysis of all extracellular and intracellular metabolite isotopomers. Unfortunately, it is highly challenging to analyze all positional isotopomers in practice, e.g., using nuclear magnetic resonance spectroscopy (NMR) techniques, and also the information content finally depends on measurement sensitivity. The much more efficient way is to determine mass isotopomers using mass spectrometry (MS), which outperforms NMR with respect to sensitivity, as well as precision (Haunschild et al. 2005; Wittmann and Heinzle 1999a). Thus, diverse MS-based analytical techniques have been developed for the mass isotopomer analysis (Haunschild et al. 2005; Yang et al. 2009). For <sup>13</sup>C-based metabolic flux analysis (<sup>13</sup>CMFA), the mass isotopomers of intracellular, extracellular metabolites, and/or biomass constituents can be used. The analysis of intracellular metabolites is often challenging, e.g., due to low concentrations close to or below detection limits as well as often limited stability and short time constants of certain compounds such as glycolytic metabolites. Amino acids contained in cellular proteins reflect the labeling patterns of various central key metabolites at steady state. They can be easily analyzed by NMR (Maaheimo et al. 2001; Marx et al. 2003; Sauer et al. 1997), gas chromatography-mass spectrometry (GC-MS) (Becker et al. 2007; Becker et al. 2008b; Christensen and Nielsen 1999; Dauner and Sauer 2000; Hans et al. 2001; Wittmann 2007), or matrix-assisted laser desorption/ionization time-of-flight mass spectrometry (MALDI-TOF MS) (Wittmann and Heinzle 2001a). Methods have been developed to take into account natural isotope abundances of the analytes (Wittmann and Heinzle 1999a; Yang et al. 2009). In recent years, the combination of GC-MS and parameter estimation methods using network simulation techniques has been well developed and most frequently applied in metabolic flux

analysis (Antoniewicz et al. 2007; Dauner and Sauer 2000; Nanchen et al. 2007; Schmidt et al. 1998; Wittmann 2007; Yang et al. 2008; Yang et al. 2004).

Another challenge in <sup>13</sup>C-based metabolic flux analysis is that experiments are limited to small scales. So far labeling experiments have been restricted to laboratory-scale fermentation, shake flasks, and microtiter plates (Velagapudi et al. 2007; Wittmann et al. 2004) due to the requirement for high degree of <sup>13</sup>C-labeled substrate (generally 100% tracer substrate) and the resulting high cost. Experiments on a laboratory scale, however, cannot usually represent conditions on much larger scales that are industrially much more relevant. In this regard, a method of <sup>13</sup>CMFA applicable to large-scale biotechnological processes is highly desired. Hereto, applying a small amount of isotopic tracer substrates for labeling experiments is a possible solution, yet it leads to extremely low <sup>13</sup>C enrichments of labeling in proteinogenic amino acids and, consequently, a poor flux resolution. Since <sup>13</sup>C isotopic enrichments in amino acids in proteins is usually low (0.001-0.05 atom percent excess-APE) as determined in protein turnover experiments (Godin et al. 2007a), the labeling patterns of metabolites cannot reliably be measured by GC-MS, which has a measurable range of only higher than 0.5 APE (Meier-Augenstein 1999b). In contrast, GC-C-IRMS is capable of measuring isotopic composition at low enrichment and even natural abundance level (-0.1 to +2.0 APE) with high precision (0.0002 APE) and accuracy (Meier-Augenstein 1999b). Thus, GC-C-IRMS has a great potential for the application to cases with extremely low <sup>13</sup>C enrichments in metabolites.

Since the first report of determination of the  $\delta^{13}\text{C}$  values of individual amino acid from the Murchison meteorite using GC-C-IRMS (Engel et al. 1990), this analytical technique has been widely adopted as a strategy using an identified amino acid as marker for the study of turnover and synthesis rates of proteins (de Sain-van der Velden et al. 1998; Reijngoud et al. 1998a) and other metabolic and nutritional research due to its high-precision and reliability for low <sup>13</sup>C enrichment detection (Meier-Augenstein 1999b; Meier-Augenstein et al. 1995). In recent years, more efforts have been put to the optimization of derivatization procedures (Corr et al. 2007; Godin et al. 2007a), and a new correction approach was introduced for the elimination of kinetic isotope effects to improve the accuracy of isotopic measurement (Heinzle et al. 2008a). High chromatographic resolution of amino acids, high precision of isotopic measurement, and high reliability make this technique potentially very suitable for the <sup>13</sup>C

labeling experiments involving just a small amount of <sup>13</sup>C-tracers, e.g., in a large scale fermentation, where extremely low <sup>13</sup>C labeling enrichments in metabolites are expected.

To prove our concept, we implemented <sup>13</sup>C labeling experiments using different content of <sup>13</sup>C glucose mixed with non-labeled glucose. Cultivations were carried out using *Corynebacterium glutamicum* which is the most important bacterium for the production of amino acids in industry. In our former study (Heinzle et al. 2008a), an experimental protocol to measure <sup>13</sup>C fractional enrichments in proteinogenic amino acids by GC-C-IRMS was developed, and a method for the correction of isotope kinetic isotopic effects was established. Based on the protocol, the <sup>13</sup>C fractional enrichment data were corrected from GC-C-IRMS measurements, and applied to <sup>13</sup>CMFA to verify the potential of GC-C-IRMS for an industrial scale <sup>13</sup>CMFA. Results were compared with those from conventional <sup>13</sup>CMFA using 99% [1-<sup>13</sup>C]glucose and GC-MS as well as with literature values.

### 3.2 Materials and Methods

#### 3.2.1 Reagents.

[1-<sup>13</sup>C] glucose (99 atom-% <sup>13</sup>C) was purchased from Cambridge Isotope Laboratories Inc. (Andover, USA). All other chemicals were from Sigma-Aldrich (St. Louis, USA). For all experiments the same batch of chemicals was used.

#### 3.2.2 Microorganism

*C. glutamicum* ATCC 13032 wild type was purchased from the American Type Strain and Culture Collection (Manassas, USA).

#### 3.2.3 Growth and labeling of *C. glutamicum*

*C. glutamicum* ATCC 13032 was cultivated in 25 ml baffled shake flasks, cultivations with low fractions of [1-<sup>13</sup>C] glucose from 0 to 10% were already described previously (Heinzle et al. 2008a). In parallel, experiments with high fractions of mixtures of [1-<sup>13</sup>C] glucose (99% isotope purity) and natural labeled glucose, 20, 50, 80, and 100% (w/w) [1-<sup>13</sup>C] glucose were also carried out for reference.

### 3.2.4 Sample preparation for labeling analysis

For both GC-MS and GC-C-IRMS, the sample preparation and the derivatization procedures were identical as described previously elsewhere (Heinzle et al. 2008a).

### 3.2.5 Analytics

Mass isotopomer distributions of proteinogenic amino acids and of trehalose from the culture medium were measured by GC-MS. The quantitative measurements of glucose, glycerol, dihydroxyacetone and organic acids were performed by HPLC (Kontron Instruments, Neufahrn, Germany) with an Aminex HPX 87-H column (Biorad). Quantification of free extracellular amino acids was carried out by HPLC (Kontron Instruments, Neufahrn, Germany) with precolumn OPA derivatization. Cell concentration was assessed by a spectrophotometer at 660 nm (Pharmacia Biotech, Novaspec II, Cambridge, England) and dry weight analysis. The correlation factor between dry biomass and  $D_{660}$  was determined as 0.353 g dry biomass per unit at  $D_{660}$ . Each measurement was performed at least in triplicate.

### 3.2.6 GC-C-IRMS

<sup>13</sup>C fractional enrichments from five samples of low [ $1-^{13}\text{C}$ ] glucose labeling cultivations were measured on a GC-C-IRMS instrument equipped with an HP6890 gas chromatograph (Agilent 6890, Agilent Technologies, Palo Alto, CA, USA), a standard GC/C III interface with a Ni/Cu/Pt combustion reactor operated at 940 °C (Thermo Fisher Scientific, Bremen, Germany) and a MAT 253 gas isotope mass spectrometer (Thermo Fischer Scientific MAT, Bremen, Germany). Most reliable measurement is possible between 0 and 5 % carbon enrichment using this instrument and prevailing settings. The analytical procedure for GC-C-IRMS is the same as described previously (Heinzle et al. 2008a).

### 3.2.7 Central metabolic network

In this study, the metabolic network included all major central metabolic cycles in wild type *C. glutamicum*, i.e. glycolysis, pentose phosphate pathway (PPP), and tricarboxylic acid cycle (TCA). All the involved reactions carried out for both GC-MS method and GC-C-IRMS method are listed in Appendix A. The pools of pyruvate and phosphoenolpyruvate as well as the pools of oxaloacetate and malate are lumped, and each flux represents the net flux of the reaction catalyzed by all the related enzymes.  $\text{CO}_2$  producing and consuming reactions were implemented in the network, the <sup>13</sup>C labeling from  $\text{CO}_2$  into oxaloacetate/malate pool was also

taken into account. The fluxes for the byproduct formation (Table 1) and for the anabolic demand were considered as well.

### 3.2.8 Metabolic modeling

Metabolic network simulations for both GC-MS data and GC-IRMS data were performed using the MATLAB version 7.8 (Mathworks Inc., Natick, MA, USA). For the both approaches, the network parametrization and numerical flux estimation were implemented using the algorithm developed in Yang et al. (2008) and the concept of elementary metabolite units (Antoniewicz et al. 2007). Different from the GC-MS method, during GC-CIRMS measurement all derivatized amino acid are combusted into CO<sub>2</sub> which has only one carbon atom. Therefore, the problem becomes simply the first level of the elementary metabolite units, which also corresponds to the atomic level problem described elsewhere (Zupke and Stephanopoulos 1994).

## 3.3 Results

### 3.3.1 Linearity of <sup>13</sup>C fractional labeling

According to theory, the fraction of carbon atom should be always proportional to the input labeling (Heinzle et al. 2008a). A series of experiments were designed to prove this theory employing a wide range of substrate labeling. The experiments were divided into two groups, i.e., lower fraction of <sup>13</sup>C-substrates containing 0, 0.5, 1, 2 and 10% [1-<sup>13</sup>C] glucose, and higher fraction containing 20, 50, 80 and 100% [1-<sup>13</sup>C] glucose. According to the reported measurement ranges for GC-MS of 0.5 -100 APE and GC-C-IRMS -0.1 to +2.0 APE (Meier-Augenstein 1999b), samples from the lower fraction group were measured by GC-C-IRMS due to their low <sup>13</sup>C enrichment in amino acids (< 0.5 APE in derivatized analytes). The obtained  $\delta$  values of individual amino acids were then converted to <sup>13</sup>C enrichment and corrected for the kinetic isotope effect as described previously (Heinzle et al. 2008a). Samples from the higher fraction group were measured by GC-MS and then obtained mass isotopomer distributions of individual amino acids were converted into the fractional <sup>13</sup>C enrichment or fractional labeling, *FL*, using the following equation:

$$FL = \frac{\sum_{i=0}^x i \cdot y_{m+i}}{x} \quad (1)$$

Here,  $y$  is the carbon mass isotopomer fraction of an amino acid,  $i$  the mass shift by <sup>13</sup>C incorporation, and  $x$  the number of carbon atoms of the amino acid. All experimental results are listed in Table 2. Except glycine, the squared correlation coefficients ( $R^2$ ) from the listed amino acids were close to 1 ( $> 0.9999$ ) at the range from 0 to 10% of [1-<sup>13</sup>C] glucose fraction obtained from GC-C-IRMS data. For the whole range from 0 to 100%,  $R^2$  resulting from the amino acids, again except glycine, were also quite close to 1 ( $>0.99$ ). The experiments were carried out on different days using two different mass spectrometric methods, yet the measurements of <sup>13</sup>C fractional enrichments gave an excellent linearity and consistency. Because histidine peaks overlaid with other unknown substances in the GC-MS chromatogram, no satisfactory histidine values could be obtained using GC-MS. Therefore, only GC-C-IRMS  $R^2$  values are listed in the table. In this study, <sup>13</sup>C enrichment of histidine was assumed to be linear over the whole range. The high linear correlation over the whole range tested allows us to predict <sup>13</sup>C enrichment of unknown labeling (e.g. 100% [1-<sup>13</sup>C] glucose fraction) using extrapolation.

**Table 1.** Biomass and metabolites yields of *C. glutamicum* ATCC 13032 cultured on glucose. All yields are given in (C-mol product)/(C-mol glucose), except the yield for biomass that is given in (g dry cell mass)/(mmol glucose).

Biomass and metabolites	Yield
Biomass	0.095±0.004
Lactate	0.0087±0.0007
Trehalose	0.0083±0.0007
2-Oxoglutarate	0.001±0.0001

### 3.3.2 Biomass yield and extracellular metabolites

The yield coefficients for the formation of biomass and extracellular products on glucose during the exponential phase are listed in Table 1.

### 3.3.3 Anabolic demand

Precursor demands used for biomass formation in *C. glutamicum* are listed in Table 3. The values were obtained from literature (Marx et al. 2003; Yang et al. 2005).

**Table 2.** <sup>13</sup>C fractional labeling of proteinogenic amino acids from 0 to 100% input [<sup>1-<sup>13</sup>C</sup>] labeled glucose.

%	[ <sup>1-<sup>13</sup>C</sup> ]glucose fraction of feed glucose (%)									<i>R</i> <sup>2</sup> <sup>c</sup>	<i>R</i> <sup>2</sup> <sup>d</sup>
	0 <sup>a</sup>	0.5 <sup>a</sup>	1 <sup>a</sup>	2 <sup>a</sup>	10 <sup>a</sup>	20 <sup>b</sup>	50 <sup>b</sup>	80 <sup>b</sup>	100 <sup>b</sup>		
Ala	0.0098	0.0109	0.0118	0.0140	0.0315	0.0356	0.0723	0.1063	0.1296	0.9999	0.9957
Ser	0.0094	0.0101	0.0107	0.0121	0.0230	0.0356	0.0700	0.1030	0.1258	1.0000	0.9993
Glu	0.0100	0.0109	0.0117	0.0136	0.0285	0.0474	0.1007	0.1481	0.1848	1.0000	0.9995
His	0.0103	0.0108	0.0114	0.0127	0.0228					0.9999	0.9999
Val	0.0102	0.0111	0.0119	0.0137	0.0283	0.0373	0.0784	0.1184	0.1463	0.9999	0.9992
Thr	0.0097	0.0106	0.0114	0.0132	0.0277	0.0404	0.0853	0.1260	0.1595	1.0000	0.9993
Gly	0.0092	0.0092	0.0094	0.0096	0.0106	0.0172	0.0205	0.0228	0.0257	0.9919	0.9315
Asp	0.0097	0.0106	0.0113	0.0131	0.0268	0.0431	0.0887	0.1283	0.1615	1.0000	0.9991
Ile	0.0104	0.0113	0.0121	0.0139	0.0286	0.0591	0.1044	0.1527	0.1890	0.9999	0.9958
Leu	0.0104	0.0114	0.0122	0.0141	0.0294	0.0697	0.1181	0.1745	0.2145	1.0000	0.9935
Phe	0.0106	0.0111	0.0115	0.0126	0.0204	0.0363	0.0638	0.0919	0.1114	1.0000	0.9974
Pro	0.0104	0.0113	0.0121	0.0139	0.0285	0.0440	0.0942	0.1411	0.1772	1.0000	0.9998

<sup>a</sup> Measured by GC-C-IRMS.

<sup>b</sup> Measured by GC-MS and converted to FL (Equation 1).

<sup>c</sup> *R*<sup>2</sup> values for the experiments with [<sup>1-<sup>13</sup>C</sup>] glucose fraction from 0 to 10%.

<sup>d</sup> *R*<sup>2</sup> values for the whole range of [<sup>1-<sup>13</sup>C</sup>] glucose fraction from 0 to 100%.

**Table 3.** Anabolic demand of *C. glutamicum* ATCC 13032 on glucose.

Precursor	Demand mmol/(g dry cell mass)
Glucose-6-phosphate	0.205
Fructose-6-phosphate	0.308
Pentose-5-phosphate	0.879
Erythrose-4-phosphate	0.268
Glyceraldehyde-3-phosphate	0.129
3-Phosphoglycerate	1.292
Pyruvate/Phosphoenolpyruvate	3.256
$\alpha$ -Ketoglutarate	1.224
Oxaloacetate	1.682
Acetyl CoA	3.177

### 3.3.4 Correction of GC-C-IRMS data for kinetic isotope effects

For GC-C-IRMS based method, the produced  $\delta$  value for each amino acid was converted into <sup>13</sup>C enrichment, corrected for natural isotopes (Yang et al. 2009), and eventually for the kinetic isotope effect. The later was done by subtraction of the <sup>13</sup>C fractional enrichment from the experiment solely using non-labeled glucose (Heinzle et al. 2008a). This correction method is especially important for the experiments with low <sup>13</sup>C glucose fraction because kinetic isotope effects influence the results in these cases. This is clearly seen when comparing uncorrected and corrected fractional labeling in the amino acids at different fractions of [1-<sup>13</sup>C] glucose applied (Table A1 in the Appendix). After the data correction, mean values from two parallel experiments were calculated as listed in Table 4. Based on <sup>13</sup>C fractional enrichments from three labeling experiments with 0.5%, 1% and 2% of [1-<sup>13</sup>C] glucose, the <sup>13</sup>C fractional enrichments of amino acids were linearly extrapolated to 100% labeling for convenience, and these <sup>13</sup>C enrichments of 100% labeling were applied directly for the numerical flux estimation. Errors associated with this linear extrapolation were estimated using standard Gaussian error propagation rules based on the assumed normal

**Table 4.** Mass isotopomer fractions of proteinogenic amino acids based on GC-MS measurement and GC-C-IRMS measurement during cultivation of *C. glutamicum* ATCC 13032.

Analyte	GC-MS			GC-C-IRMS		
		M <sub>0</sub>	M <sub>1</sub>	M <sub>2</sub>	M <sub>0</sub>	M <sub>1</sub>
Alanine (m/z 260)	Exp	0.633	0.345	0.020	Exp	
	Calc	0.638	0.344	0.018	Calc	
Glutamic acid (m/z 432)	Exp	0.342	0.431	0.192	Exp	0.814
	Calc	0.359	0.436	0.177	Calc	0.816
Histidine (m/z 440)	Exp	0.404	0.390	0.142	Exp	0.874
	Calc	0.405	0.388	0.170	Calc	0.874
Valine (m/z 288)	Exp	0.419	0.438	0.134	Exp	
	Calc	0.427	0.437	0.128	Calc	
Threonine (m/z 404)	Exp	0.481	0.415	0.099	Exp	0.819
	Calc	0.480	0.413	0.100	Calc	0.827
Glycine (m/z 246)	Exp	0.952	0.045	0.003	Exp	0.987
	Calc	0.952	0.047	0.001	Calc	0.983
Aspartate (m/z 418)	Exp	0.479	0.416	0.100	Exp	0.829
	Calc	0.480	0.413	0.100	Calc	0.827
Isoleucine (m/z 200)	Exp				Exp	0.818
	Calc				Calc	0.816
Leucine (m/z 200)	Exp				Exp	0.809
	Calc				Calc	0.810
Phenylalanine (m/z 336)	Exp	0.330	0.428	0.197	Exp	0.901
	Calc	0.326	0.428	0.200	Calc	0.901
Proline (m/z 286)	Exp				Exp	0.818
	Calc				Calc	0.816
Tyrosine (m/z 466)	Exp	0.323	0.423	0.201	Exp	
	Calc	0.326	0.428	0.200	Calc	
Arginine (m/z 442)	Exp	0.287	0.411	0.226	Exp	
	Calc	0.300	0.423	0.219	Calc	

Note: **Exp** represents experimental data from both GC-MS and GC-C-IRMS measurement. **Calc** represents values predicted by the mathematical model corresponding to the optimized set of fluxes. M<sub>0</sub> means the amount of non-labeled mass isotopomer fraction, M<sub>1</sub> the amount of singly-labeled mass isotopomer fraction and corresponding terms refer to a higher labeling. GC-MS experimental data were from labeling experiment using 99% [1-<sup>13</sup>C] glucose. GC-C-IRMS experimental data were from labeling experiments using three different low fractions of [1-<sup>13</sup>C] glucose (0.5%, 1%, 2%) and extrapolated to 100% [1-<sup>13</sup>C] glucose as described in the Materials and Methods section. Empty data fields indicate that these data were not used for flux estimation.

distribution of experimental data (Desire et al. 1997). The resulting errors in slope, intercept and value extrapolated to 100% labeling are listed in Table 5. The latter estimated error was further used as input variance for Monte-Carlo simulations applied in the statistical analysis of the actual flux calculation. In parallel we also calculated fluxes from single labeling experiments both from corrected and uncorrected fractional enrichment data (Table A1) and compared with those from extrapolated data (Table A2). It was not possible to calculate physically meaningful fluxes with uncorrected labeling data from 0.5 and 1% [<sup>13</sup>C] glucose labeling (no data shown in Table A2. All other flux estimations with uncorrected data resulted in gross errors (Cases 4, 6, 11 and 12 in Table A2). Interestingly the data combining all four applied labeling data, 0.5, 1 2 and 10 % and those only applying 10% [<sup>13</sup>C] glucose resulted in slightly larger errors than those using only 1 or 2% or combining 0.5, 1 and 2% [<sup>13</sup>C] glucose. This may be caused by reaching almost the upper measurement limit of the GC-C-IRMS instrument with applied instrument settings. Even applying only the measurements from the 0.5% [<sup>13</sup>C] glucose measurement yielded reliable data for fluxes as is also seen in Figure. 2 where data from 99% [<sup>13</sup>C] glucose and GC-MS measurement are compared with single labeling experiments using 0.5, 1 and 2% [<sup>13</sup>C] glucose and literature data (Kim et al. 2006b). The data depicted in Figure. 1 also illustrate the high reliability of the method.

### 3.3.5 Flux estimation in central metabolic pathways of *C. glutamicum* wild type

Figure 1 shows the carbon fluxes through the central metabolic pathways of *C. glutamicum* based on the new method using GC-C-IRMS data using combined experiments with 0.5, 1 and 2% [<sup>13</sup>C] glucose and the traditional method based on GC-MS data. In addition, the corresponding data from a previous publication are listed as well (Kim et al. 2006b). Data from all Generally, the estimated fluxes were very similar in all three cases. The fluxes from glucose 6-phosphate into the pentose phosphate pathway were about 20% relative lower than those into glycolysis. All central metabolic fluxes down to pyruvate had approximately double error in the GC-C-IRMS method compared to the GC-MS method. Largest standard deviations of 5 mole-% corresponding to a relative value of 11 % were found for fluxes leading from succinate to the oxaloacetate/malate pool. Standard deviations in the lower pentose phosphate pathway fluxes were about mole-0.4%, i.e. about 4% relative. In the lower glycolysis the error was about 1.5 mole-%, i.e. less than 1 % relative. Central metabolic fluxes below pyruvate were estimated slightly lower using GC-C-IRMS but again within standard

deviations that were about 3.5 mole-% compared to about 3.3 mole-% using GC-MS. Furthermore, the flux distributions obtained from GC-C-IRMS method and GC-MS method, respectively, were very similar to the literature values given for the wild-type of *C. glutamicum* (Kim et al. 2006b).

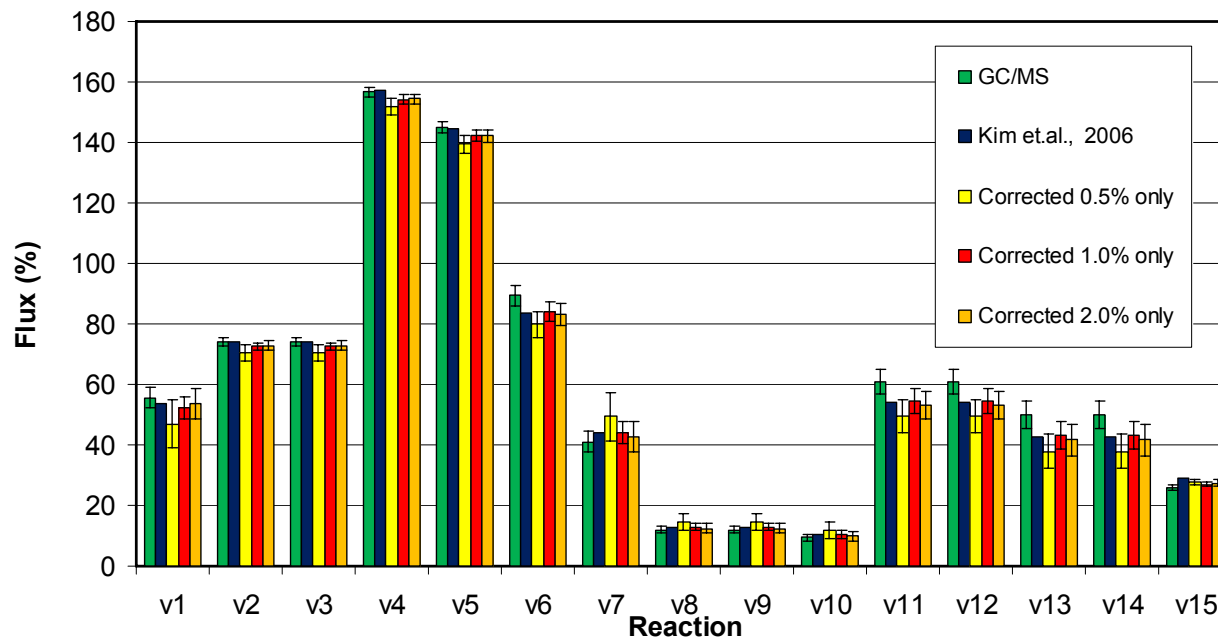


**Figure 1.** Comparison of estimated fluxes. GC/MS – flux analysis using 99% [1-<sup>13</sup>C] glucose; Literature data ((Kim et al. 2006b); GC-C-IRMS from single labeling experiment using 0.5, 1 and 2% [1-<sup>13</sup>C] glucose corrected for natural isotope abundance in culture with naturally labeled glucose. Detailed data are provided in Table A2 in the Appendix.

## Permeabilization for intracellular enzyme activity measurement

**Table 5.** Data extrapolation and error estimation of labeling experiments with four fractions of labeling using Gaussian error propagation (Desire et al. 1997).

Amino acids	1- <sup>13</sup> C fraction of feeding glucose								Slope error*	Intercept error*	Gaussian Error estimation (100%)*
		0.5%	1%	2%	Slope	Intercept	R <sup>2</sup>	100%			
Glutamic acid	M+0	0.99907	0.99823	0.99638	-0.00180	1.00000	0.99946	0.8199	4.21E-05	5.56E-05	0.00421
	M+1	0.00093	0.00177	0.00362	0.00180	0.00000	0.99946	0.1801	4.21E-05	5.56E-05	0.00421
Histidine	M+0	0.99943	0.99890	0.99764	-0.00120	1.00006	0.99831	0.8798	4.95E-05	6.55E-05	0.00495
	M+1	0.00057	0.00110	0.00236	0.00120	-0.00006	0.99831	0.1202	4.95E-05	6.55E-05	0.00495
Threonine	M+0	0.99911	0.99832	0.99655	-0.00172	1.00000	0.99925	0.8284	4.70E-05	6.22E-05	0.00470
	M+1	0.00089	0.00168	0.00345	0.00172	0.00000	0.99925	0.1716	4.70E-05	6.22E-05	0.00470
Glycine	M+0	0.99993	0.99982	0.99955	-0.00026	1.00007	0.99766	0.9745	1.24E-05	1.64E-05	0.00124
	M+1	0.00007	0.00018	0.00045	0.00026	-0.00007	0.99766	0.0255	1.24E-05	1.64E-05	0.00124
Aspartic acid	M+0	0.99915	0.99837	0.99667	-0.00166	1.00000	0.99956	0.8340	3.46E-05	4.58E-05	0.00346
	M+1	0.00085	0.00163	0.00333	0.00166	0.00000	0.99956	0.1660	3.46E-05	4.58E-05	0.00346
Isoleucine	M+0	0.99913	0.99835	0.99658	-0.00171	1.00002	0.99908	0.8290	5.20E-05	6.87E-05	0.00520
	M+1	0.00087	0.00165	0.00342	0.00171	-0.00001	0.99908	0.1710	5.20E-05	6.87E-05	0.00520
Leucine	M+0	0.99905	0.99821	0.99636	-0.00180	0.99998	0.99946	0.8198	4.21E-05	5.56E-05	0.00421
	M+1	0.00095	0.00179	0.00364	0.00180	0.00003	0.99946	0.1802	4.21E-05	5.56E-05	0.00421
Phenylalanine	M+0	0.99950	0.99905	0.99804	-0.00098	1.00001	0.99923	0.9021	2.72E-05	3.60E-05	0.00272
	M+1	0.00050	0.00095	0.00196	0.00098	0.00000	0.99923	0.0979	2.72E-05	3.60E-05	0.00272
Proline	M+0	0.99907	0.99827	0.99651	-0.00171	0.99995	0.99947	0.8285	3.96E-05	5.24E-05	0.00396
	M+1	0.00093	0.00173	0.00349	0.00171	0.00005	0.99947	0.1715	3.96E-05	5.24E-05	0.00396

Slopes and intercepts were calculated using the function LINEST of Excel 2003 (Microsoft). These errors were applied for the calculation of extrapolated errors of 100% labeling using Gaussian error propagation.

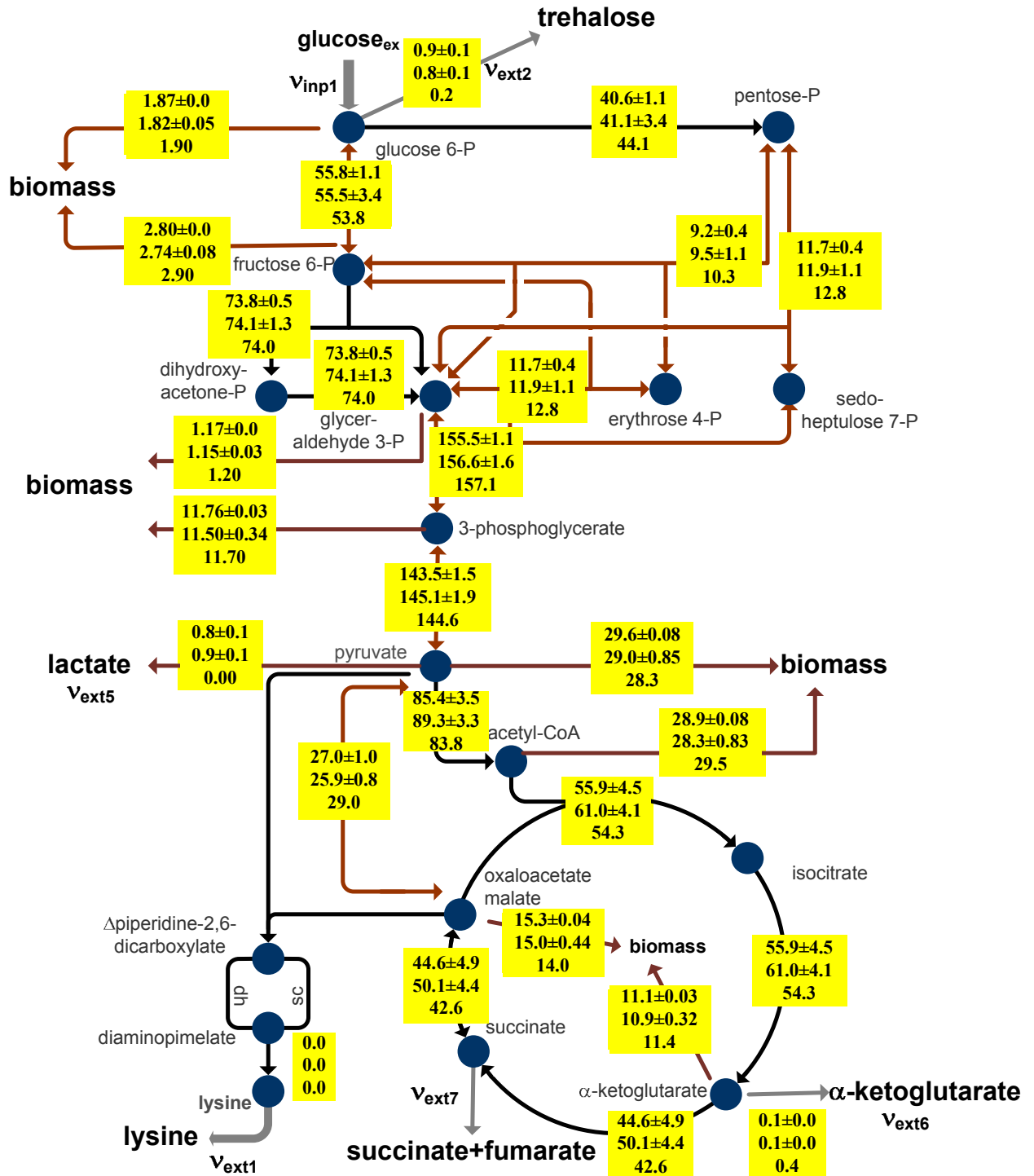


**Figure 2.** In vivo carbon fluxes estimation in the central metabolism of *C. glutamicum* ATCC 13032. Fluxes in molar % of glucose uptake flux with estimated standard deviations are given in square boxes. Upper values are estimated fluxes based on GC-C-IRMS method using combined labeling experiments with 0.5, 1 and 2% [1-<sup>13</sup>C] glucose; middle values are

estimated fluxes based on GC-MS method using 99% [1-<sup>13</sup>C] glucose; bottom values are estimated fluxes from literature (Kim et al. 2006b).

### 3.4 Discussion

The aim of this present study was to develop a new straightforward and cost-efficient approach for the quantification of the *in vivo* flux distribution in the central metabolism of *C. glutamicum*, e.g., in industrial scale fermentation. Based on a model-based experimental design (Mollney et al. 1999), [1-<sup>13</sup>C] glucose was selected as the tracer substrate because of its commercial availability and low cost. Due to the ability for the detection of extremely low isotopic enrichment and high precision, GC-C-IRMS measurement of isotope enrichment was chosen for this study (Heinzle et al. 2008a). To our knowledge, GC-C-IRMS has not been applied on isotope-based *in vivo* flux analysis yet. Our present study opens up the door for the application of GC-C-IRMS to *in vivo* <sup>13</sup>CMFA even at industrially relevant fermentation scales *in situ*. This is of increasing importance with increasing competition, e.g. in the production of biopharmaceuticals (Boghigian et al.)

The theoretically expected linear relationship between input <sup>13</sup>C labeling content and the <sup>13</sup>C enrichment of metabolic products was also observed experimentally, which suggests the GC-C-IRMS applicability for <sup>13</sup>CMFA. As verified for the proteinogenic amino acids investigated herein, other metabolic products can also be applied to <sup>13</sup>CMFA using this novel approach, e.g., some intracellular metabolites. With our method, it is possible to calculate <sup>13</sup>C enrichment at any input <sup>13</sup>C substrate content by extrapolation with at least two or more different amounts of <sup>13</sup>C substrate in mixtures with non-labeled ones.  $R^2$  values from GC-C-IRMS data were closer to 1, compared to those resulting from GC-MS values (Table 2). This is owing to the extremely high precision of GC-C-IRMS for the measurements of <sup>13</sup>C enrichment as well as the absence of any effects from naturally occurring isotopes other than carbon and oxygen. The number of necessary labeling points needed for this extrapolation depends on the accuracy and precision of both experiments and measurements. Typically, we need at least 3 points in order to estimate the accuracy and precision by statistical method such as linear regression analysis. In addition, according to GC-MS results, the relative molar

fraction of each mass isotopomer pool of an individual proteinogenic amino acid is also linear with <sup>13</sup>C input labeling (data not shown).

Due to the high sensitivity, this new approach relies more on the accuracy of experimental operations and measurements, i.e., <sup>13</sup>C-tracer preparation, sampling, GC separation, isotopic calibration etc. Theoretically, one labeling experiment with one low labeling tracer (e.g. 1%) is enough for the extrapolation considering natural substrate as the second point. In this case, it is more difficult to determine the statistical quality of the calculated results. Three or more experiments with different degrees of labeling would improve this.

Typically, commercially available 99% [1-<sup>13</sup>C] glucose applied in <sup>13</sup>C labeling experiment contains 1% <sup>12</sup>C in the first carbon and natural abundance of isotopes of carbon and other elements at other positions. Additionally, elements with natural isotope abundance are introduced during derivatization, e.g., silicon and nitrogen. In case of GC-MS based estimation, the effect of all these naturally labeled atoms can be eliminated by a matrix correction (van Winden et al. 2002; Yang et al. 2009). The so-called correction matrix represents the abundance of naturally occurring isotopes other than the carbon atoms in the skeleton of a metabolite. Therefore, the reliability of carbon mass isotopomer distributions computed from measurements can be subject to the reliability of the data given for the natural abundance of isotopes. In contrast, all the separated derivatized analytes are combusted to CO<sub>2</sub> in GC-C-IRMS measurement and only CO<sub>2</sub> is analyzed afterwards. Therefore, only carbon and oxygen need to be considered for the correction. In this regard, the corrected GC-C-IRMS data should have a higher accuracy than the corrected GC-MS data.

The new approach with the use of low degree <sup>13</sup>C substrate and GC-C-IRMS measurement allows *in vivo* flux estimation in central metabolism, and the final estimated fluxes showed a slightly lower precision only at very low labeling input of 0.5% [1-<sup>13</sup>C] glucose compared with those from high degree labeling and GC-MS measurement. Additionally, many reactions in the central metabolism which are regarded as reversible, e.g. the transaldolase and transketolase reactions in the PPP; phosphoenolpyruvate carboxylase (oxaloacetate to phosphoenolpyruvate), malic enzyme (malate to phosphoenolpyruvate) and oxaloacetate decarboxylase (oxaloacetate to pyruvate) cannot be determined by the new approach with [1-<sup>13</sup>C] glucose as only tracer substrate. Therefore, only the net fluxes were determined using GC-C-IRMS data in this study. The above limitation can be overcome, e.g., by a parallel

experimental design using tracer substrates with different positional labeling to increase information content as was shown by Yang et al. (Yang et al. 2006b; Yang et al. 2006c) measuring only CO<sub>2</sub> labeling. In terms of information content GC-MS measurement is superior to GC-C-IRMS since it allows the determination of mass isotopomer distribution for each analyte, whereas GC-C-IRMS determines only average carbon labeling. The present approach has a great potential for <sup>13</sup>C MFA at low labeling degree of substrates and, especially, is the most promising one for investigating *in vivo* fluxes in a large scale bioprocess *in situ*.

### 3.5 Conclusion

In this study, we introduced a novel strategy to estimate metabolic fluxes using GC-C-IRMS at low degree of labeling. Its applicability was demonstrated using 4 different low labeling fractions from 0.5 to 10% [1-<sup>13</sup>C] labeled glucose, mixed with non-labeled glucose, for the estimation of fluxes in the central metabolism of *C. glutamicum*. The reliability of obtained results was confirmed by checking the accordance with parallel experiments using conventional GC-MS method applying 99% [1-<sup>13</sup>C] glucose. Also, the flux values obtained from the labeling measurements were found to be well consistent with a previous report using the GC-MS method under the same condition (Kim et al. 2006b).

The whole range of labeling degrees from 0 to 100% [1-<sup>13</sup>C] glucose was applied, and the mass isotopomers of proteinogenic amino acids were measured by both GC-C-IRMS and GC-MS in their respective measurement ranges. <sup>13</sup>C fractional labeling of each amino acid for the whole range of labeling was found to be proportional to the input labeling, as also expected theoretically. This provides the possibility to use an extremely small amount of <sup>13</sup>C substrates for the estimation of *in vivo* fluxes in the central metabolism. The reliability of the final results was found to greatly depend on the reproducibility of experimental procedure and measurement accuracy. This novel technique can cut the cost of the tracer substrate to 100 times or even more lower than those using conventional GC-MS method. Hence, the method developed in the present work is promising for the investigation of metabolic fluxes in industrially relevant organisms on larger scales. The method might also be successfully applied for dynamic metabolic flux analysis to determine very initial changes after a carbon-isotope perturbation of previously naturally labeled substrate.

## References:

- Antoniewicz MR, Kelleher JK, Stephanopoulos G. 2007. Elementary metabolite units (EMU): a novel framework for modeling isotopic distributions. *Metab Eng* 9(1):68-86.
- Bailey JE. 1991. Toward a Science of Metabolic Engineering. *Science* 252(5013):1668-1675.
- Becker J, Klopprogge C, Herold A, Zelder O, Bolten CJ, Wittmann C. 2007. Metabolic flux engineering of L-lysine production in *Corynebacterium glutamicum*--over expression and modification of G6P dehydrogenase. *J Biotechnol* 132(2):99-109.
- Becker J, Klopprogge C, Wittmann C. 2008. Metabolic responses to pyruvate kinase deletion in lysine producing *Corynebacterium glutamicum*. *Microb Cell Fact* 7:8.
- Boghigian BA, Seth G, Kiss R, Pfeifer BA. 2009. Metabolic flux analysis and pharmaceutical production. *Metab Eng*.
- Christensen B, Nielsen J. 1999. Isotopomer analysis using GC-MS. *Metab Eng* 1(4):282-90.
- Corr LT, Berstan R, Evershed RP. 2007. Optimisation of derivatisation procedures for the determination of delta13C values of amino acids by gas chromatography/combustion/isotope ratio mass spectrometry. *Rapid Commun Mass Spectrom* 21(23):3759-71.
- Dauner M, Sauer U. 2000. GC-MS analysis of amino acids rapidly provides rich information for isotopomer balancing. *Biotechnol Prog* 16(4):642-9.
- de Sain-van der Velden MG, Rabelink TJ, Gadellaa MM, Elzinga H, Reijngoud DJ, Kuipers F, Stellaard F. 1998. In vivo determination of very-low-density lipoprotein-apolipoprotein B100 secretion rates in humans with a low dose of l-[1-<sup>13</sup>C]valine and isotope ratio mass spectrometry. *Anal Biochem* 265(2):308-12.
- Engel MH, Macko SA, Silfer JA. 1990. Carbon Isotope Composition of Individual Amino-Acids in the Murchison Meteorite. *Nature* 348(6296):47-49.
- Godin JP, Faure M, Breuille D, Hopfgartner G, Fay LB. 2007. Determination of <sup>13</sup>C isotopic enrichment of valine and threonine by GC-C-IRMS after formation of the N(O,S)-ethoxycarbonyl ethyl ester derivatives of the amino acids. *Anal Bioanal Chem* 388(4):909-18.
- Hans MA, Heinzle E, Wittmann C. 2001. Quantification of intracellular amino acids in batch cultures of *Saccharomyces cerevisiae*. *Appl Microbiol Biotechnol* 56(5-6):776-9.

- Haunschild MD, Freisleben B, Takors R, Wiechert W. 2005. Investigating the dynamic behavior of biochemical networks using model families. *Bioinformatics* 21(8):1617-1625.
- Heinzle E, Yuan Y, Kumar S, Wittmann C, Gehre M, Richnow HH, Wehrung P, Adam P, Albrecht P. 2008. Analysis of <sup>13</sup>C labeling enrichment in microbial culture applying metabolic tracer experiments using gas chromatography-combustion-isotope ratio mass spectrometry. *Anal Biochem* 380(2):202-10.
- Iwatani S, Yamada Y, Usuda Y. 2008. Metabolic flux analysis in biotechnology processes. *Biotechnol Lett* 30(5):791-9.
- Kim HM, Heinzle E, Wittmann C. 2006. Deregulation of aspartokinase by single nucleotide exchange leads to global flux rearrangement in the central metabolism of *Corynebacterium glutamicum*. *J Microbiol Biotechnol* 16:1174-1179.
- Maaheimo H, Fiaux J, Cakar ZP, Bailey JE, Sauer U, Szyperski T. 2001. Central carbon metabolism of *Saccharomyces cerevisiae* explored by biosynthetic fractional (<sup>13</sup>C) labeling of common amino acids. *Eur J Biochem* 268(8):2464-79.
- Marx A, de Graaf AA, Wiechert W, Eggeling L, Sahl H. 1996. Determination of the fluxes in the central metabolism of *Corynebacterium glutamicum* by nuclear magnetic resonance spectroscopy combined with metabolite balancing. *Biotechnol Bioeng* 49(2):111-29.
- Marx A, Hans S, Mockel B, Bathe B, de Graaf AA, McCormack AC, Stapleton C, Burke K, O'Donohue M, Dunican LK. 2003. Metabolic phenotype of phosphoglucose isomerase mutants of *Corynebacterium glutamicum*. *Journal of Biotechnology* 104(1-3):185-97.
- Massart DL, Vandeginste BGM, Buydens LMC, de Jong S, Lewi PJ, Smeyers-Verbeke J. 1997. *Handbook of Chemometrics and Qualimetrics: Part A*. Amsterdam: Elsevier.
- Meier-Augenstein A, Rating D, Hoffmann GF, Wendel U, Matthiesen U, Schadewaldt P. 1995. Determination of <sup>13</sup>C Enrichment by Conventional GC-MS and GC-(MS)-CIRMS. *Isotopes Environ. Health Stud.* 31(3):261-266.
- Meier-Augenstein W. 1999. Use of gas chromatography-combustion-isotope ratio mass spectrometry in nutrition and metabolic research. *Curr Opin Clin Nutr Metab Care* 2(6):465-70.

- Mollney M, Wiechert W, Kownatzki D, de Graaf AA. 1999. Bidirectional reaction steps in metabolic networks: IV. Optimal design of isotopomer labeling experiments. *Biotechnol Bioeng* 66(2):86-103.
- Nanchen A, Fuhrer T, Sauer U. 2007. Determination of metabolic flux ratios from <sup>13</sup>C-experiments and gas chromatography-mass spectrometry data: protocol and principles. *Methods in Molecular Biology* 358:177-97.
- Reijngoud DJ, Hellstern G, Elzinga H, de Sain-van der Velden MG, Okken A, Stellaard F. 1998. Determination of low isotopic enrichment of L-[1-<sup>13</sup>C]valine by gas chromatography/combustion/isotope ratio mass spectrometry: a robust method for measuring protein fractional synthetic rates in vivo. *J Mass Spectrom* 33(7):621-6.
- Schmidt K, Carlsen M, Nielsen J, Villadsen J. 1997. Modeling isotopomer distributions in biochemical networks using isotopomer mapping matrices. *Biotechnol Bioeng* 55(6):831-840.
- Schmidt K, Marx A, de Graaf AA, Wiechert W, Sahm H, Nielsen J, Villadsen J. 1998. <sup>13</sup>C tracer experiments and metabolite balancing for metabolic flux analysis: comparing two approaches. *Biotechnol Bioeng* 58(2-3):254-7.
- van der Werf MJ, Takors R, Smedsgaard J, Nielsen J, Ferenci T, Portais JC, Wittmann C, Hooks M, Tomassini A, Oldiges M and others. 2007. Standard reporting requirements for biological samples in metabolomics experiments: microbial and in vitro biology experiments. *Metabolomics* 3(3):189-194.
- van Winden WA, Wittmann C, Heinzle E, Heijnen JJ. 2002. Correcting mass isotopomer distributions for naturally occurring isotopes. *Biotechnology and Bioengineering* 80(4):477-479.
- Velagapudi VR, Wittmann C, Schneider K, Heinzle E. 2007. Metabolic flux screening of *Saccharomyces cerevisiae* single knockout strains on glucose and galactose supports elucidation of gene function. *J Biotechnol* 132(4):395-404.
- Wiechert W. 2001. <sup>13</sup>C metabolic flux analysis. *Metab Eng* 3(3):195-206.
- Wiechert W, de Graaf AA. 1996. In vivo stationary flux analysis by <sup>13</sup>C labeling experiments. *Advances in Biochemical Engineering/Biotechnology* 54:109-54.
- Wittmann C. 2007. Fluxome analysis using GC-MS. *Microbial Cell Factories* 6:-.
- Wittmann C, Heinzle E. 1999. Mass spectrometry for metabolic flux analysis. *Biotechnol Bioeng* 62(6):739-750.

- Wittmann C, Heinzle E. 2001. Application of MALDI-TOF MS to lysine-producing *Corynebacterium glutamicum* - A novel approach for metabolic flux analysis. *European Journal of Biochemistry* 268(8):2441-2455.
- Wittmann C, Heinzle E. 2008. Metabolic Network Analysis and Design in *Corynebacterium glutamicum*. In: Burkovski A, editor. *Corynebacteria. Genomics and Molecular Biology*. Norfolk UK: Caister Academic Press. p 79-112.
- Wittmann C, Kim HM, Heinzle E. 2004. Metabolic network analysis of lysine producing *Corynebacterium glutamicum* at a miniaturized scale. *Biotechnol Bioeng* 87(1):1-6.
- Yang TH, Bolten CJ, Coppi MV, Sun J, Heinzle E. 2009. Numerical bias estimation for mass spectrometric mass isotopomer analysis. *Anal Biochem* 388(2):192-203.
- Yang TH, Frick O, Heinzle E. 2008. Hybrid optimization for <sup>13</sup>C metabolic flux analysis using systems parametrized by compactification. *BMC Syst Biol* 2:29.
- Yang TH, Heinzle E, Wittmann C. 2005. Theoretical aspects of C-13 metabolic flux analysis with sole quantification of carbon dioxide labeling. *Computational Biology and Chemistry* 29(2):121-133.
- Yang TH, Wittmann C, Heinzle E. 2004. Metabolic network simulation using logical loop algorithm and Jacobian matrix. *Metabolic Engineering* 6(4):256-267.
- Yang TH, Wittmann C, Heinzle E. 2006a. Respirometric <sup>13</sup>C flux analysis - Part II: in vivo flux estimation of lysine-producing *Corynebacterium glutamicum*. *Metab Eng* 8(5):432-46.
- Yang TH, Wittmann C, Heinzle E. 2006b. Respirometric <sup>13</sup>C flux analysis, Part I: design, construction and validation of a novel multiple reactor system using on-line membrane inlet mass spectrometry. *Metab Eng* 8(5):417-31.
- Zupke C, Stephanopoulos G. 1994. Modeling of isotope distributions and intracellular fluxes in metabolic networks using atom mapping matrixes. *Biotechnol Prog* 10(5):489-98.

## APPENDIX

### Reactions in the central network in Figure. 1.

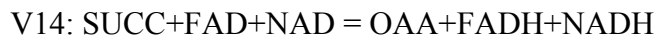
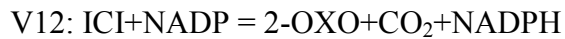
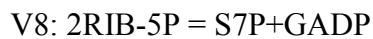
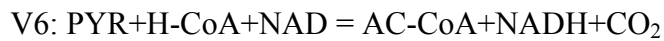


TABLE A1 <sup>13</sup>C fractional enrichments and standard deviations of proteinogenic amino acids before and after correction of carbon contribution from derivatization reagent at different fractions of [1-<sup>13</sup>C] glucose used

		[1- <sup>13</sup> C] Glucose fraction (%)								
		Uncorrected					Corrected			
		0	0.5	1	2	10	0.5	1	2	10
Alanin	Mean	0.00982	0.01088	0.01180	0.01398	0.03150	0.00105	0.00198	0.00416	0.02168
	SD	5.7E-05	3.9E-07	1.0E-05	0.00014	0.00231	5.8E-05	5.8E-05	0.00015	0.00231
Serin	Mean	0.00938	0.01008	0.01068	0.01205	0.02301	0.00070	0.00130	0.00267	0.01363
	SD	2.3E-05	4.1E-05	2.9E-06	8.6E-05	0.00124	4.7E-05	2.4E-05	9.0E-05	0.00124
Glutamat	Mean	0.00998	0.01091	0.01174	0.01364	0.02849	0.00093	0.00177	0.00366	0.01851
	SD	4.3E-05	3.0E-05	9.2E-06	0.00012	0.00162	5.3E-05	4.4E-05	0.00013	0.00162
Histidin	Mean	0.01026	0.01083	0.01137	0.01265	0.02280	0.00057	0.00110	0.00239	0.01253
	SD	7.3E-06	3.3E-05	1.2E-05	8.7E-05	0.00103	3.3E-05	1.4E-05	8.7E-05	0.00103
Valin	Mean	0.01025	0.01114	0.01190	0.01370	0.02830	0.00089	0.00165	0.00345	0.01805
	SD	4.2E-05	2.9E-05	2.6E-06	0.00011	0.00185	5.1E-05	4.2E-05	0.00012	0.00185
Threonin	Mean	0.00973	0.01062	0.01140	0.01322	0.02774	0.00089	0.00168	0.00349	0.01801
	SD	5.5E-05	3.5E-05	1.3E-05	0.00012	0.00160	6.5E-05	5.6E-05	0.00014	0.00160
Glycin	Mean	0.00917	0.00924	0.00936	0.00962	0.01055	0.00007	0.00018	0.00044	0.00138
	SD	9.3E-06	3.5E-05	4.9E-05	6.4E-05	0.00022	3.6E-05	5.0E-05	6.4E-05	0.00022
Aspartat	Mean	0.00972	0.01057	0.01134	0.01308	0.02676	0.00085	0.00163	0.00337	0.01705
	SD	3.3E-05	2.8E-05	6.8E-06	0.00012	0.00147	4.3E-05	3.4E-05	0.00012	0.00147
Isoleucin	Mean	0.01043	0.01131	0.01209	0.01390	0.02856	0.00087	0.00165	0.00347	0.01813
	SD	3.7E-05	4.2E-05	1.2E-05	0.00014	0.00165	5.6E-05	3.9E-05	0.00014	0.00165
Leucin	Mean	0.01040	0.01135	0.01219	0.01408	0.02944	0.00095	0.00179	0.00368	0.01904
	SD	3E-05	3.8E-05	1.7E-06	0.00012	0.00155	4.8E-05	3.0E-05	0.00012	0.00155
Phenylalanin	Mean	0.01057	0.01107	0.01152	0.01256	0.02044	0.00050	0.00095	0.00198	0.00987
	SD	2.2E-05	3.2E-05	1.0E-05	7.6E-05	0.00086	3.9E-05	2.5E-05	7.9E-05	0.00086
Prolin	Mean	0.01037	0.01130	0.01210	0.01391	0.02851	0.00093	0.00173	0.00354	0.01814
	SD	3.7E-05	6.2E-05	2.7E-05	0.00015	0.00164	7.2E-05	4.6E-05	0.00016	0.00164

TABLE A2. Flux estimation results based on trace experiments with different fractions of [1-<sup>13</sup>C] glucose.

Case		v1	v2	v3	v4	v5	v6	v7	v8	v9	v10	v11	v12	v13	v14	v15
1	GCMS <sup>1</sup>	55.53 ±3.35	74.14 ±1.27	74.14 ±1.27	156.61 ±1.6	145.10 ±1.9	89.32 ±3.34	41.05 ±3.35	11.87 ±1.10	11.87 ±1.10	9.48 ±1.08	61.00 ±4.13	61.00 ±4.13	50.10 ±4.44	50.10 ±4.44	25.90 ±0.75
2	Kim et.al.,2006 <sup>2</sup>	53.80	74.00	74.00	157.10	144.60	83.80	44.10	12.80	12.80	10.30	54.30	54.30	42.60	42.60	29.00
3	Corrected 0.5-10 (%) <sup>3</sup>	48.49 ±7.83	71.39 ±2.76	71.39 ±2.76	153.23 ±3.0	141.43 ±3.0	84.33 ±3.10	47.81 ±7.64	14.08 ±2.54	14.08 ±2.54	11.63 ±2.54	55.32 ±3.17	55.32 ±3.17	44.15 ±3.19	44.15 ±3.19	26.53 ±0.07
4	Uncorrected 0.5-10 (%) <sup>4</sup>	60.94 ±2.98	75.39 ±0.88	75.39 ±0.88	156.98 ±0.8	144.88 ±0.9	86.28 ±1.73	35.49 ±3.02	9.92 ±1.03	9.92 ±1.03	7.41 ±1.06	56.51 ±2.31	56.51 ±2.31	45.05 ±2.54	45.05 ±2.54	27.22 ±0.58
5	Corrected 0.5-2.0(%) <sup>5</sup>	55.83 ±1.09	73.77 ±0.53	73.77 ±0.53	155.51 ±1.1	143.51 ±1.5	85.42 ±3.46	40.62 ±1.09	11.65 ±0.37	11.65 ±0.37	9.16 ±0.41	55.92 ±4.49	55.92 ±4.49	44.55 ±4.90	44.55 ±4.90	26.99 ±0.96
6	Uncorrected 0.5-2.0 (%) <sup>6</sup>	64.82 ±0.81	76.89 ±0.43	76.89 ±0.43	158.81 ±0.9	146.94 ±1.3	89.45 ±3.13	31.65 ±0.81	8.68 ±0.29	8.68 ±0.29	6.22 ±0.33	60.27 ±4.09	60.27 ±4.09	49.02 ±4.46	49.02 ±4.46	26.70 ±0.88
7	Corrected 0.5(%) <sup>7</sup>	46.95 ±8.02	70.53 ±2.67	70.53 ±2.67	151.81 ±2.8	139.48 ±3.0	79.80 ±4.38	49.44 ±8.03	14.54 ±2.69	14.54 ±2.69	11.98 ±2.70	49.49 ±5.33	49.49 ±5.33	37.81 ±5.71	37.81 ±5.71	27.73 ±1.04
8	Corrected 1.0(%) <sup>8</sup>	52.20 ±3.68	72.56 ±1.23	72.56 ±1.23	154.27 ±1.4	142.26 ±1.7	84.08 ±3.23	44.24 ±3.70	12.85 ±1.24	12.85 ±1.24	10.36 ±1.26	54.54 ±4.13	54.54 ±4.13	43.16 ±4.48	43.16 ±4.48	27.02 ±0.88
9	Corrected 2.0 (%) <sup>9</sup>	53.60 ±4.86	72.87 ±1.59	72.87 ±1.59	154.34 ±1.7	142.15 ±2.0	83.14 ±3.63	42.81 ±4.87	12.35 ±1.64	12.35 ±1.64	9.82 ±1.67	53.16 ±4.65	53.16 ±4.65	41.61 ±5.05	41.61 ±5.05	27.42 ±1.01
10	Corrected 10.0(%) <sup>10</sup>	41.55 ±8.69	68.65 ±2.89	68.65 ±2.89	149.80 ±3.0	137.38 ±3.2	77.26 ±4.61	54.83 ±8.73	16.32 ±2.92	16.32 ±2.92	13.74 ±2.93	46.71 ±5.57	46.71 ±5.57	34.94 ±5.95	34.94 ±5.95	27.94 ±1.06
11	Uncorrected 2.0 (%) <sup>11</sup>	95.82 ±0.07	85.43 ±0.07	85.43 ±0.07	164.52 ±0.1	150.87 ±0.1	84.73 ±0.15	0.00 ±0.00	2.15 ±0.00	2.15 ±0.00	4.98 ±0.00	51.17 ±0.15	51.17 ±0.15	38.23 ±0.15	38.23 ±0.15	30.70 ±0.00
12	Uncorrected 10.0 (%) <sup>12</sup>	96.43 ±0.16	87.23 ±0.52	87.23 ±0.52	168.83 ±1.3	156.74 ±1.8	98.18 ±4.32	0.00 ±0.00	1.91 ±0.08	1.91 ±0.08	4.41 ±0.19	68.44 ±5.62	68.44 ±5.62	56.99 ±6.12	56.99 ±6.12	27.20 ±1.19

Flux results are based on trace experiments with [1-<sup>13</sup>C] glucose fractions of:

- 1) 99% and GCMS measurement.
- 2) 99% and GDMS measurement (Kim et al., 2006).
- 3) 0.5, 1, 2 and 10% and GCCIRMS measurement. <sup>13</sup>C enrichments were corrected as described in the text.
- 4) 0.5, 1, 2 and 10% and GCCIRMS measurement. <sup>13</sup>C enrichments were not corrected.
- 5) 0.5, 1 and 2% and GCCIRMS measurement. <sup>13</sup>C enrichments were corrected as described in the text.
- 6) 0.5, 1 and 2% and GCCIRMS measurement. <sup>13</sup>C enrichments were not corrected.
- 7) 0.5% and GCCIRMS measurement. <sup>13</sup>C enrichments were corrected as described in the text.
- 8) 0% and GCCIRMS measurement. <sup>13</sup>C enrichments were corrected as described in the text.
- 9) 2.0% and GCCIRMS measurement. <sup>13</sup>C enrichments were corrected as described in the text.
- 10) 0% and GCCIRMS measurement. <sup>13</sup>C enrichments were corrected as described in the text.
- 11) 2.0% and GCCIRMS measurement. <sup>13</sup>C enrichments were not corrected.
- 12) 10.0% and GCCIRMS measurement. <sup>13</sup>C enrichments were not corrected.

## Chapter 4

# Permeabilization of *Corynebacterium glutamicum* for NAD(P)H-dependent intracellular enzyme activity measurement

### Abstract

Permeabilization of *Corynebacterium glutamicum* cells permits direct determination of enzyme activity measuring NAD(P)H after appropriate calibration and correction for cell density. The optimized conditions found were the treatment of 10 mg cells/ml (dry weight) by Triton X-100 at a final concentration of 0.05 % for 5 min at room temperature. Glucose-6-phosphate dehydrogenase and 6-phosphogluconate dehydrogenase activities were very close to those determined in cell-free extract. In cell-free extracts malic enzyme activity was about double and that of isocitrate dehydrogenase about triple the values in permeabilized cells.  $K_m$  values were similar in cell-free extract and permeabilized cell but larger than literature values obtained with purified enzymes.

This chapter has been published as: Yuan Y, Heinzle E. 2009. Permeabilization of *Corynebacterium glutamicum* for NAD(P)H-dependent intracellular enzyme activity measurement. *Comptes Rendus Chimie* 12(10-11):1154-1162.

### 4.1 Introduction

Accurate enzyme kinetic parameters are highly desirable for metabolic kinetic analysis (Miranda et al. 2006). Usually purified enzymes are utilized to characterize their kinetic behavior in unnatural buffer systems. Unfortunately, these artificial conditions usually cannot provide correct information on how an enzyme fulfils its physiological role in the living cell (Wittmann et al. 2005). There is plenty of evidence that channeling, i.e. the preferential direct transfer of a product of an enzymatic reaction to the next enzyme, is an important phenomenon that cannot be studied with purified enzymes. Recent protein localization studies in *Arabidopsis thaliana* showed, e.g., that dynamic association of glycolytic enzymes with mitochondria is a function of mitochondrial activity thus supporting channeling (Graham et al. 2007a). Channeling was also shown for glycolysis even in bacteria (Shearer et al. 2005b). Application of cell-free extracts obtained from the water-soluble part of the cell lysate is the classical way for intracellular enzyme study, but the requirement of complete disruption of the cell integrity may result in an inactivation of enzymes and dissociation of enzyme complexes, especially those associated more weakly. In addition, the procedure for purifying enzymes or preparation of cell-free extract is laborious and time consuming (Miozzari et al. 1978). Permeabilization of the cellular membrane without complete cell disintegration promises to solve above mentioned problems to a certain extent. After the treatment of cells with appropriate organic solvents, such as ethanol (Somkuti et al. 1998), toluene-ethanol mixtures (Chelico and Khachatourians 2003; Choudary 1984), detergents like Triton X-100 (Galabova et al. 1996; Miozzari et al. 1978) and other organic chemicals (Gowda et al. 1991; Gowda et al. 1988), the cell membrane becomes permeable allowing small molecules to freely enter and leave the cell while keeping the morphology of the cell intact. This method permits keeping most cellular structures, protein-protein interactions, and most of intracellular enzymes in their original environment which is very important for metabolic processes analysis (Felix 1982). Kinetics measured under permeabilization conditions, which is often called *in situ*, is regarded as an intermediate stage between *in vivo* and *in vitro*. Compared to *in vitro* methods, permeabilized cells still keep their macromolecular structure intact that is important for channeling and protein-protein interaction phenomena.

Many intracellular oxidation-reduction reactions involve the inter-conversion of the oxidized and reduced forms of NAD(P), and for monitoring such reactions, the large

absorbance of NAD(P)H at 340 nm can be measured continuously by a spectrophotometer (Cornish-Bowden, 2004). Normally such spectrophotometric assays need an optically clear reaction system for a detection linear with concentration of NAD(P)H. Therefore, NAD(P)H-dependent enzyme assays in a cell suspension system have not been deeply studied yet.

Whole-cell permeabilization for enzyme activity measurement has been applied in many organisms until now (Alamae and Jarviste 1995; Chelico and Khachatourians 2003; Crotti et al. 2001; Galabova et al. 1996; Gowda et al. 1991; Somkuti et al. 1998; Vanderwerf et al. 1995). *Corynebacterium glutamicum* is intensively used for the industrial production of amino acids such as glutamate and lysine (Kelle et al. 2005; Kimura 2005; Wittmann and Becker 2007a). The mostly used method for enzyme activity measurement in such cells uses cell lysis (Becker et al. 2005; Kromer et al. 2006; Yokota and Lindley 2005). In vivo activity of the enzyme of the entire metabolic network is determined using various methods of metabolic flux analysis (Becker et al. 2005; Heinzle et al. 2008a; Kiefer et al. 2004; Krömer et al. 2004; Wittmann and de Graaf 2005; Wittmann and Heinzle 2001b; Wittmann and Heinzle 2002a; Wittmann and Heinzle 2008; Wittmann et al. 2004; Yang et al. 2006a).

In this investigation, we focus on NAD(P)H-dependent enzyme assays in a cell suspension system, in particular on obtaining a rapid, simple permeabilization method in *C. glutamicum* for potential determination of enzymatic kinetic parameters which are important for metabolic pathway analysis and modeling. The effect of the nonionic surfactant Triton X-100, toluene-ethanol mixtures (TE), CTAB, digitonin and ethanol on the permeability of *C. glutamicum* cells was examined and four enzyme activities, glucose-6-phosphate dehydrogenase, isocitrate dehydrogenase, 6-phosphogluconate dehydrogenase and malic enzyme, were analyzed as model systems.

## 4.2 Materials and methods

### 4.2.1 Strain

*Corynebacterium glutamicum* ATCC 13032 was obtained from the American Type Culture Collection (Manassas, USA).

### 4.2.2 Chemicals

Triton X-100 was purchased from Fluka (Buchs, Switzerland). Malate, NADP and glucose-6-phosphate were from Sigma (Steinheim, Germany). All other chemicals were from Sigma (St. Louis, USA), Merck (Darmstadt, Germany) or Fluka (Buchs, Switzerland) and of analytical grade. For all experiments the same batch of chemicals was used.

### 4.2.3 Strain cultivation

The cultivation of *C. glutamicum* ATCC 13032 was the same as described in (Heinzle et al. 2008a). Cells in the exponential growth phase ( $OD_{660}=10$ ) were harvested by centrifugation (8500 rpm, 5 min, 4 °C), and then washed by Tris-HCl buffer (100 mM Tris, 200 mM KCl, pH=7.8) for twice. The pellet was weighted and appropriate volume of Tris-HCl buffer was added and adjusted to required cell density (mg cell dry weight /ml) for the next cell disruption.

### 4.2.4 Preparation of crude extract and permeabilization

**Permeabilization.** Washed cells were resuspended to a cell density of 10 mg/ml (CDW), 1 ml of cell suspension was transferred into a 1.5 ml Eppendorf tube and a defined amount of permeabilization agent was added to give a desired concentration. After 30 s swirling the cell suspension was incubated for a defined period of time. The final permeabilized cell suspension was directly used for enzyme activity measurement.

**Glass beads treatment.** Washed cells were resuspended to a cell density of 10 mg/ml(CDW), 400  $\mu$ l cell suspension and 400 mg glass beads ( $\leq 0.25$  mm in diameter) were mixed in a 1.5 ml Eppendorf tube and shaken for 15 min (Frequency: 30/s). The supernatant was transferred into another pre-cooled Eppendorf tube and centrifuged at 13000 rpm (15500 g) for 15 min. The final supernatant was used for enzyme activity measurement. Samples were kept at 4 °C.

### 4.2.5 Enzymes assays

All of the following enzyme activities were measured spectrophotometrically by detecting the change in the absorption of NADPH at 340 nm ( $\epsilon=6.223 \text{ l}\times\text{mmol}^{-1}\times\text{cm}^{-1}$ ) at 30 °C.

## Permeabilization for intracellular enzyme activity measurement

---

**Malic enzyme.** The 1 ml reaction system contains 890  $\mu$ l Tris-HCl buffer (100 mM Tris-HCl, 200 mM KCl, pH=7.8), 10  $\mu$ l MgCl<sub>2</sub> solution (2 mM), 10  $\mu$ l NADP solution (1 mM) and 50  $\mu$ l cell extract or permeabilized cell suspension. 40  $\mu$ l of malate solution was added to start the reaction.

**Glucose-6-phosphate dehydrogenase.** The 1 ml reaction system contained 880  $\mu$ l Tris-HCl buffer (100 mM Tris-HCl, 200 mM KCl, pH=7.8), 10  $\mu$ l MgCl<sub>2</sub> solution (10mM), 10  $\mu$ l NADP solution (1 mM) and 50  $\mu$ l cell extract or permeabilized cell suspension. 50  $\mu$ l of glucose-6-phosphate was added to start the reaction.

**Isocitrate dehydrogenase.** The 1 ml reaction system contained 915  $\mu$ l Tricine-KOH buffer (100 mM Tricine-KOH, pH=8.0), 10  $\mu$ l MgCl<sub>2</sub> solution (10 mM), 5  $\mu$ l NADP<sup>+</sup> solution (1 mM) and 50  $\mu$ l cell extract or permeabilized cell suspension. 20  $\mu$ l of DL-isocitric acid solution was added to start the reaction.

**6-Phosphogluconate-dehydrogenase.** The 1 ml reaction system contained 910  $\mu$ l Tris-HCl buffer (100 mM Tris-HCl, pH=7.5), 10  $\mu$ l MgCl<sub>2</sub> (10mM), 10  $\mu$ l NADP (1mM) and 50  $\mu$ l cell extract or permeabilized cell suspension. 20  $\mu$ l of 6-phosphogluconate was added to start the reaction.

**Phosphoglucose isomerase.** The 1 ml reaction system contained 925  $\mu$ l Tris-HCl buffer (100 mM Tris-HCl, pH=7.5), 10  $\mu$ l MgCl<sub>2</sub> (10mM), 5  $\mu$ l NADP (0.5 mM), 1 U glucose-6-phosphate dehydrogenase and 50  $\mu$ l cell extract or permeabilized cell suspension. 10  $\mu$ l of fructose-6-phosphate was added to start the reaction.

**Enzyme activity unit:** One unit of enzyme is defined as the amount of enzyme producing 1  $\mu$ mol NADPH per min under the assay conditions. Enzymatic activities are given per mg of dry cells unless specially defined. All absorbance measurements were carried out in a spectrophotometer at controlled temperature.

**Cell density in enzyme assay:** Permeabilized cell suspension was diluted 20 times starting usually at 10 mg/ml and yielding 0.5 mg/ml in the reaction cuvette.

### 4.3 Results

#### 4.3.1 NAD(P)H measurement in permeabilized cells

## Permeabilization for intracellular enzyme activity measurement

In optically clear solution the measured absorbance is usually linear with concentration following Lambert Beer's law. During activity measurement with permeabilized cells, the absorption of NAD(P)H is measured in a cell suspension disturbing its measurement. It was therefore essential to study whether NAD(P)H could be measured in a permeabilized cell suspension. Various amounts of NADPH were mixed with permeabilized cell suspensions to give final concentrations from 0 to 50  $\mu\text{g/ml}$ . Plots of the absorbance at 340 nm,  $A_{340}$ , against NADPH concentration are depicted in Figure 1. The range of linear correlation decreased with increasing cell concentration (Table 1). The corresponding  $R^2$ -values are listed in Table 1. A

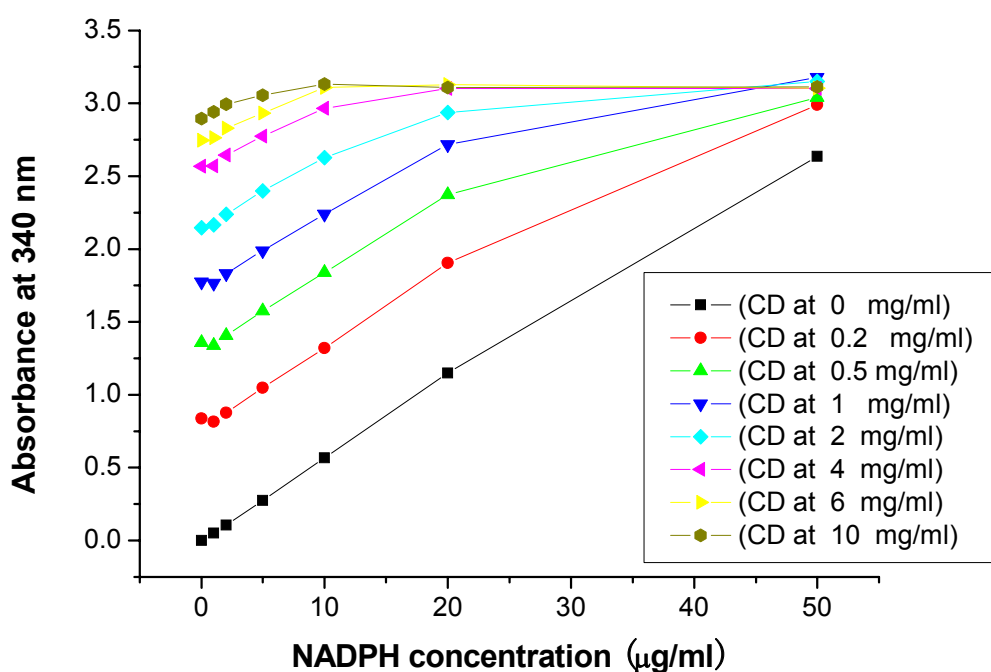


Figure 1. Plot of absorbance against NADPH concentration in various permeabilized cell densities. Harvested cells were washed 3 times with Tris-HCl buffer (pH=7.8) and centrifuged. Afterwards the suspension was diluted with the same buffer to desired cell densities, followed by permeabilization with Triton X-100. After permeabilization, cell suspensions were diluted 20 times (the same ratio as in enzyme assay) with buffer to final cell densities (CD) of 0 mg/ml, 0.2 mg/ml 0.5 mg/ml, 1mg/ml, 2 mg/ml, 4 mg/ml, 6 mg/ml, 10 mg/ml. For each cell density, 8 ml diluted cell suspension was divided evenly into 8 cuvettes and added various amount of NADPH to final concentrations of 0  $\mu\text{g/ml}$ , 1  $\mu\text{g/ml}$ , 2  $\mu\text{g/ml}$ , 5  $\mu\text{g/ml}$ , 10  $\mu\text{g/ml}$ , 20  $\mu\text{g/ml}$ , 50  $\mu\text{g/ml}$ . Absorbance was measured with spectrophotometer at 340 nm.

## Permeabilization for intracellular enzyme activity measurement

good linear relationship was obtained for a range of NADPH concentration from 1 µg/ml to 20 µg/ml for cell densities below 1 mg/ml (CDW). The highest  $A_{340}$  value in this linear range was 2.77. For cell densities between 1 to 6 mg/ml, the corresponding  $A_{340}$  values were linear at NADPH concentrations from 1 µg/ml to only 10 µg/ml with a highest  $A_{340}$  value of 3.11.  $A_{340}$  values below 2.77 increased linearly with rising NADPH concentration at cell densities below 6 mg/ml. For cell densities higher than 6 mg/ml  $A_{340}$  values were still linear although only in a small range from 1 to 10 µg/ml. It was concluded that cell densities above 6 mg/ml are not suitable for enzyme activity measurement.

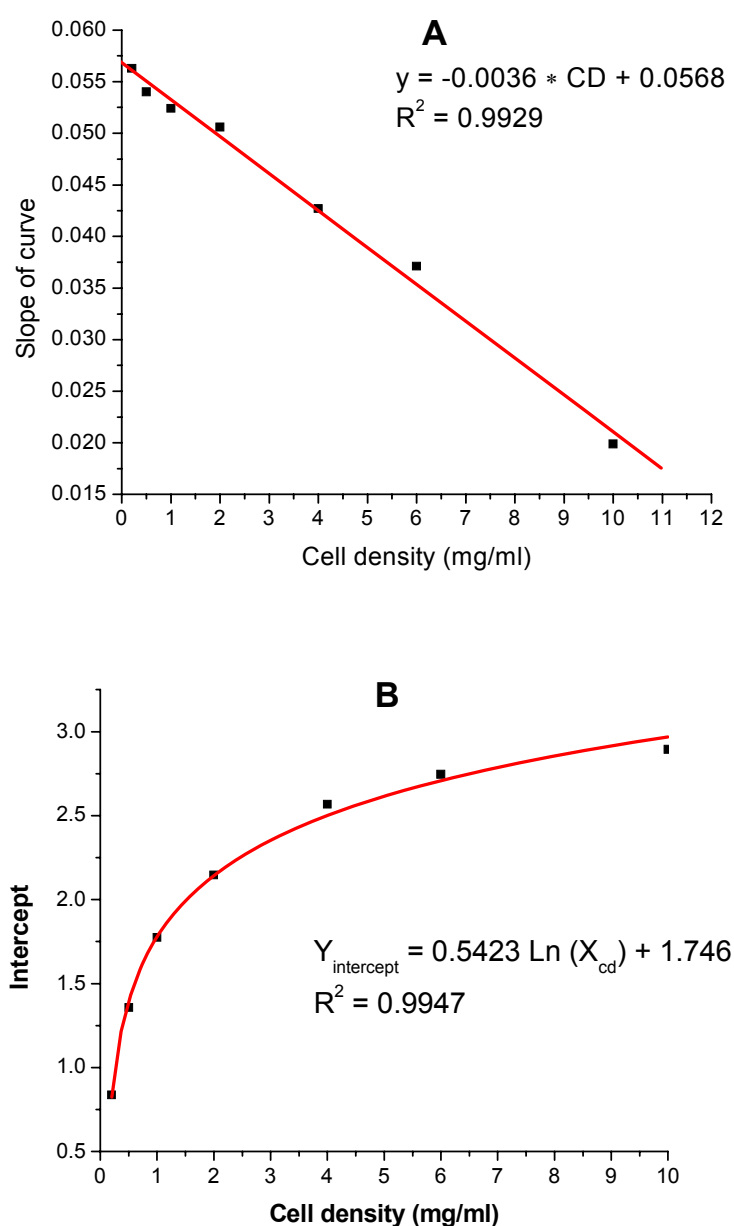


Figure 2. Plot of slopes (A) and intercepts (B) of Table 1 against cell density.

## Permeabilization for intracellular enzyme activity measurement

Table 1 Linear dependency of the absorbance at 340 nm,  $A_{340}$ , on the concentration of NADPH,  $C_{\text{NADPH}}$ , at various cell densities as depicted in Figure 1.

Cell density (mg/ml)	Slope, SL (ml/ $\mu$ g NADPH)	Intercept, IC	$R^2$	$C_{\text{NADPH, max}}$ ( $\mu$ g/ml)
0	0.053	0.0162	0.9986	20
0.2	0.0563	0.759	0.9998	20
0.5	0.054	1.2949	0.9996	20
1	0.0524	1.7216	0.9989	10
2	0.0506	2.1304	0.995	10
4	0.0427	2.5464	0.9917	10
6	0.0371	2.7413	0.9935	10
10	0.0171	2.9634	0.9926	10

Slopes, SL, and intercepts, IC, of the linear parts of the calibration curves depicted in Figure 1 and listed in Table 1 depended on cell densities,  $X_{\text{CD}}$ , in a regular way as is shown in Figure 2. This is described by the equation

$$\text{SL} = -0.0036 X_{\text{CD}} + 0.0568 \quad (1)$$

The intercept depended linearly on the logarithm of cell density as given by

$$\text{IC} = 0.5423 \ln(X_{\text{CD}}) + 1.746 \quad (2)$$

From the above relationships and equations it is possible to determine the NAD(P)H concentration in a cell suspension just by measurement of two different absorptions,  $A_{660}$  and  $A_{340}$ , respectively. The measurement of  $A_{660}$  that is linearly correlated with cell density directly yields slope and intercept using equations 1 and 2. Similar to Lambert-Beer's law, a linear correlation exists between the absorbance at 340 nm,  $A_{340}$ , and NADPH concentration,  $C_{\text{NADPH}}$

$$A_{340} = SL C_{\text{NADPH}} + IC \quad (3)$$

Rearrangement of this equation yields

$$C_{\text{NADPH}} = \frac{A_{340} - IC}{SL} \quad (4)$$

Measurement of  $A_{660}$  and  $A_{340}$  with time eventually allows the determination of enzyme activity.

### 4.3.2 Permeabilization optimization

#### 4.3.2.1 Selection of agents for permeabilization.

Table 2 summarizes effects of treatment using different permeabilization agents on four intracellular enzyme activities: glucose 6-phosphate dehydrogenase, G6PDH, malic enzyme, ME, isocitrate dehydrogenase, IDH, and 6-phospho-gluconate dehydrogenase, 6-PGDH. Untreated cells (control) did not show any activity in contrast to treated cells which show significant variation on different treatments. Except for G6PDH higher activity was observed in cell-free extracts than in permeabilized cells. For G6PDH and 6PGDH the measured activities were very similar for cell-free extract, Triton X-100 and TE. The activities for ME and particularly IDH were significantly higher in cell-free extracts than in permeabilized cells. CTAB treatment was comparable to other permeabilization methods for ME and 6PGDH. In this study, Triton X-100 and TE were investigated in more detail.

#### 4.3.2.1 Effect of cell density on permeabilization.

Washed cells were diluted to final cell densities between 2 mg/ml and 20 mg/ml (CDW). Figure 3A shows that malic enzyme and G6PDH activities increased linearly in Triton X-100 permeabilized cells with cell densities up to 10 mg/ml. The same trend was observed with ME activity in TE permeabilized cells as depicted in Figure 3B. It was reported that permeabilization depends primarily on the ratio of the permeabilization agent to cell number rather than its concentration (Gowda et al. 1991). This means that at higher cell density a higher agent concentration is required which may cause problems in following

## Permeabilization for intracellular enzyme activity measurement

analysis steps. On the other hand, a relatively high protein concentration and therefore high cell concentration is required for a sensitive activity measurement. 10 mg/ml was identified as the optimal cell density for permeabilization in this study.

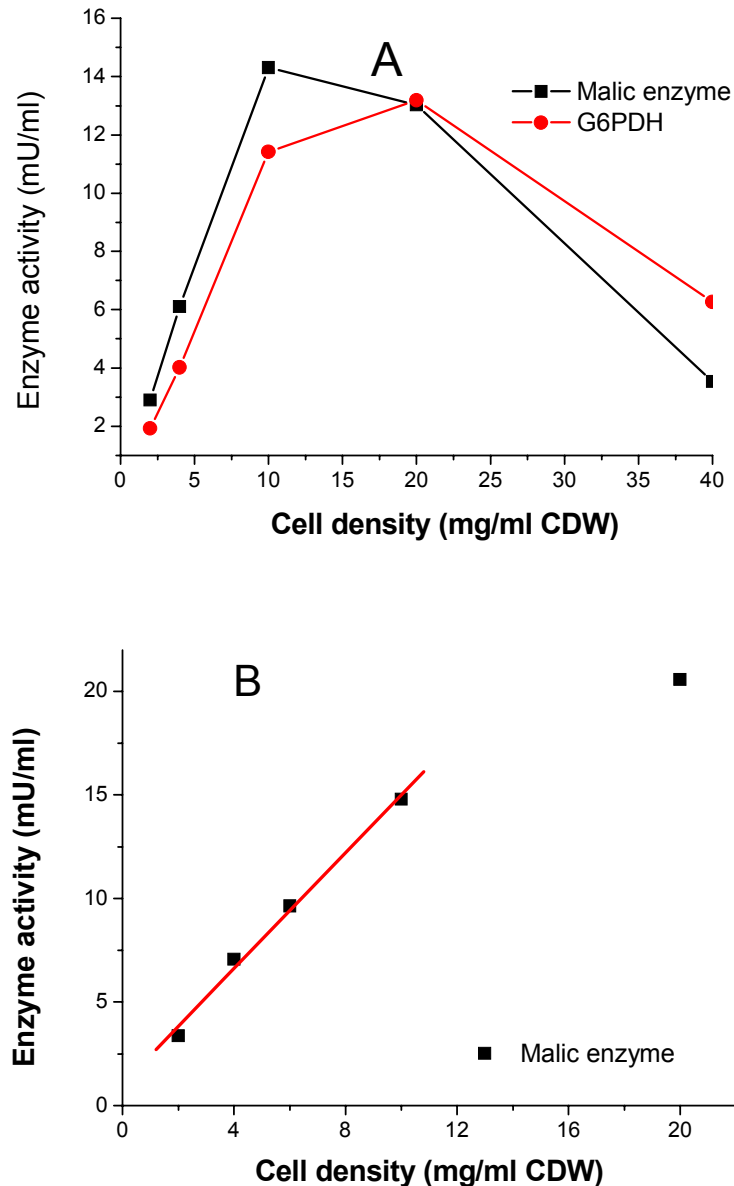


Figure 3. Influence of cell densities on permeabilization in *C. glutamicum*. Enzyme activities in this figure were defined as mU per 1ml reaction system in a cuvette. A: Washed cells were resuspended in Tris-HCl buffer at various densities from 2 to 40 mg/ml (CDW). Triton X-100 was added to each cell density and adjusted to the same final concentration of 0.05 % and then incubated at room temperature for 30 min. B: Washed cells were resuspended in Tris-HCl buffer at different densities from 2 to 20mg/ml (CDW). TE was added to each cell density and adjusted to the same final concentration of 10 % and then incubated at room temperature for 30 min.

### 4.3.2.3 Effect of agent concentration for permeabilization.

Figure 4A shows the effect of Triton X-100 concentration on enzyme activity. The level of both enzyme activities of permeabilized cells increased significantly but not linearly with the Triton X-100 concentration from 0.02 % to 0.05 %. Higher Triton X-100 concentration did not result in any further increase for both enzymes. In contrast relatively high TE concentration was necessary for permeabilization to get highest enzyme activities (Figure 4B). For malic enzyme activity a concentration higher than 20 % was required for the highest activity, but for G6PDH, the highest activity was found at a TE concentration of 10 % and the activity decreased at higher concentrations than 10 %.

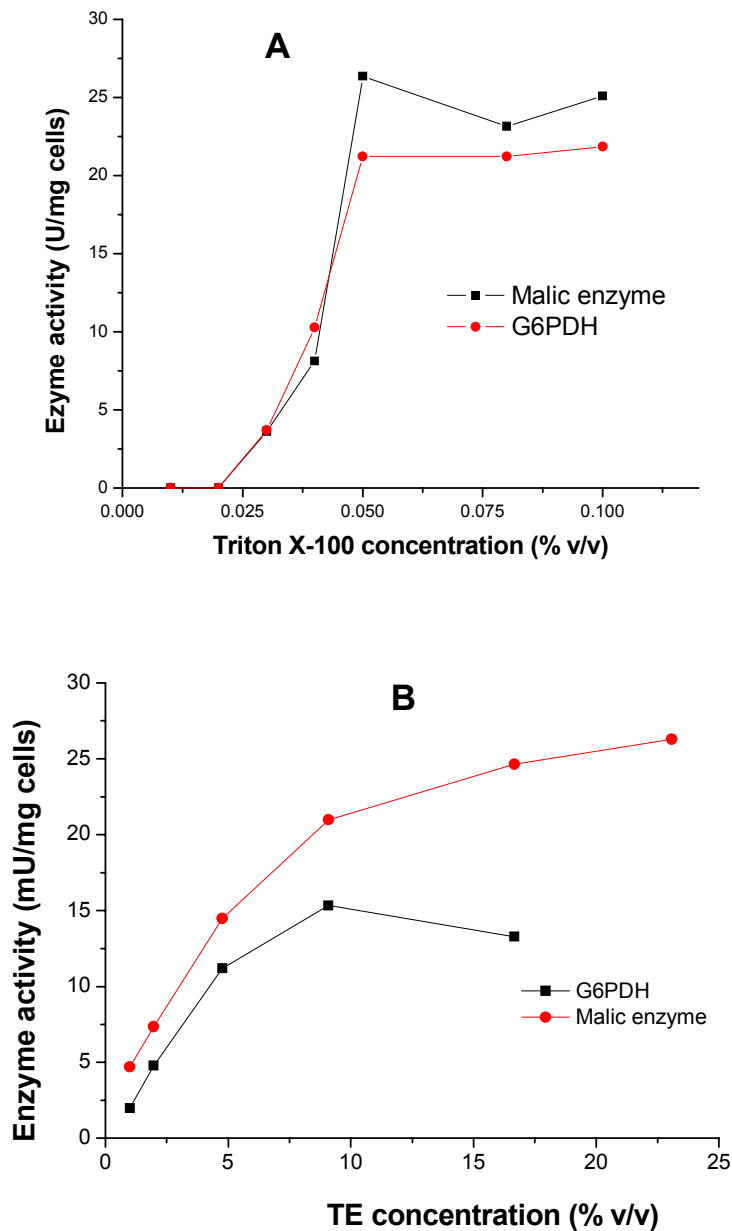


Figure 4. Influence of agent concentration on permeabilization in *C. glutamicum*. Washed cells were resuspended in Tris-HCl buffer at a density of 10 mg/ml (CDW). A: Triton X-100 was added to yield different concentrations from 0.01 % to 0.2 %. B: Triton TE was added to give different concentrations from 1 % to 23 %. The suspension was incubated at room temperature for 30 min and assayed for enzyme activity.

### 4.3.2.4 Effect of incubation condition on permeabilization.

Several different conditions suggested in the literature were tested and results are shown in Figure 5. No significant differences were found under the conditions tested with Triton X-100 permeabilized cells, i.e. freeze/thaw cycles with -70 °C, -20 °C, dry ice bath and incubation at room temperature. Continuous shaking during the incubation at room temperature also did not affect enzyme activities. Room temperature incubation without shaking was found most appropriate and was further studied. For Triton X-100 treated cells, the effect of varying incubation time at room temperature was investigated (Figure 6A). The activities of ME and G6PDH both reached top values after an incubation of 5 minutes and decreased slightly with increasing time. For TE treated permeabilized cells (Figure 6B), a longer time was necessary for both enzymes. After 40 min incubation, ME reached its top activity but G6PDH activity remained constant after 40 min.

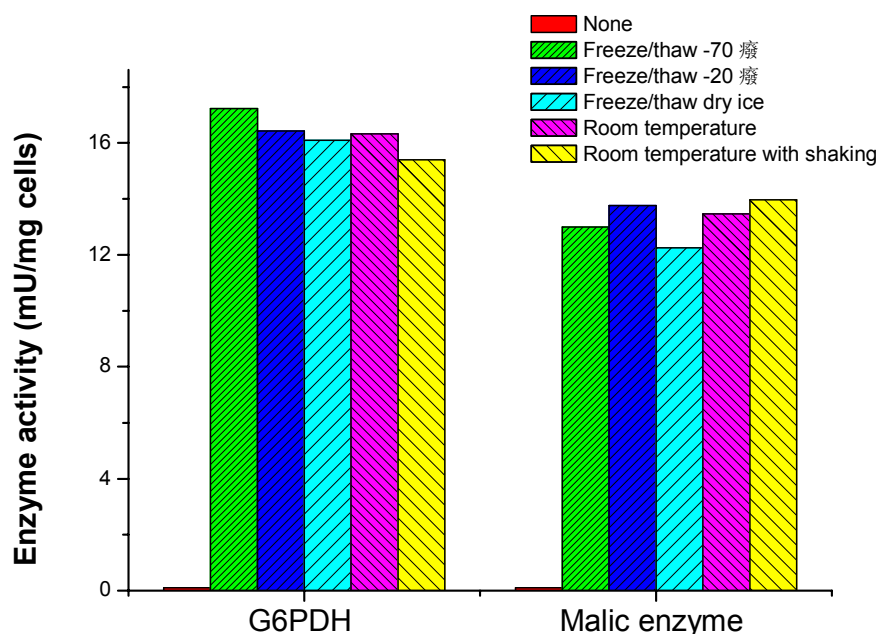


Figure 5. Enzyme activity on permeabilization under different incubation conditions *C. glutamicum* cells were harvested during the exponential growth phase and washed twice with Tris-HCl buffer. The pellet was resuspended in the same buffer to 10 mg/ml (CDW)

## Permeabilization for intracellular enzyme activity measurement

---

and divided into several portions, subjected to further Triton X-100 treatments as indicated below.

Freeze/thaw at -70 °C: Cells were frozen in -70 °C freezer for 24 h and thawed by swirling in a water bath at 30 °C.

Freeze/thaw at -20 °C: Cells were frozen in -20 °C freezer for 24 h and thawed by swirling in a water bath at 30 °C.

Freeze/thaw in dry ice bath: Cells were frozen in dry ice bath for 2 h and thawed by swirling in a water bath at 30 °C.

Room temperature: Triton X-100 was added to a final concentration of 0.05 % and kept at room temperature for 30 min.

Room temperature with shaking: Triton X-100 was added to a final concentration of 0.05 % and the cell suspension was kept shaking at a speed of 500 rpm for 30 min.

### **4.3.2.5 Enzyme-substrate affinity in permeabilized cells.**

The substrate affinity to an enzyme, usually characterized by the Michaelis-Menten kinetic parameter,  $K_m$ , is a key characteristic of an enzyme. In this study,  $K_m$  values of several intracellular enzymes from both cell-free extract and permeabilized cells were determined and compared with literature values for purified enzymes (Table 3).  $K_m$  values of all four enzymes were similar in cell-free extracts and permeabilized cells (Gourdon et al. 2000; Moritz et al. 2000b; Yokota and Lindley 2005)

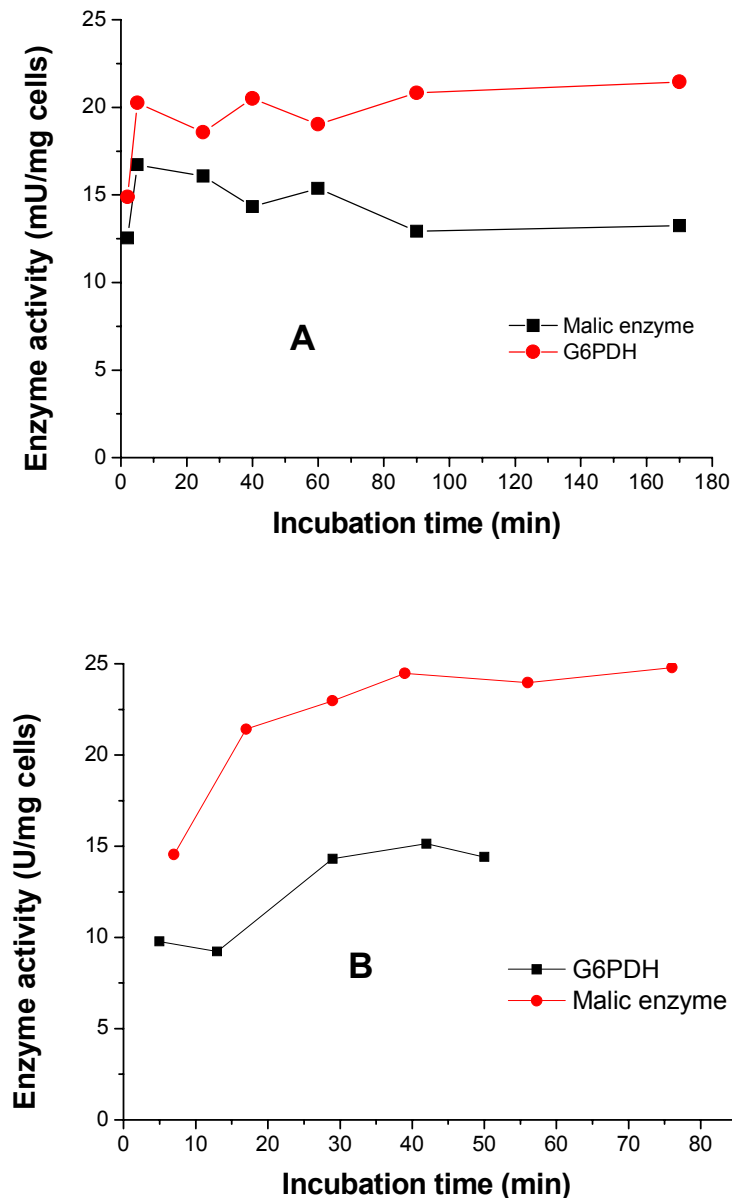


Figure 6. Influence of various incubation times on permeabilization in *C. glutamicum*. Washed cells were resuspended in Tris-HCl buffer at a density of 10mg/ml (CDW). A: Triton X-100 was added to a final concentration of 0.5 %. The suspension was incubated at room temperature for various times from 0 to 170 min and assayed for enzyme activity. B: TE was added to a final concentration of 10 %. The suspension was stored at room temperature for various times from 0 to 80 min and assayed for enzyme activity.

### 4.3.3 Protein release

After washing permeabilized cells, all the supernatants were collected and analyzed for protein secretion. Protein concentration was determined by the Bradford method, bovine

serum albumin was used as the standard. Analyzed protein levels in the supernatant were always below 2 mg/ml, i.e. less than 5 % of the total protein. (data not shown here).

### **4.3.4 Activity analysis in fermentation broth without washing step**

The developed method was also applied directly to fermentation broth without any washing. A cell suspension from a growing culture was taken, directly treated by Triton X-100 and used for enzyme activity measurement. In these experiments linear relationships were also obtained between absorbance at 340nm and NADPH concentration, but the coefficient in equation 1 changed from -0.0036 to -0.0202. Enzyme activities under this condition were only about half of those obtained with a washing step (data not shown here).

Table 2 Activity of selected intracellular enzymes of *C. glutamicum* using enzyme extraction and different methods of permeabilization. All activities are given in mU/mg dry cells.

Enzyme	Control untreated cells	Cell-free extract <sup>a</sup>	TritonX-100 permeabilized cells <sup>b</sup>	TE permeabilized cells <sup>c</sup>	CTAB permeabilized cells <sup>d</sup>	Digitonin permeabilized cells <sup>e</sup>	Ethanol permeabilized cells <sup>f</sup>
Malic enzyme	0	51.1 ± 5.7	20.5 ± 1.9	41.7 ± 3.6	23.7 ± 4.7	16.1±3.6	1.0±0.3
G6PDH	0	22.6 ± 1.5	24.1 ± 2.0	22.0 ± 2.9	5.5 ± 1.8	12.1±3.1	8.8±0.9
IDH	0	304 ± 30	109 ± 13	96.6 ± 12.4	-	-	-
6PGDH	0	36.4 ± 4.4	26.5 ± 4.4	25.6 ± 5.1	24.4 ± 2.4	-	-

*C. glutamicum* cells were harvested during the exponential growth phase and washed twice with Tris-HCl buffer. The pellet was resuspended in the same buffer and diluted to a final cell density of 10 mg/ml (CDW), diluted cells were divided into several aliquots, and subjected to further treatment as indicated below.

<sup>a</sup> Glass-bead treatment followed by direct analysis of enzyme activity in cell-free extract.

<sup>b</sup> Triton X-100 was added to yield a final concentration of 0.05 % and kept at room temperature for 30 min.

<sup>c</sup> TE was added to a final concentration of 10 % and kept at room temperature for 30 min.

<sup>d</sup> CTAB was added to a final concentration of 0.1 % and kept at room temperature for 30 min

<sup>e</sup> Digitonin was added to a final concentration of 0.1 % and kept at room temperature for 30 min.

<sup>f</sup> Ethanol was added to a final concentration of 40 % and kept at room temperature for 30 min.

<sup>b-f</sup> in all cases of permeabilization enzyme activity was directly measured in the resulting cell suspension.

## Permeabilization for intracellular enzyme activity measurement

Table 3  $K_m$  values of enzymes from cell-free extract, permeabilized cells in *C. glutamicum* and literature values of purified enzymes.

$K_m$ value (mM)	Malic enzyme		G6PDH	PGI
	For Malate	For NADP <sup>+</sup>	For G-6-P	For F-6-P
Cell-free extract	13.9±5.2	0.17±0.12	0.14±0.0005	0.34±0.15
Permeabilized cells	10.7±4.0	0.23±0.03	0.092±0.017	0.42±0.12
Data from the literature	3.8±0.6*	0.083±0.017*	0.15±0.021**	0.54***

\*(Gourdon et al. 2000)

\*\* (Moritz et al. 2000a)

\*\*\* (Yokota and Lindley 2005)

Cells were washed by Tris-HCl buffer three times and diluted by the same buffer to 10 mg /ml (CDW). Triton X-100 was added to the cell suspension to a final concentration of 0.05 %. After 30 seconds vortexing, suspension was incubated at room temperature for 10 min, activity measurements were carried out using different substrate concentrations. Measured initial rates were used in a *Lineweaver-Burk plot* to determine  $K_m$  values.

Data from three or four independent experiments (average±standard deviation) are listed.

### 4.4 Discussion

There is an ongoing discussion whether *in vitro* enzyme characteristics can be directly applied for describing the dynamics of complex metabolic networks (Reuss et al. 2007). It is very difficult and sometimes even not possible to directly measure intracellular enzyme activity and kinetic characteristics in intact whole cells due to the cell membrane permeability barrier. Only pulse techniques combined with appropriate measurement of intracellular metabolite profiles and modelling permits the *in vivo* kinetic analysis (Nikerel et al. 2009; Reuss et al. 2007). For metabolic enzyme kinetic research, traditional studies using purified enzymes or cell-free extracts, which are called *in vitro* conditions, is restricted because many unknown interactions, e.g. between enzymes and other effecting proteins, may influence the final results that will then be different from *in vivo* conditions (Reuss et al. 2007). In addition, the preparation procedure is generally complex and time consuming. Enzymes in gently

## Permeabilization for intracellular enzyme activity measurement

---

permeabilized cells are assumed to be much closer to their *in vivo* condition and therefore more suitable to be applied in metabolic studies. In this article, permeabilization of *C. glutamicum* was investigated for potential applications for metabolic enzyme kinetic study.

The influence of cell density on the absorbance at 340 nm for NADPH determination was investigated in detail in this study, which is very important for NAD(P)H-dependent enzyme activity measurement. Absorbance values of the enzymatic reaction system containing permeabilized cells cannot be directly used for activity calculation only after appropriate correction. Since NADH has an absorption spectrum very similar to NADPH, the results of this report are directly applicable to NADH dependant enzymes.

The results using crude fermentation broth indicate the possibility of high-throughput screening of mutants using the permeabilization method in microtiter plates. After pipetting into wells, mixing with the permeabilization agent and corresponding enzyme substrates and incubating for appropriate time, absorbances at 660 nm and 340 nm could be read with a microplate reader. After correction of absorbance using equation 4, activities can be easily calculated and compared. In this way a large number of mutants could be screened in a short time. Besides to *C. glutamicum*, this method could be also applied to other organisms.

Many agents have been applied for permeabilization in various organisms. The efficiency of different agents on permeabilization are different (Table 2). Triton X-100 and TE were most suitable for *C. glutamicum* for enzyme activity measurement. Compared to TE, treatment with Triton X-100 needs much lower concentration and shorter incubation time. If other analytical methods, e.g. using mass spectrometry with ion spray ionization or MALDI, are applied, it might be necessary to remove the permeabilizing agent. Since Triton X-100 is a detergent, it is very difficult to remove. However, TE could be removed easily by evaporation.

The environment of enzymes in permeabilized cells (*in situ*) is thought to be closer to that in living cells (*in vivo*) compared to cell-free extract (*in vitro*). Therefore, the kinetics of enzymes *in situ* is assumed be closer to *in vivo* conditions than *in vitro* kinetics.  $K_m$  value is regarded as a key parameter for kinetic study and values from *in situ* condition are assumed to be closer to those *in vivo* condition. In our experiments  $K_m$  values of enzymes measured in

permeabilized cells were similar to those from cell-free extract, whereas other reports reported differences, however using different cells (Alamae and Jarviste 1995; Serrano et al. 1973). In this study,  $K_m$  values of both malic enzyme and G6PDH were clearly higher than those of purified enzymes reported in the literature (Gourdon et al. 2000; Moritz et al. 2000b). Only for PGI  $K_m$  values measured here were slightly lower than those reported in the literature (Yokota and Lindley 2005).

### 4.5 Conclusion

NAD(P)H-dependent intracellular enzyme assays in permeabilized cell suspension were investigated in this study. Permeabilization of *C. glutamicum* cells depends on several variables such as agent type, cell density, agent concentration but less on the incubation condition. The optimized permeabilization condition in *C. glutamicum* by Triton X-100 was obtained with CDW concentration of 10 mg/ml and treatment with 0.05 % Triton X-100 at room temperature for only 5 minutes. TE treatment needed a concentration of 10 % and a much longer incubation time of more than 40 min to get the highest enzyme activity. Compared to cell-free extract preparation, permeabilization is a rapid, simple and mild technique. Using this method single enzyme activity measurements for the dehydrogenases G6PDH, 6PGDH and ME as well as for PGI were carried out successfully. Furthermore, permeabilized cells can provide intracellular enzymes whose properties are assumed to be more similar to those of *in-vivo* conditions.

### References:

- Alamae T, Jarviste A. 1995. Permeabilization of the Methylophilic Yeast *Pichia-Pinus* for Intracellular Enzyme Analysis - a Quantitative Study. *Journal of Microbiological Methods* 22(2):193-205.
- Becker J, Klopprogge C, Zelder O, Heinzle E, Wittmann C. 2005. Amplified expression of fructose 1,6-bisphosphatase in *Corynebacterium glutamicum* increases in vivo flux through the pentose phosphate pathway and lysine production on different carbon sources. *Appl Environ Microbiol* 71(12):8587-96.
- Chelico L, Khachatourians GG. 2003. Permeabilization of *Beauveria bassiana* blastospores for in situ enzymatic assays. *Mycologia* 95(5):976-981.
- Choudary PV. 1984. A simple micromethod for rapid kinetic analyses of yeast enzymes in situ. *Anal Biochem* 138(2):425-9.
- Crotti LB, Drgon T, Cabib E. 2001. Yeast cell permeabilization by osmotic shock allows determination of enzymatic activities in situ. *Anal Biochem* 292(1):8-16.
- Felix H. 1982. Permeabilized cells. *Anal Biochem* 120(2):211-34.
- Galabova D, Tuleva B, Spasova D. 1996. Permeabilization of *Yarrowia lipolytica* cells by Triton X-100. *Enzyme and Microbial Technology* 18(1):18-22.
- Gourdon P, Baucher MF, Lindley ND, Guyonvarch A. 2000. Cloning of the malic enzyme gene from *Corynebacterium glutamicum* and role of the enzyme in lactate metabolism. *Appl Environ Microbiol* 66(7):2981-7.
- Gowda LR, Bachhawat N, Bhat SG. 1991. Permeabilization of Bakers-Yeast by Cetyltrimethylammonium Bromide for Intracellular Enzyme Catalysis. *Enzyme and Microbial Technology* 13(2):154-157.
- Gowda LR, Joshi MS, Bhat SG. 1988. In situ assay of intracellular enzymes of yeast (*Kluyveromyces fragilis*) by digitonin permeabilization of cell membrane. *Anal Biochem* 175(2):531-6.
- Graham JW, Williams TC, Morgan M, Fernie AR, Ratcliffe RG, Sweetlove LJ. 2007. Glycolytic enzymes associate dynamically with mitochondria in response to respiratory demand and support substrate channeling. *Plant Cell* 19(11):3723-38.
- Heijnen JJ. 2005. Approximative kinetic formats used in metabolic network modeling. *Biotechnol Bioeng* 91(5):534-45.

- Heinzle E, Yuan Y, Kumar S, Wittmann C, Gehre M, Richnow HH, Wehrung P, Adam P, Albrecht P. 2008. Analysis of <sup>13</sup>C labeling enrichment in microbial culture applying metabolic tracer experiments using gas chromatography-combustion-isotope ratio mass spectrometry. *Anal Biochem* 380(2):202-10.
- Kelle R, Hermann T, Bathe B. 2005. L-Lysine Production. In: Eggeling L, Bott M, editors. *Handbook of Corynebacterium glutamicum*. Boca Raton: CRC Press. p 465-488.
- Kiefer P, Heinzle E, Zelder O, Wittmann C. 2004. Comparative metabolic flux analysis of lysine-producing *Corynebacterium glutamicum* cultured on glucose or fructose. *Appl Environ Microbiol* 70(1):229-39.
- Kimura E. 2005. L-Glutamate Production. In: Eggeling L, Bott M, editors. *Handbook of Corynebacterium glutamicum*. Boca Raton: CRC Press. p 439-464.
- Kromer JO, Heinzle E, Schroder H, Wittmann C. 2006. Accumulation of homolanthionine and activation of a novel pathway for isoleucine biosynthesis in *Corynebacterium glutamicum* McbR deletion strains. *J Bacteriol* 188(2):609-18.
- Krömer JO, Sorgenfrei O, Klopprogge K, Heinzle E, Wittmann C. 2004. In-depth profiling of lysine-producing *Corynebacterium glutamicum* by combined analysis of the transcriptome, metabolome, and fluxome. *Journal of Bacteriology* 186(6):1769-84.
- Miozzari GF, Niederberger P, Hutter R. 1978. Permeabilization of microorganisms by Triton X-100. *Anal Biochem* 90(1):220-33.
- Miranda HV, Ferreira AE, Cordeiro C, Freire AP. 2006. Kinetic assay for measurement of enzyme concentration in situ. *Anal Biochem* 354(1):148-50.
- Moritz B, Striegel K, De Graaf AA, Sahm H. 2000. Kinetic properties of the glucose-6-phosphate and 6-phosphogluconate dehydrogenases from *Corynebacterium glutamicum* and their application for predicting pentose phosphate pathway flux *in vivo*. *European Journal of Biochemistry* 267(12):3442-52.
- Nikerel IE, van Winden WA, Verheijen PJ, Heijnen JJ. 2009. Model reduction and a priori kinetic parameter identifiability analysis using metabolome time series for metabolic reaction networks with linlog kinetics. *Metab Eng* 11(1):20-30.
- Reuss M, Aguilera-Vázquez L, Mauch K. 2007. Reconstruction of dynamic network models from metabolite measurements. In: Nielsen J, Jewett MC, editors. *Metabolomics - A Powerful Tool in Systems Biology*. Heidelberg: Springer. p 97-127.

## Permeabilization for intracellular enzyme activity measurement

---

- Serrano R, Gancedo JM, Gancedo C. 1973. Assay of yeast enzymes in situ. A potential tool in regulation studies. *Eur J Biochem* 34(3):479-82.
- Shearer G, Lee JC, Koo JA, Kohl DH. 2005. Quantitative estimation of channeling from early glycolytic intermediates to CO in intact *Escherichia coli*. *Febs J* 272(13):3260-9.
- Somkuti GA, Dominiecki ME, Steinberg DH. 1998. Permeabilization of *Streptococcus thermophilus* and *Lactobacillus delbrueckii* subsp. *bulgaricus* with ethanol. *Curr Microbiol* 36(4):202-6.
- Vanderwerf MJ, Hartmans S, Vandentweel WJJ. 1995. Permeabilization and Lysis of *Pseudomonas Pseudoalcaligenes* Cells by Triton X-100 for Efficient Production of D-Malate. *Applied Microbiology and Biotechnology* 43(4):590-594.
- Wittmann C, Becker J. 2007. The L-lysine story: From metabolic pathways to industrial production. *Microbiology Monographs: Springer Berlin/ Heidelberg* p39-70.
- Wittmann C, de Graaf A. 2005. Metabolic flux analysis in *Corynebacterium glutamicum*. In: Eggeling L, Bott M, editors. *Handbook of Corynebacterium glutamicum*. Boca Raton: CRC Press. p 277-304.
- Wittmann C, Heinzle E. 2001. Application of MALDI-TOF MS to lysine-producing *Corynebacterium glutamicum*: a novel approach for metabolic flux analysis. *Eur J Biochem* 268(8):2441-55.
- Wittmann C, Heinzle E. 2002. Genealogy profiling through strain improvement by using metabolic network analysis: metabolic flux genealogy of several generations of lysine-producing corynebacteria. *Appl Environ Microbiol* 68(12):5843-59.
- Wittmann C, Heinzle E. 2008. Metabolic Network Analysis and Design in *Corynebacterium glutamicum*. In: Burkovski A, editor. *Corynebacteria. Genomics and Molecular Biology*. Norfolk UK: Caister Academic Press. p 79-112.
- Wittmann C, Kim HM, Heinzle E. 2004. Metabolic network analysis of lysine producing *Corynebacterium glutamicum* at a miniaturized scale. *Biotechnol Bioeng* 87(1):1-6.
- Yang TH, Wittmann C, Heinzle E. 2006. Respirometric <sup>13</sup>C flux analysis--Part II: in vivo flux estimation of lysine-producing *Corynebacterium glutamicum*. *Metab Eng* 8(5):432-46.
- Yokota A, Lindley ND. 2005. Central metabolism: Sugar uptake and conversion. In: Eggeling L, Bott M, editors. *Handbook of Corynebacterium glutamicum*. Boca Raton: CRC Press. p 215-240.

## Chapter 5

### ***In-situ* multi-enzyme network kinetics study using MALDI-TOF MS**

#### **Abstract**

A novel strategy was developed for the determination of *in-situ* enzymatic network kinetics combining permeabilization and matrix-assisted laser desorption/ionization time-of-flight mass spectrometry (MALDI-TOF-MS) quantification. Quantification of small molecular mass metabolites in glycolysis and pentose-phosphate pathway using MALDI-TOF-MS with [U-<sup>13</sup>C<sub>6</sub>] glucose-6-phosphate as single internal standard was established. Signal suppression during MALDI analysis could be compensated by applying the standard addition method. Permeabilized cells are considered closer to the *in-vivo* situation than purified enzyme(s) for the study of kinetics. Adding selected substrates and cofactors, kinetics of glycolysis and pentose-phosphate pathways could be characterized using this method. During the experiment the carbon balance was nearly closed indicating quantitative analysis of all important substrates and products accumulated in the reaction mixture.

This chapter has been submitted to Analytical Biochemistry as: Yuan Y, Heinzle E. 2010. *in-situ* multi-enzyme network kinetics study using MALDI-TOF MS.

### 5.1 Introduction

For one century, enzymologists utilize isolated enzymes for their kinetic characterization. The increasing involvement in describing metabolic network kinetics in a systems biological context uncovers limitations of this classical approach. Metabolite channeling, characterized by the direct transfer of intermediates from one enzyme to the next (Graham et al. 2007b), and macromolecular crowding effects causing modified enzyme kinetic properties (Minton 2006; Zhou et al. 2008) can cause differences between *in-vivo* and *in-vitro* kinetics. Therefore, determining enzyme kinetic parameters directly inside the living cell is highly expected to overcome the limitations listed above (Snoep and Rohwer 2005; van Dam et al. 2002). This is however experimentally limited as it requires the analysis of intracellular metabolites, which is a partly still unsolved problem (Bolten et al. 2007). Additionally, it allows only limited perturbation of the system because of the limited transport of substrate through the cell membrane. Careful permeabilization of the cell keeps its morphology largely intact, and most of the intracellular enzymes seem to be active and stay in their original macromolecular environment (Felix 1982; Yuan and Heinzle 2009). This condition is called *in-situ* and is regarded as closer to the *in-vivo* state than commonly used *in-vitro* conditions. It is therefore promising for intracellular enzymatic network kinetic investigations (Martins et al. 2001a; Martins et al. 2001b; Serrano et al. 1973).

MALDI-TOF MS is utilized mainly to determine the molecular weight of macro-molecules like peptides by detecting the time of flight to a detector in an electric field. By the use of appropriate matrices and internal standard, a wide range of biomolecules can be analyzed by MALDI-TOF MS (Lasaosa et al. 2009a; Lasaosa et al. 2009b; Simm et al. 2009; Tholey et al. 2002). Due to its high sensitivity, good mass resolution, high speed and simplicity (Duncan et al. 2008; Szajli et al. 2008), recently it was also applied to quantitative determination of low molecular mass compounds of biological interest without analyte separation step (Zabet-Moghaddam et al. 2004a) as well as involving appropriate analyte separation (Mims and Hercules 2003; Mims and Hercules 2004). There are, however, some limitations for quantification using MALDI-TOF MS. Suppression effects, either originating from the matrix or from the analytes themselves, are one of the major impediments for quantitative measurement (Lou et al. 2009; Vaidyanathan et al. 2006). In complex samples, some analytes which are more competing for the available protons can suppress other analytes. Separation

## *In situ* network kinetic study using MALDI-TOF MS

and clean-up operations can partly eliminate this suppression, but make the protocol much more complicated. Therefore this can be applied only in cases in which more accurate information is required. In practice, the analysis of a large number of biological samples requires high speed analysis without pretreatment steps, and a slight reduction of accuracy is acceptable.

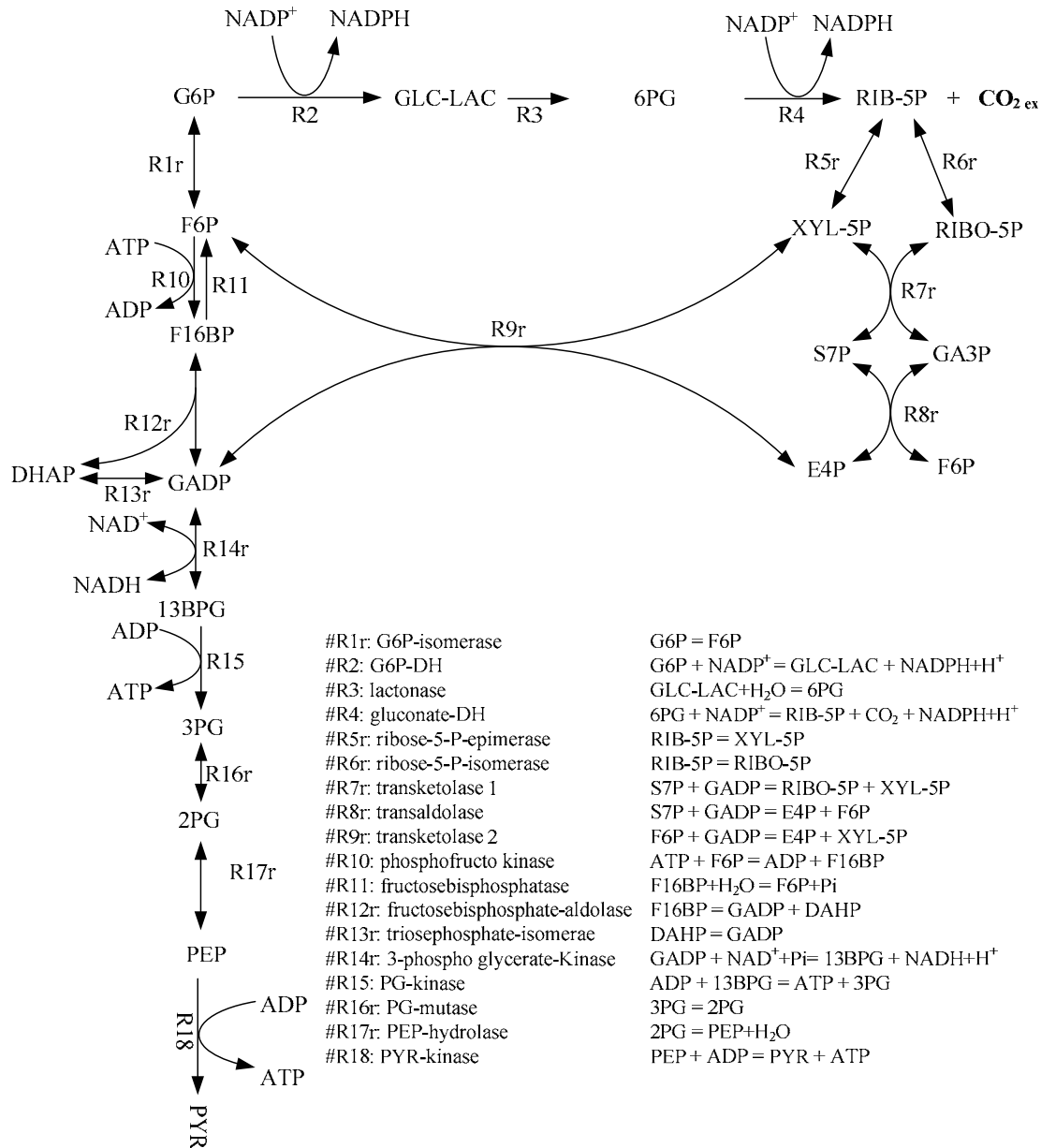


Figure 1. Schematic diagram of the metabolic network investigated in this study.

The suitability for metabolome analyses using MALDI has been investigated using the conventional matrices DHB and CHCA and measuring in the positive ion mode

(Vaidyanathan et al. 2006). Several metabolites in a synthetic mixture can be detected using both solid and ionic liquid matrices in parallel. Another matrix, 9-aminoacridine, was more recently tested and regarded as more suitable for the detection of low molecular mass metabolites (Edwards and Kennedy 2005; Rachal L. Vermillion-Salsbury 2002), as well as for quantification (Mims and Hercules 2003; Mims and Hercules 2004; Vaidyanathan and Goodacre 2007).

Internal standards are necessary for quantification to compensate for the inhomogeneous distribution of matrix and target molecules in samples. Selection of internal standard is critical for the measurement (Wilkinson et al. 1997). Stable-isotope labeled forms (isotopomers) of the analyte has been proven an ideal internal standard because of their highest possible chemical, physical, and mass similarity to the analyte (Duncan et al. 2008). Unfortunately, for many compounds such standards are not commercially available.

The first objective of this study was to develop a sensitive and rapid method for quantitative measurement of low molecular mass metabolites involved in glycolysis and pentose-phosphate pathway (Figure.1). Some pioneering investigations have already been carried out applying MALDI-TOF MS for enzyme activity measurement (Tholey et al. 2002) and low molecular mass quantification (Tholey et al. 2002; Zabet-Moghaddam et al. 2004a). In this study we investigated quantitative measurement of metabolites with MALDI mass spectrometry using 9-aminoacridine as matrix. [U-<sup>13</sup>C<sub>6</sub>] glucose-6-phosphate, enzymatically synthesized from [U-<sup>13</sup>C<sub>6</sub>] glucose, was tested as a single internal standard to quantify other metabolites of glycolysis and the pentose-phosphate pathway. Kinetics of these two pathways was investigated by the combination of the developed quantification method and permeabilization technique.

## In situ network kinetic study using MALDI-TOF MS

Table1. Negative ion signals of metabolites used in this study as observed in MALDI-TOF MS.

No.	Metabolite	Abbreviation	[M-H] <sup>-</sup>
1	Glucose-6-phosphate / Fructose-6-phosphate	G6P/ F6P	259.30
2	Fructose-1, 6-biphosphate	F16BP	339.36
3	Dihydroxyacetone phosphate / Glyceraldehydes 3-phosphate	DHAP/ GADP	169.16
4	3-phosphoglycerate/2-phosphoglycerate	3PG/2PG	185.17
5	Phosphoenolpyruvate	PEP	167.14
6	Pyruvate	PYR	87.06
7	6-phosphogluconate	6PG	275.32
8	Ribulose 5-phosphate/Ribose 5-phosphate/Xylulose 5-phosphate	P5P	229.25
9	Sedoheptulose 7-phosphate	S7P	289.34
10	1, 3-bisphosphoglycerate	13BPG	265.23
11	Erythrose 4-phosphate	E4P	199.21
12	[U- <sup>13</sup> C <sub>6</sub> ] Glucose-6-phosphate	[U- <sup>13</sup> C <sub>6</sub> ] G6P	265.33

## 5.2 Materials and methods

### Chemicals and enzyme

[U-<sup>13</sup>C<sub>6</sub>] Glucose (99 atom % <sup>13</sup>C) was purchased from Cambridge Isotope Laboratories (Andover, MA, USA). The matrix, 9-aminoacridine (9AA), was purchased from Sigma-Aldrich (St Louis, Mo, USA). All the commercially available metabolites listed in Table 1 were from Sigma-Aldrich (St Louis, Mo, USA). Water was purified by a Millipore water purification system (Bedford, MA, USA). Hexokinase from *Saccharomyces cerevisiae* with an activity of 2285 U/mg was purchased from Sigma-Aldrich (St Louis, Mo, USA).

### Microorganism

*C. glutamicum* ATCC 13032 wild type was purchased from the American Type Strain and Culture Collection (Manassas, USA).

### Sample preparation

The cultivation of *C. glutamicum* ATCC 13032 was the same as described earlier (Heinzle et al. 2008b). Cells in the exponential growth phase (OD<sub>660</sub>=10) were harvested and permeabilized as described before (Yuan and Heinzle 2009). Permeabilized cells were

subsequently washed 3 times by centrifugation (5000 rpm, 5 min, 4 °C) with ammonium bicarbonate buffer (100 mM NH<sub>4</sub>HCO<sub>3</sub>, pH adjusted to 7.8 by acetic acid). Washed cells were diluted with the same ammonium bicarbonate buffer to a cell density of 200 mg/mL (wet weight).

### **Enzyme stability comparison between in-vitro and in-situ**

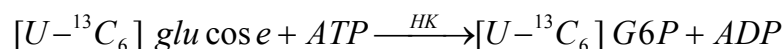
Experimental procedures for cell disruption using glass beads (in-vitro) and permeabilization (in-situ) were applied as described earlier (Yuan and Heinzle 2009). After treatment both solutions containing enzymes were kept on ice in a 4°C cold room. The malic enzyme and glucose 6-phosphate dehydrogenase activities from above two sources were tested over 48 h. Activities in the supernatant (the supernatant directly harvested after Triton X-100 treatment) of permeabilized cells were measured as well. Detailed enzyme assays were described earlier (Yuan and Heinzle 2009).

### ***In-situ* kinetic experiment and sampling**

15 mL Eppendorf tube (EP) containing diluted permeabilized cells was pre-warmed in a water bath for 2 min at 30°C. Substrates and cofactors were added to designed concentrations to start reaction. During the whole reaction, EP tube was shaken manually from time to time. Samples were collected and treated in two different ways: (A) during the first 2 min of incubation samples were taken and filtered through a 0.2 µm cellulose acetate membrane filter (VWR, USA) connected to a 5 mL syringe (Tuttlingen, Germany). The filtrate was collected and stored at -20°C; (B) after 2 min samples were quickly centrifuged for 1 min at 5000 rpm and -9 °C, supernatants were stored at -20°C.

### **Synthesis of internal standard**

In this study, [U-<sup>13</sup>C<sub>6</sub>] glucose 6-phosphate was tested as internal standard for the quantitation of several metabolites. It was synthesized using hexokinase (HK):



1 mL ammonium bicarbonate-acetic acid buffer reaction system (pH=7.8) containing 2 mM [U-<sup>13</sup>C<sub>6</sub>] glucose, 2 mM ATP and 10 mM Mg<sup>2+</sup> was pre-warmed at 25°C for 2 min. 100 units of hexokinase was added to start the reaction. After 30 min, the enzyme was removed by

## *In situ* network kinetic study using MALDI-TOF MS

---

centrifugation using 10 kDa NMWL (Nominal Molecular Weight Limit) filter (Millipore) and the supernatant was stored at -20°C until used.

### **MALDI-TOF mass spectrometry**

The experiments were carried out on a 4800 TOF/TOF Analyzer mass spectrometer (Applied Biosystems, Darmstadt, Germany) in negative ion reflector mode. A pulsed 200 Hz solid state Nd: Yag laser with a wavelength of 355 nm was utilized in the system. The laser energy was set from 3000 units to 5000 units for both metabolite standards and real samples. One single mass spectrum was formed from 25 sub-spectra per spot using 50 accepted laser shots each. More details were described earlier (Tholey et al. 2002).

### **MALDI sample preparation**

The matrix 9AA was dissolved in methanol to a concentration of 9 mg/mL. All standard metabolites were dissolved in Milli-Q water. The dried droplet method was applied for sample preparation. Matrix-to-analyte ratio (M/A ratio) was set in the range of 2.5: 1 to 50: 1 and optimized during experiments. For mass spectrometry measurement, equal volumes of the analyte(s) solution and matrix solutions were mixed and 0.6 µl of this mixture was spotted on a stainless steel 384-well MALDI-MS target plate and dried in air for 5 min.

### **Quantitative MALDI-TOF MS analysis**

Samples from experiments were mixed with [U-<sup>13</sup>C<sub>6</sub>] G6P internal standard at an optimized volume ratio and analyzed by MALDI-TOF MS. The peak height ratio of metabolite to internal standard was calculated. The concentrations of metabolites were subsequently calculated by the use of obtained calibration curves (see next section).

### **Calibration curves**

For the test of suppression effects, the standard curves were prepared in two ways: (1) each individual metabolite standard was serially diluted to desired concentrations and then mixed with internal standard and matrix; (2) equal amounts of all metabolite standards were mixed and serially diluted to required concentrations and then mixed with internal standard and matrix. Metabolite standard, internal standard and matrix were mixed at a volume ratio of 1:1:2, this ratio was later optimized. The peak height ratio for each individual sample,  $R_{ind}$ ,

which contained a single metabolite standard, and the peak height ratio for the same metabolite in the mixture,  $R_m$ , were calculated. The average ratio of the peak heights was then plotted against the concentration of the metabolite.

### **Estimation of metabolite concentration in kinetic experiment samples**

The matrix effects and signal suppression required an extension of the analytical procedure for the kinetic experiments using the standard addition method (Duncan et al. 2008). A mixture of 15 samples form a kinetic experiment (see Table 2) was used as background for all measurements. To this, different concentrations of metabolite standard mixtures were added and measured using MALDI-TOF MS as described above. Calibration curves were created by plots of ratios of peak height for each metabolite standard and [U- $^{13}$ C $_6$ ] glucose internal standard against the real concentrations for 6 metabolite standards. The ratio of metabolites to IS ( $R_A$ ) was calculated as given below:

$$\text{Intensity ratio} = \frac{\text{Metabolites intensity}}{\text{Internal standard intensity}} \quad (1)$$

$$R_A = \text{Intensity ratio}(\text{background} + \text{standard}) - \text{Intensity ratio}(\text{background}) \quad (2)$$

For samples with higher concentrations of F16BP it was necessary to carry out the standard addition method for each individual sample instead of using the mixture of 15 samples. The calibration curve was calculated using linear regression of Microsoft Excel 2003.

## **5.3 Results and discussion**

### **Mass spectrum of metabolites**

A negative-ion MALDI spectrum of metabolites and internal standard cocktail using 9AA as matrix is depicted in Figure. 2. The internal standard, [U- $^{13}$ C $_6$ ] G6P, has a peak at 265.33 m/z. The metabolites show peaks in the range of 167.1 m/z to 339.4 m/z. Other peaks also can be

seen which are either from matrix or other unknown origin. However, these unknown peaks did not interfere with the peaks of interest.

### **Calibration curves and suppression**

The intensity obtained from MALDI-TOF MS can not be directly used for quantification because of its dependence on other metabolite and buffer concentrations. Therefore, internal standard is necessary for quantitative measurement. It is expected to compensate for systematic and random errors and partly eliminate influences from other compounds in the sample.

Figure. 3 shows calibration curves by plots of ratios of peak height for each metabolite standard and [U-<sup>13</sup>C<sub>6</sub>] G6P internal standard against the real concentrations for 6 metabolite standards. For all metabolites, the resulting calibration curves, either spiked individually or in a mixture, show good linear relationships. Correlation coefficients ( $R^2$ ) are from 0.9876 to 1. Except for G6P/F6P, the slopes of the standard mixture are significantly different from the individual metabolites. The largest and smallest differences of the slopes were for 6PG and G6P/F6P, which differed 6.7-fold and by 8.8%, respectively. Other 4 metabolites have differences from 22.7% to 33.4%.

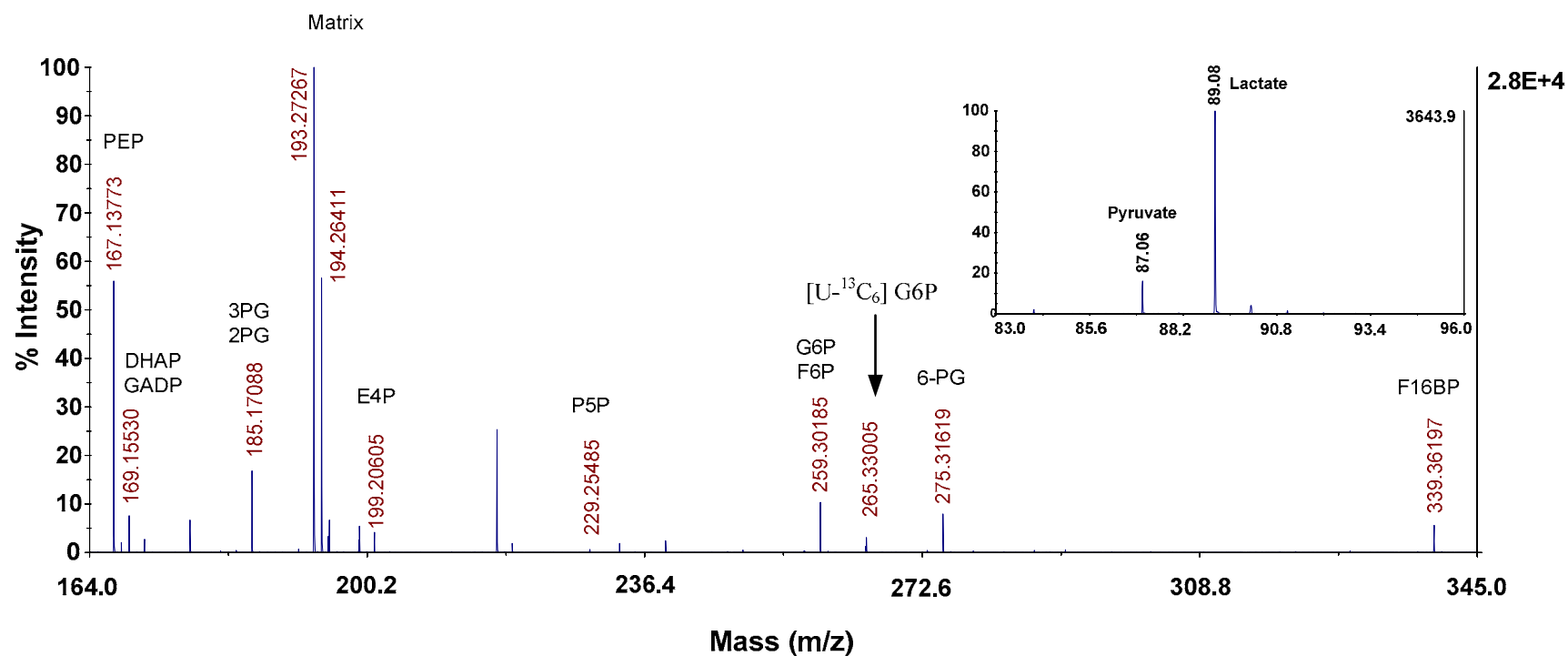


Figure 2. MALDI mass spectrum of the metabolite cocktail in the negative ion mode using 9AA as matrix. The mass-spectrum was obtained from a sample containing 1  $\mu$ M of each metabolite and internal standard. Details of sample preparation are provided in the Materials and Methods section.

Generally, for quantification of low molecular mass compounds, stable isotope labeled isotopomers of each analyte would be the optimal internal standard (Duncan et al. 2008) but are not available as stated earlier. However, since calibration curves from all these 6 metabolites depicted in Figure. 3 show very good linearity, this internal standard seems applicable not only for G6P, but also for the other 5 metabolites. Measurements under the same condition but without internal standard were also performed. However, obtained calibration curves were not linear (data not shown here). These 6 metabolites in glycolysis and pentose-phosphate pathway have quite similar structures, especially they are all phosphorylated. Therefore they are expected to have chemical and physical properties, e.g. charge, very close to the internal standard. Systematic and random errors can be compensated by the use of the internal standard [ $U\text{-}^{13}\text{C}_6$ ] G6P, but errors originating from signal suppression, which is caused by the changes of concentrations of other compounds in the samples, could not be compensated completely. The influence of this suppression can be seen from the different slopes of calibration curves in Figure. 3. The use of internal standard and the optimization of the measurement parameters could significantly decrease this suppression, but could not completely eliminate it. Compared to the other 5 metabolites, the slope differences of G6P/F6P were much smaller, most likely caused by the closer similarity to the internal standard and analyte. Based on this finding, the ideal internal standard would consist of stable isotopomers of all individual metabolites.

The variations of concentration of other components, e.g. buffer, can also cause analyte suppression. To test the degree of suppression in real samples, each metabolite standard sample was mixed with a real experimental sample as background which contained all these 6 metabolites as well as the corresponding buffer. The added volume and component of this real experimental sample is identical for all standards (Figure. 4). Correlation coefficients ( $R^2$ ) of calibration curves are from 0.9802 to 0.9997. Differences between two slopes using standard mixture and those from individual metabolites are from 1% to 11.8%. These differences are much smaller compared to those without background subtraction. High linearity and low differences of the slopes made these calibration curves suitable for quantification. Based on above observations, the calibration curve for each metabolite was made individually using the same background which consisted of an equal volume of each sample from one kinetic experiment.

### **Determination of glycolysis and pentose-phosphate pathway kinetics applying MALDI quantification**

For a long time, kinetic studies have been investigated using purified single enzymes or small networks containing few purified enzymes (Ishii et al. 2007). But parameters obtained from these so called *in-vitro* conditions can not completely match in *in-vivo* conditions. Cells permeabilized using appropriate conditions do not cause the release of proteins during kinetic experiments and also keep most cellular structures and protein-protein interactions intact since intracellular enzymes remain in their original macromolecular environment which is very similar to their *in-vivo* condition (Felix 1982). Therefore *in-situ* kinetics is expected to be superior for kinetic network studies. By the addition of selected substrates and cofactors, metabolites are converted only within a restricted part of the network. Kinetics of glycolysis and pentose-phosphate pathway was determined using G6P as substrate combined with the addition of the cofactors ATP, ADP, NADP<sup>+</sup> and NAD<sup>+</sup>. Samples were taken over a period of 120 min and subsequently measured by MALDI-TOF MS using the standard addition method as described above. Calculating an overall carbon balance, it was found that F16BP was significantly over-estimated in the higher concentration range (2400 s and 3600 s) using only the mixture of the 15 samples as background. Using each individual sample with the standard addition method for the quantification of F16BP, however, provided results with a consistent carbon balance (data shown in brackets in Table 2). All other samples gave almost identical values for F16BP with both methods as depicted in Figure. 6. Differences might be caused by the significantly different molecular structure of F16BP compared to the applied internal standard [U-<sup>13</sup>C<sub>6</sub>] G6P particularly concerning the two phosphate groups in one molecule in combination with the changing composition of the reaction mixture. The resulting concentration profiles of 6 metabolites are depicted in Figure 6. G6P/F6P concentration decreased during the whole period from 3 mM to only 0.3 mM. F16BP concentration (full diamonds in Figure. 6) increased in the first 3600 s, reaching a top concentration of about 1.43 mM and then quickly decreasing to a plateau value of 0.76 mM at the end of this experiment. 3PG/2PG and DHAP/GADP concentrations increased initially showing a similar shape and after reaching a plateau at around 3600 s increased again towards the end of the experiment. The almost identical shape indicates that these compounds are nearly in equilibrium throughout the experiment. PEP appeared at 1200 s and then increased to the final

## *In situ* network kinetic study using MALDI-TOF MS

---

concentration of 0.05mM. The shape of this curve is similar to those of 3PG/2PG and DHAP/GADP but with a certain delay. For 6PG, the concentration jumped from 0 to 0.11 mM in the first 300 s, then decreased very quickly to almost zero after about 3600 s. This means that the rate of formation of 6PG is not proportional to the concentration of G6P/F6P alone but is most likely inhibited by its product NADPH (Moritz et al. 2000a) and other products formed during the reaction.

Metabolite concentrations and total amount of carbon are listed in table 2. Detection limits of metabolites are specified there as well. The starting molar carbon concentration was 18 mM, all contained in G6P. The differences between the sum of the carbon contained in measured metabolites and initial carbon were lower than 17%. The total detected carbon remained reasonably constant during the whole period of the kinetic experiment. Deviations originate from: (i) other unknown and not detected metabolites, (ii) loss by decarboxylation in the pentose-phosphate pathway and (iii) experimental error.

Table 2. Concentrations of observed metabolites measured by MALDI-TOF MS and resulting total carbon concentrations.

		Concentrations of metabolites (mM)										Total carbon (mM)	Carbon Recovery (%)	
		G6P /F6P	F16BP	DHAP / GADP	13BPG	3PG /2PG	PEP	PYR	6PG	P5P	S7P			E4P
Carbon number		6	6	4	3	3	3	3	6	5	7	4		
Time points (min)	0	3.00	ND	ND	ND	ND	ND	ND	ND	ND	ND	ND	18.00	100
	15	2.69	0.021	0.0023	ND	0.0054	ND	ND	0.0082	ND	ND	0.030	16.48	92
	30	3.28	0.023	0.0000	ND	0.0000	ND	ND	0.0090	ND	ND	0.026	19.95	111
	60	3.20	0.023	0.0045	ND	0.0103	ND	ND	0.0135	ND	ND	ND	19.44	108
	90	2.94	0.029	0.0066	ND	0.0076	ND	ND	0.0256	ND	ND	0.035	18.14	101
	120	2.76	0.073	0.0226	ND	0.0261	ND	ND	0.0655	ND	ND	0.066	17.79	99
	180	2.83	0.115	0.0590	ND	0.0455	ND	ND	0.0918	ND	ND	0.076	18.86	105
	300	2.63	0.143	0.1121	ND	0.0416	ND	ND	0.1084	ND	ND	0.065	18.02	100
	600	2.23	0.366	0.3630	ND	0.1346	ND	ND	0.0687	ND	ND	0.056	17.68	98
	1200	2.01	0.807	0.6118	ND	0.2269	ND	ND	0.0327	ND	ND	0.044	19.80	110
	2400	1.16	1.853 <sup>#</sup> (1.20)	1.3067	ND	0.4846	0.012	ND	0.0218	ND	0.03*	0.074	23.93 <sup>#</sup> (20.00)	133 <sup>#</sup> (111)
	3600	0.75	2.908 <sup>#</sup> (1.43)	1.6654	ND	0.6176	0.020	ND	ND	ND	0.03*	0.063	29.10 <sup>#</sup> (20.25)	162 <sup>#</sup> (112)
	4800	0.48	1.311	1.7079	ND	0.6334	0.024	ND	ND	ND	0.02*	ND	17.83	99
	6000	0.35	0.805	1.9726	ND	0.7316	0.031	ND	0.0023	ND	0.02*	ND	15.18	84
7200	0.30	0.759	2.5020	ND	0.9279	0.052	ND	ND	ND	0.02*	0.027	16.89	94	

ND, not detected. Detection limits: FBP $\leq$ 0.02mM; DHAP/GADP $\leq$ 0.002mM; 2PG/3PG $\leq$ 0.001mM; PEP $\leq$ 0.001mM; 6PG $\leq$ 0.001mM;

E4P $\leq$ 0.02mM; Pyr $\leq$ 0.002mM; P5P $\leq$ 0.02mM. For 13BPG, Pyr and P5P, corresponding peaks at 265.23, 87.06 and 229.25 were not detected.

\* For S7P, corresponding peak at 289.34 was detected after 40 min, but the peaks were very small. The values in the table are the ratios of height of S7P peaks to the height of internal standard peaks, corresponding concentrations were expected to be lower than 0.01 mM, and they were not included in the carbon calculation.

# Values in brackets were corrected using another calibration curve made with a higher F16BP concentration background.

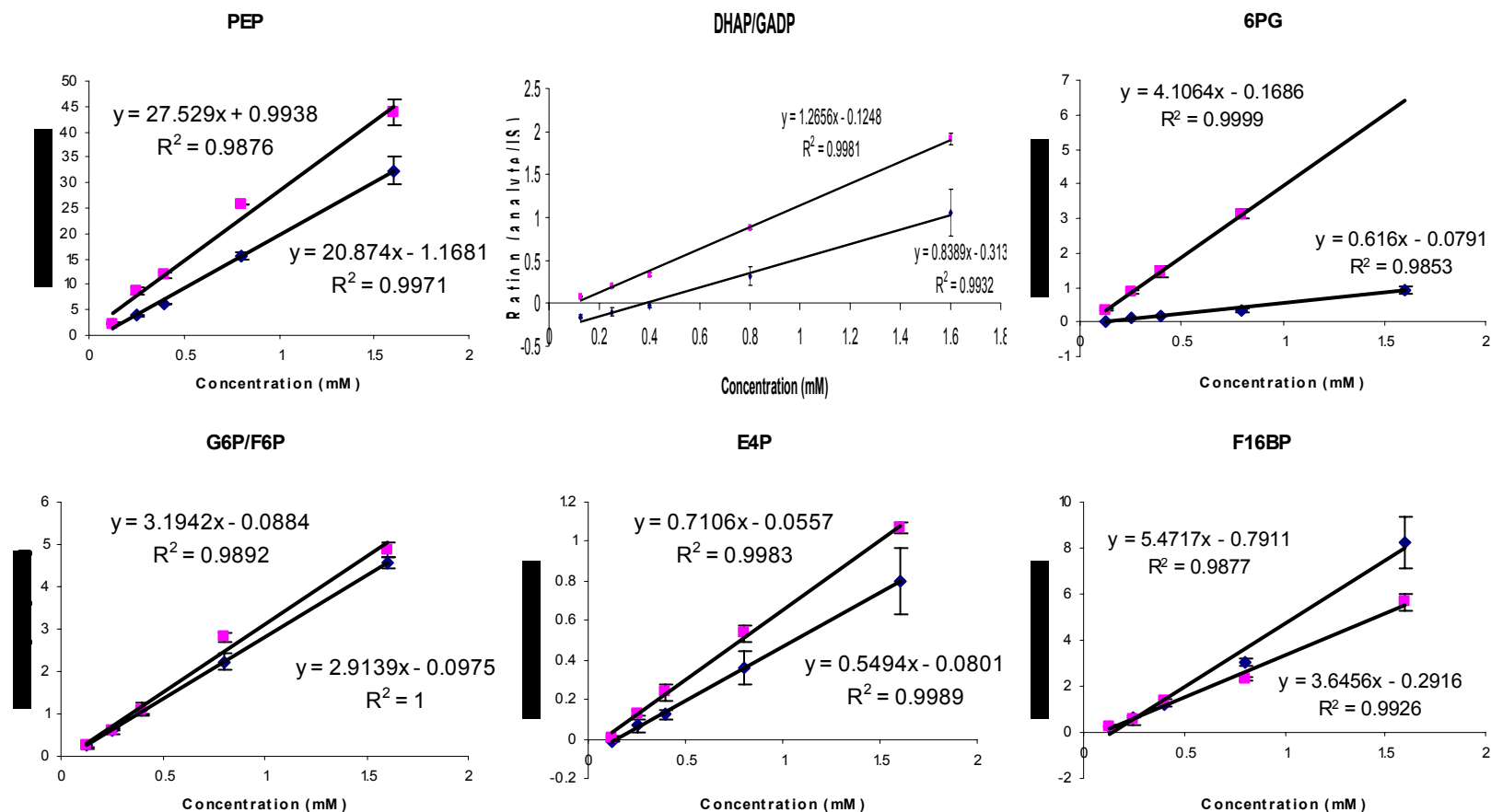


Figure.3. Calibration curves determination by MALDI-TOF mass spectrometry. [ $U\text{-}^{13}\text{C}_6$ ] G6P was used as internal standard at a fixed concentration whereas the concentration of the metabolite was varied. Peak heights of internal standard and each metabolite were calculated and the ratios of the internal standard to metabolite heights were determined. Calibration curves were constructed by plotting ratios against metabolite concentrations.  $\blacksquare$ : all 6 metabolite standards were measured in a mixture;  $\blacklozenge$ : all 6 metabolite standards were measured individually. Details of sample preparation are provided in Materials and Methods section.

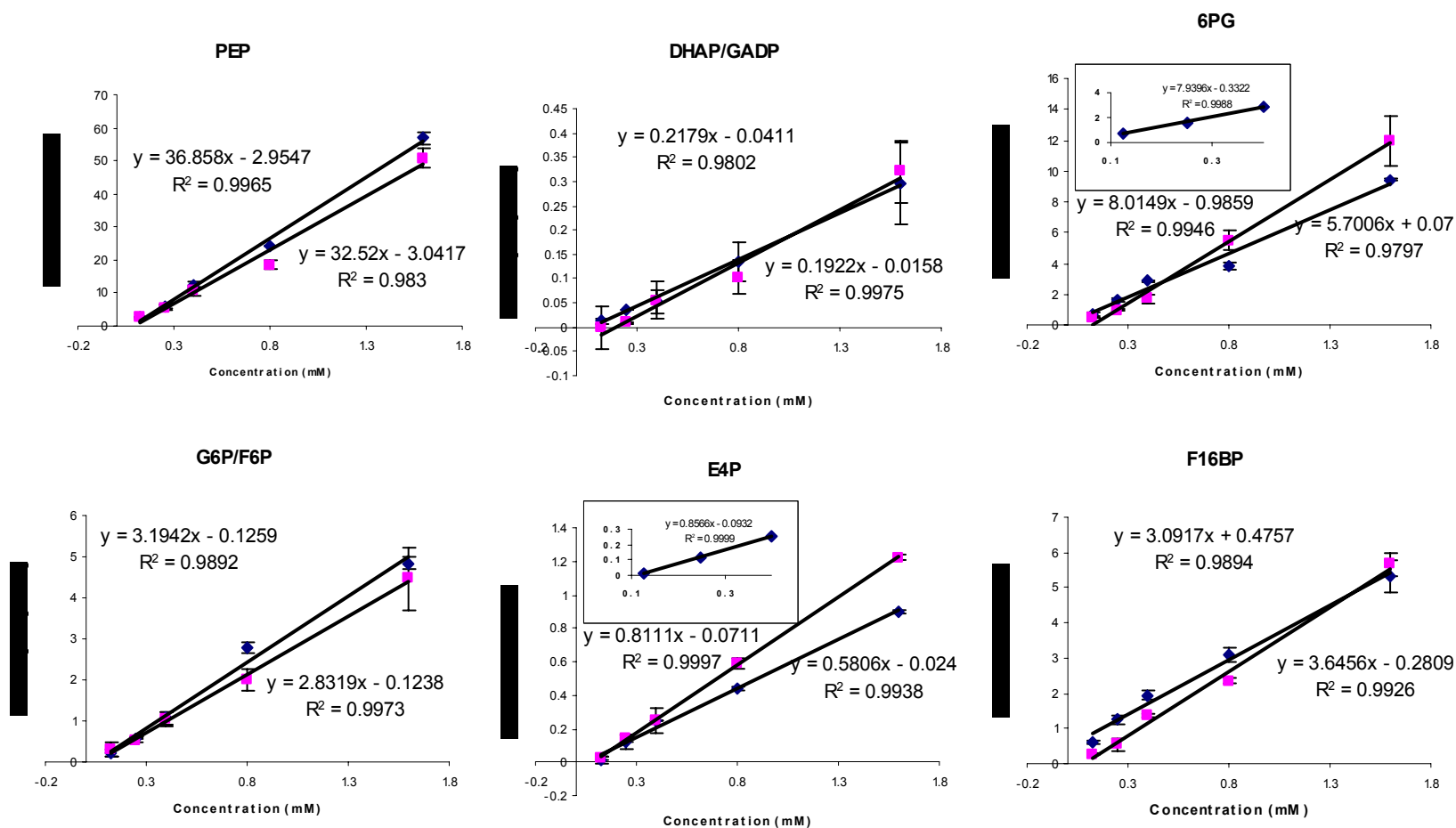


Figure.4. Calibration curves used for metabolite quantification by MALDI-TOF mass spectrometry. The difference of the sample preparation is that each standard sample was mixed with a real experimental sample  $\blacksquare$ : all 6 metabolite standards were measured in a mixture;  $\blacklozenge$ : all 6 metabolite standards were measured individually. Inserts indicate individually measured standards at low concentration.

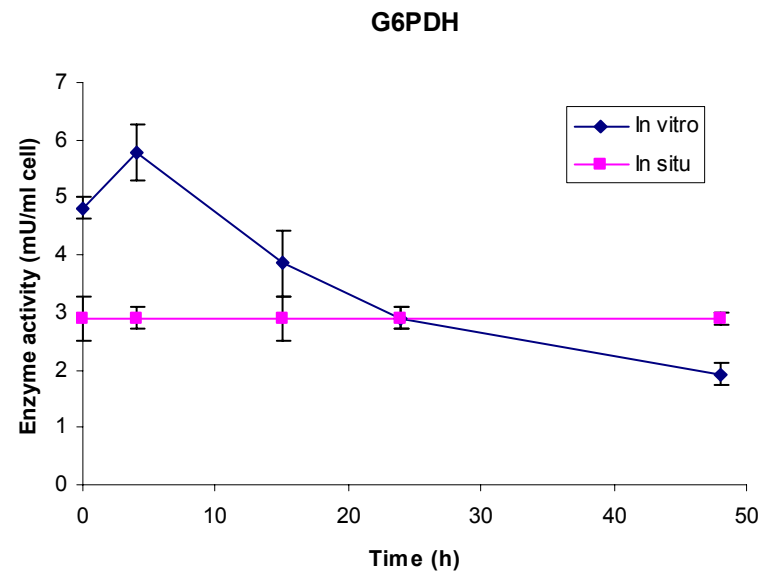
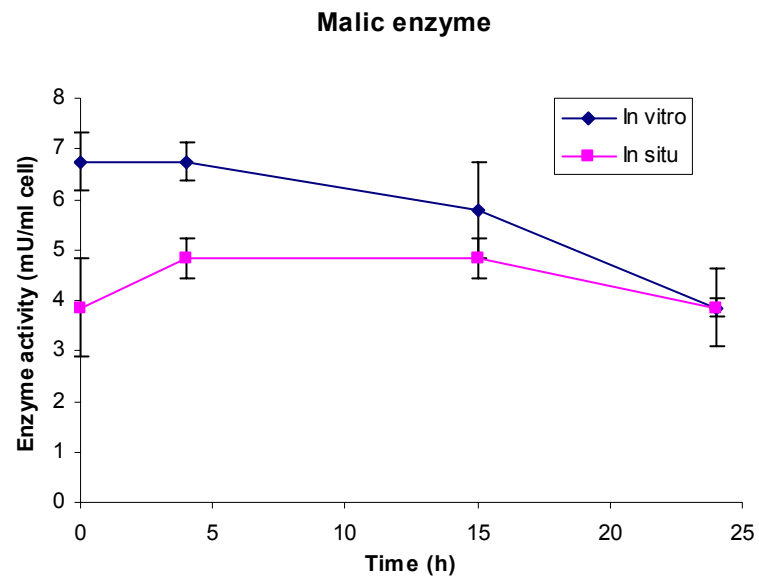


Figure.5. Stability comparison between *in-vitro* and *in-situ* conditions. Malic enzyme and G6PDH were then measured as described in Materials and methods section.

Many individual enzymes in glycolysis and the pentose-phosphate pathway in permeabilized cells have been proven active using established assays for activity measurement (Yuan and Heinzle 2009). It was already shown earlier that only a very small amount of proteins was released during permeabilization. In this study it was shown that only activities lower than 2% (0.001 mU/ml) were detected in the supernatant of the permeabilized cells for the tested malic enzyme and G6PDH. Furthermore, all of the major metabolites were detected during the kinetic experiments described here indicating that all of major enzymes were still inside the cells and active after permeabilization. It was shown earlier that the enzymes inside the cells are generally more stable than purified enzymes and can thus improve kinetic experiments (Ishii et al. 2007). Figure 5 depicts the comparison of the stability of two enzymes *in-vitro* and *in-situ*. After 48 h, malic enzyme and glucose 6-phosphate dehydrogenase lost their activities by 43% and 60% at *in-vitro* conditions. Both enzyme activities exhibited much more constant activities *in-situ*. Kinetic experiments using enzymes in permeabilized cells lasted for several minutes to a less than two hours. Therefore, the inactivation can be ignored since activity loss was not observed during this period. The degradation of G6P was also tested by keeping it in buffer solution under the identical conditions for 4 hours. No significant conversion of G6P could be detected.

For each experiment, the substrates and cofactors and their concentrations should be well selected and designed according to the purpose of the experiment. The selection of the substrate(s) depends on the network to be investigated. For networks producing non-phosphorylated metabolites the MALDI quantification method should be modified considering internal standards and matrices. ATP and ADP always could be detected by MALDI-TOF MS with peaks at 506.57 and 426.51, respectively. But they were not successfully quantified using the internal standard in this study so far. NADP(H) and NAD(H) could not even be detected reliably by MALDI-TOF MS, probably because of their limited stability. Some intermediates of the network, i.e. 13BPG, PYR, P5P, S7P and E4P were either detected at very low concentrations or were below the detection limits as specified in Table 2. This means that the rates of reactions consuming these metabolites were larger than or equal to those of the corresponding synthesizing reactions.

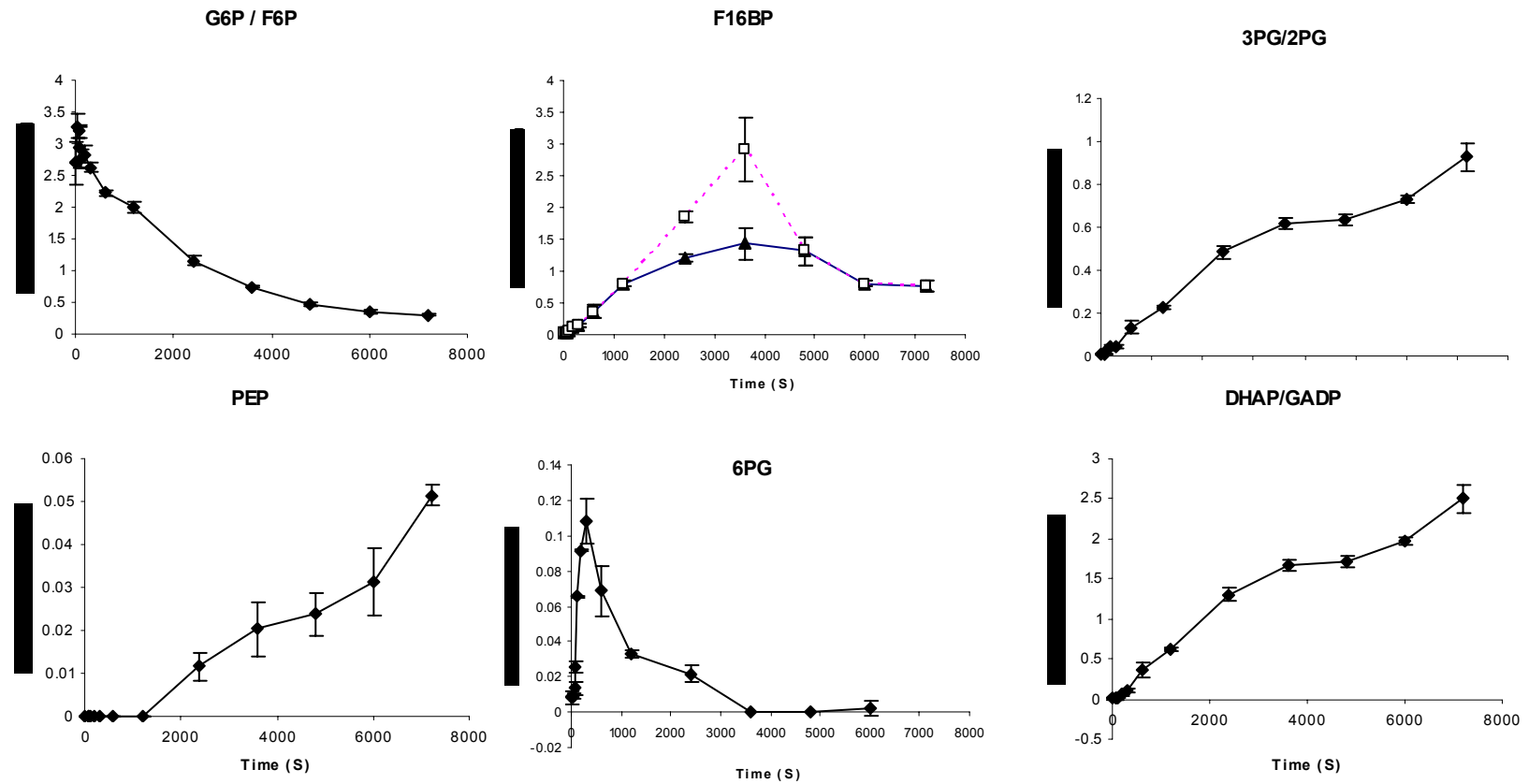


Figure.6. Time courses of 6 metabolite concentrations. Starting concentrations: G6P 3 mM, ATP 0.5 mM, ADP 1.5 mM, NADP<sup>+</sup> 2 mM, NAD<sup>+</sup> 2 mM, Mg<sup>2+</sup> 5 mM. *Corynebacterium glutamicum* cell density was 200 mg/ml (wet weight). F16BP: □-calibration using sample mixture; ▲- calibration using individual samples both combined with standard addition.

## 5.4 Conclusion

A novel strategy for enzyme network kinetic study combining permeabilization technique and MALDI quantitative measurement is described here. Quantitative measurement of small molecular mass phosphorylated metabolites using MALDI-TOF MS was tested. [U-<sup>13</sup>C<sub>6</sub>] G6P was proven to be a useful internal standard for 13 metabolites. Signal suppression could be largely eliminated by the use of this internal standard making calibration curves in a background consisting of a mixture of all metabolites of interest (standard addition method). The standard addition method had to be modified for F16BP using every single sample having higher concentrations as background. Reliable calibration curves could be made in this way and applied to the quantification of metabolites. This quantification method is applicable for determination of enzyme activities of pentose-phosphate pathway and glycolysis of other organisms.

Permeabilized cells were utilized as material for network kinetic studies, all enzymes were assumed to be at their *in-situ* conditions but accessible by substrates and metabolites, furthermore, these *in-situ* enzymes were more stable than those of purified enzymes. After adding the selected substrates and cofactors, samples containing produced metabolites could be collected and analyzed. Enzymes could be simply removed to stop reactions by centrifugation separating cells from the supernatant. 12 metabolites, or metabolite groups were quantified based on the above developed MALDI quantification method and corresponding kinetics was obtained. Activities and kinetic interactions in both pathways could be understood in considerable depth.

## References:

- Bolten CJ, Kiefer P, Letisse F, Portais J-C, Wittmann C. 2007. Sampling for Metabolome Analysis of Microorganisms. *Analytical Chemistry* 79(10):3843-3849.
- Duncan MW, Roder H, Hunsucker SW. 2008. Quantitative matrix-assisted laser desorption/ionization mass spectrometry. *Brief Funct Genomic Proteomic* 7(5):355-370.
- Edwards JL, Kennedy RT. 2005. Metabolomic analysis of eukaryotic tissue and prokaryotes using negative mode MALDI time-of-flight mass spectrometry. *Anal Chem* 77(7):2201-9.
- Felix H. 1982. Permeabilized cells. *Anal Biochem* 120(2):211-34.
- Graham JWA, Williams TCR, Morgan M, Fernie AR, Ratcliffe RG, Sweetlove LJ. 2007. Glycolytic Enzymes Associate Dynamically with Mitochondria in Response to Respiratory Demand and Support Substrate Channeling. *Plant Cell* 19(11):3723-3738.
- Heinzle E, Yuan Y, Kumar S, Wittmann C, Gehre M, Richnow HH, Wehrung P, Adam P, Albrecht P. 2008. Analysis of C-13 labeling enrichment in microbial culture applying metabolic tracer experiments using gas chromatography-combustion-isotope ratio mass spectrometry. *Analytical Biochemistry* 380(2):202-210.
- Ishii N, Suga Y, Hagiya A, Watanabe H, Mori H, Yoshino M, Tomita M. 2007. Dynamic simulation of an in vitro multi-enzyme system. *FEBS Letters* 581(3):413-420.
- Lasaosa M, Delmotte N, Huber CG, Melchior K, Heinzle E, Tholey A. 2009a. A 2D reversed-phase x ion-pair reversed-phase HPLC-MALDI TOF/TOF-MS approach for shotgun proteome analysis. *Analytical and Bioanalytical Chemistry* 393(4):1245-1256.
- Lasaosa M, Jakoby T, Delmotte N, Huber CG, Heinzle E, Tholey A. 2009b. Rapid selection of peptide containing fractions in off-line 2-D HPLC in shotgun proteome analysis by screening with MALDI TOF MS. *Proteomics* 9(19):4577-4581.
- Lou X, van Dongen JL, Vekemans JA, Meijer EW. 2009. Matrix suppression and analyte suppression effects of quaternary ammonium salts in matrix-assisted laser desorption/ionization time-of-flight mass spectrometry: an investigation of suppression mechanism. *Rapid Commun Mass Spectrom* 23(19):3077-82.
- Martins AM, Cordeiro CA, Ponces Freire AM. 2001a. In situ analysis of methylglyoxal metabolism in *Saccharomyces cerevisiae*. *FEBS Lett* 499(1-2):41-4.

- Martins AM, Mendes P, Cordeiro C, Freire AP. 2001b. In situ kinetic analysis of glyoxalase I and glyoxalase II in *Saccharomyces cerevisiae*. *Eur J Biochem* 268(14):3930-6.
- Mims D, Hercules D. 2003. Quantification of bile acids directly from urine by MALDI-TOF-MS. *Analytical and Bioanalytical Chemistry* 375(5):609-616.
- Mims D, Hercules D. 2004. Quantification of bile acids directly from plasma by MALDI-TOF-MS. *Analytical and Bioanalytical Chemistry* 378(5):1322-1326.
- Minton AP. 2006. How can biochemical reactions within cells differ from those in test tubes? *J Cell Sci* 119(14):2863-2869.
- Rachal L, Vermillion-Salsbury DMH. 2002. 9-Aminoacridine as a matrix for negative mode matrix-assisted laser desorption/ionization. *Rapid Communications in Mass Spectrometry* 16(16):1575-1581.
- Serrano R, Gancedo JM, Gancedo C. 1973. Assay of yeast enzymes in situ. A potential tool in regulation studies. *Eur J Biochem* 34(3):479-82.
- Simm R, Morr M, Remminghorst U, Andersson M, Röling U. 2009. Quantitative determination of cyclic diguanosine monophosphate concentrations in nucleotide extracts of bacteria by matrix-assisted laser desorption/ionization-time-of-flight mass spectrometry. *Analytical Biochemistry* 386(1):53-58.
- Snoep JL, Rohwer JM. 2005. Detailed Kinetic Models Using Metabolomics Data Sets. *Metabolome Analyses: Strategies for Systems Biology*. p 215-242.
- Szajli E, Feher T, Medzihradzky KF. 2008. Investigating the Quantitative Nature of MALDI-TOF MS. *Mol Cell Proteomics* 7(12):2410-2418.
- Tholey A, Wittmann C, Kang MJ, Bungert D, Hollemeyer K, Heinzle E. 2002. Derivatization of small biomolecules for optimized matrix-assisted laser desorption/ionization mass spectrometry. *Journal of Mass Spectrometry* 37(9):963-973.
- Vaidyanathan S, Gaskell S, Goodacre R. 2006. Matrix-suppressed laser desorption/ionisation mass spectrometry and its suitability for metabolome analyses. *Rapid Commun Mass Spectrom* 20(8):1192-8.
- Vaidyanathan S, Goodacre R. 2007. Quantitative detection of metabolites using matrix-assisted laser desorption/ionization mass spectrometry with 9-aminoacridine as the matrix. *Rapid Commun Mass Spectrom* 21(13):2072-8.
- van Dam JC, Eman MR, Frank J, Lange HC, van Dedem GWK, Heijnen SJ. 2002. Analysis of glycolytic intermediates in *Saccharomyces cerevisiae* using anion exchange

- chromatography and electrospray ionization with tandem mass spectrometric detection. *Analytica Chimica Acta* 460(2):209-218.
- Wilkinson W, Gusev A, Proctor A, Houalla M, Hercules D. 1997. Selection of internal standards for quantitative analysis by matrix-assisted laser desorption-ionization (MALDI) time-of-flight mass spectrometry. *Fresenius' Journal of Analytical Chemistry* 357(3):241-248.
- Yuan YB, Heinzle E. 2009. Permeabilization of *Corynebacterium glutamicum* for NAD(P)H-dependent intracellular enzyme activity measurement. *Comptes Rendus Chimie* 12(10-11):1154-1162.
- Zabet-Moghaddam M, Heinzle E, Tholey A. 2004. Qualitative and quantitative analysis of low molecular weight compounds by ultraviolet matrix-assisted laser desorption/ionization mass spectrometry using ionic liquid matrices. *Rapid Communications in Mass Spectrometry* 18(2):141-148.
- Zhou H-X, Rivas G, Minton AP. 2008. Macromolecular Crowding and Confinement: Biochemical, Biophysical, and Potential Physiological Consequences\*. *Annual Review of Biophysics* 37(1):375-397.

## Chapter 6

### Kinetic modeling of *in-situ* enzymatic system

#### Abstract

Continuing Chapter 5, six major metabolites in pentose phosphate pathway and glycolysis were quantified using the established MALDI-TOF MS method. A mathematical model based on elementary kinetic equations was constructed and applied to simulate these six major metabolites using Berkeley Madonna software. The results show that these simulated data match experimental data very well. The obtained network kinetic parameters can be used for further simulation study.

This part is under preparation as : Yuan Y, Heinzle E. 2010. Kinetic modeling of *in-situ* enzymatic system.

### 6.1 Introduction

Kinetic reaction networks comprise a set of reactions. Modeling kinetics of a biological process has long been pursued to improve our understanding of the system. However, due to the complexity of biological systems, modeling and simulation of such a network are still limited (Resat et al. 2009). Generally the construction of a mathematical modeling comprises three steps: (1) participating metabolites identification by experimental measurement, (2) assignment of rate laws, and (3) parameter estimation (Drager et al. 2009). Traditionally, the parameter are obtained from *in vitro* conditions (Ishii et al. 2007), but such an artificial system can not represent the real conditions in a living cell, particularly considering crowding effects with multiple protein interactions effecting rates and control, e.g. channeling (Graham et al. 2007b; Minton 2006; Shearer et al. 2005a; Zhou et al. 2008). Quantified dynamic of metabolites from *in vivo* conditions are ideal for the identification of metabolic network kinetic parameters, but this is limited by the difficulties of sampling and quantification. In the past, the perturbation method was normally utilized to carry out such a kinetic experiment (Hadlich et al. 2009; Theobald et al. 1997; Visser et al. 2004). In Chapter 5, a new strategy combining permeabilization and MALDI-TOF MS quantification method were established. The obtained experimental data of metabolites are tested in a kinetic model in this chapter.

### 6.2 Kinetic network simplification

Based on the six major metabolites quantified in Chapter 5, the investigated network is simplified as depicted in Figure 1. P5P represents metabolites with 5 carbons: RIB5P, XYL5P and RIBO5P are lumped together. Except the reaction between G6P and F6P, all the other reversible reactions were simplified to irreversible reactions, only net reaction rates were calculated to reduce the number of parameters in the model.

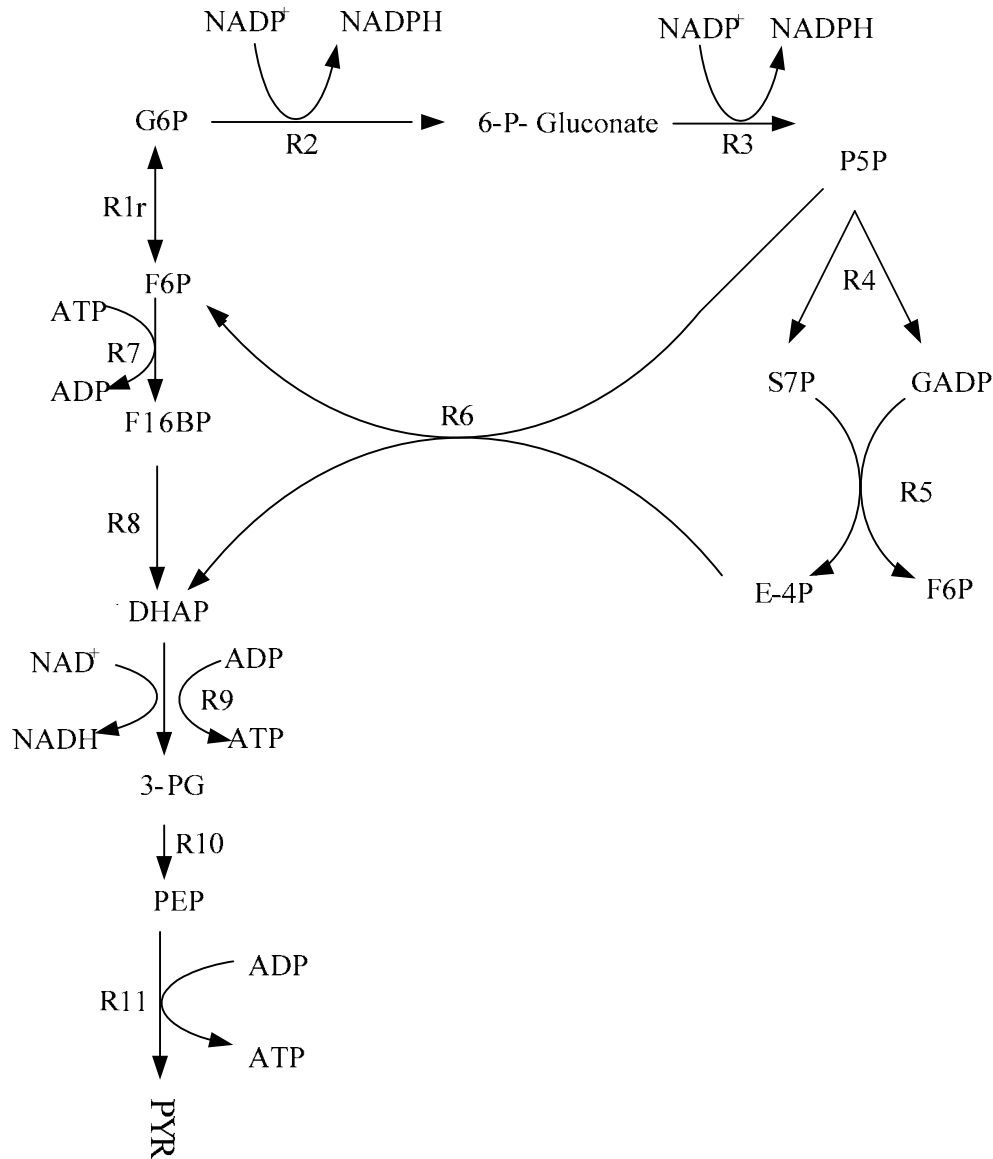
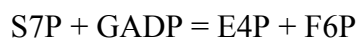
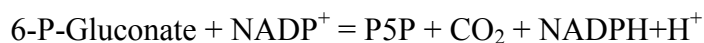
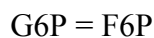
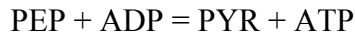
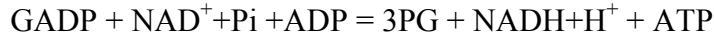
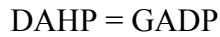
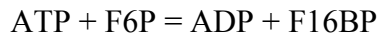
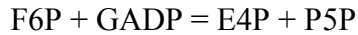


Figure 1. Simplified pentose phosphate pathway and glycolysis network.

## 6.3 Reactions in the network

According to the network in Figure 1, all reactions involved in this simulation network are listed as following:





### 6.4 Kinetic model formulation

Since most enzyme kinetics resemble Michaelis-Menten kinetics and typical intracellular concentrations are in the lower range, a first order approximation is reasonably justified. For a general Michaelis-Menten formula,

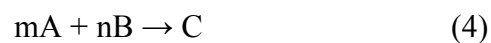
$$r = V_m \frac{S}{K_m + S} \quad (1)$$

Assume the intracellular concentrations are very low and  $S \ll K_m$ , then the formula can be converted to:

$$r = \frac{V_m}{K_m} S \quad (2)$$

$$r = kS \quad (3)$$

For a generic elementary reaction:



The rate of this reaction is expressed as:

$$r = k[\text{A}]^m[\text{B}]^n \quad (5)$$

In this study, all rates were of first order with respect to each reaction. Then the formula can be transformed as following while  $m=1$  and  $n=1$ :

$$r = k[\text{A}][\text{B}] \quad (6)$$

## Kinetic modeling of *in-situ* enzymatic system

---

Based on the above assumption and formulation, the network shown in Figure 1 can be represented as the following set of ordinary differential equations:

$$d[\text{G6P}]/dt = -V_1 - V_2 + V_{1r}$$

$$d[\text{6PG}]/dt = V_2 - V_3$$

$$d[\text{F6P}]/dt = V_1 - V_{1r} - V_7 + V_6 + V_5$$

$$d[\text{E4P}]/dt = -V_6 + V_5$$

$$d[\text{S7P}]/dt = -V_5 + V_4$$

$$d[\text{P5P}]/dt = -2 \cdot V_4 + V_3$$

$$d[\text{F16BP}]/dt = V_7 - V_8$$

$$d[\text{DHAP}]/dt = 2 \cdot V_8 + V_6 - V_9 + V_4$$

$$d[\text{3PG}]/dt = V_9 - V_{10}$$

$$d[\text{PEP}]/dt = V_{10} - V_{11}$$

$$d[\text{ATP}]/dt = -V_7 + V_9 + V_{11}$$

$$d[\text{ADP}]/dt = -d[\text{ATP}]/dt$$

$$d[\text{NADP}]/dt = -2 \cdot V_2$$

$$d[\text{NADPH}]/dt = -d[\text{NADP}]/dt$$

$$d[\text{NAD}]/dt = -V_9$$

$$d[\text{NADH}]/dt = -d[\text{NAD}]/dt$$

DHAP represents the sum of DHAP and GADP. Simulations were performed using Berkeley Madonna ([www.berkeleymadonna.com](http://www.berkeleymadonna.com)) which allows a parameter estimation using available integrators for stiff systems. Selection of initial guesses for the optimizer was critical to get optimization (Heinzle et al. 2007). All parameters (12 rate constants and 16 initial concentrations) were carefully assigned initial values. The experimental data of metabolite

## Kinetic modeling of *in-situ* enzymatic system

---

concentrations were input into the software and all parameters were evaluated using the function of curve fit. The detailed program is listed in Appendix.

### 6.5 Results and conclusion

A suitable format reduces the number of parameters and simplifies the algebraic treatment of models, several of these approximate kinetic formats, including Linear, Power law, Linlog and Generic formats, have been compared recently (Hadlich et al. 2009; Heijnen 2005). A big advantage of using permeabilized cells (*in situ*) for this kinetic experiment is that all enzymes are present and active while all intermediates were mostly washed away before starting the reactions, therefore the network can be activated from simple biochemical reactions by adding substrates and corresponding cofactors. Different from *in vivo* kinetic studies that need formulations more complex, reactions under *in situ* conditions can be described with simple linear kinetic formulations as well as make the number of parameters as less as possible. A mathematical modeling based on first order approximation was tested in this study. Besides the first order kinetics shown here, other more complex formulations were also applied, e.g. a Taylor series approximation. This, however, did not improve data fitting significantly despite the large number of parameters.

**Table 1. Estimated rate constants in equation (6).**

Reaction	Rate constant	value
V <sub>1</sub>	k1	3.40E-04
V <sub>1r</sub>	k1r	1.03E-14
V <sub>2</sub>	k2	1.74E-04
V <sub>3</sub>	k3	0.006728
V <sub>4</sub>	k4	21.9111
V <sub>5</sub>	k5	1.18E-04
V <sub>6</sub>	k6	5.94E-09
V <sub>7</sub>	k7	0.09998
V <sub>8</sub>	k8	4.66E-04
V <sub>9</sub>	k9	1.23E-04
V <sub>10</sub>	k10	2.42E-04
V <sub>11</sub>	k11	0.003233

Using Berkeley Madonna, all 28 parameters in the model were fitted to the experimental data. The entire simulation running could be finished in 5 min. All estimated reaction constants are listed in Table 1.  $K_{1r}$  is so small that it can be ignored, which means the flux from F6P to G6P

## Kinetic modeling of *in-situ* enzymatic system

---

is very small during the experiment.  $K_1$  and  $K_2$  are two important parameters that, to some extent, represent fluxes to glycolysis and pentose phosphate pathway, respectively.  $K_1$  is about 3 times larger than  $K_2$  but both values are at the same order of magnitude. It can be drawn that G6P were simultaneously converted to both directions and the flux to glycolysis might be larger than that to pentose phosphate pathway. This agree with other former reports concerning fluxes calculation (Kim et al. 2006b; Yuan et al. 2010).  $K_4$  is the highest value among these parameters and much higher than others, therefore the converted P5P can be then converted to F6P and GADP in glycolysis.

The simulated metabolite concentrations can fit the experimental data very well as shown in Figure 2. For G6P/F6P, DHAP/GADP, 3PG/2PG and PEP, the experimental data can be matched by the simulated data perfectly. G6P/F6P concentration decreased sharply in the first 5000 s and then slowly down due to the network regulation by other productions. DHAP/GADP and PEP concentrations kept increasing sharply during the whole experiment. It indicates that the entire network is far from reaching a steady state in 7200 s. Another kinetic experiment with a long time could be necessary to describe the whole map from zero to the steady state. Simulated 3PG/2PG concentration decreased after 5400 s, but it could not be reflected from experimental data around that time point. The experimental data curve of 6PG has the same shape with the simulated ones, and both curves have top peaks at about 300 s. However, the simulated concentration values around this peak are lower than measured ones. This difference might be caused by the quantitative measurement error as discussed in Chapter 5.

As a preliminary study, a mathematical model for a *in situ* metabolic network of *Corynebacterium glutamicum* was established. All parameters in the model were estimated using Berkeley Madonna software with its curve fitting function. These simulated data can match experimental data very well applying the set of these parameters. All these obtained parameters, which represent the network enzymatic kinetic properties, can be applied for further simulations in the same conditions, e.g. for metabolic control analysis to identify the limiting steps. Furthermore, it can be deeply studied by the comparison of previous reports concerning single enzymatic kinetic properties (Jonges et al. 1992; Rizzi et al. 1997; Theobald et al. 1997).

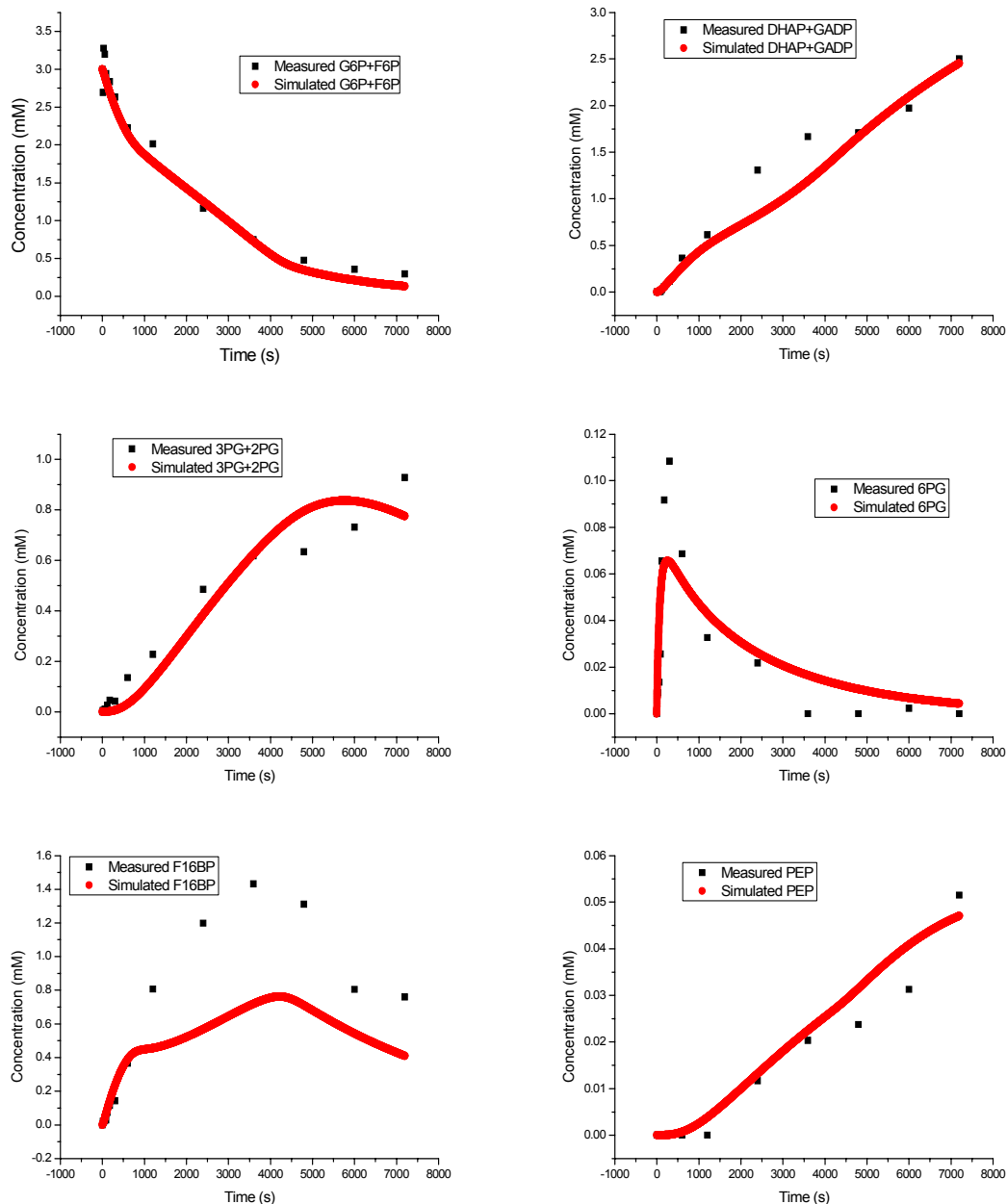


Figure 2. Metabolite concentrations simulated by the model compared with experimental data from kinetic experiments.

### References:

- Drager A, Kronfeld M, Ziller MJ, Supper J, Planatscher H, Magnus JB, Oldiges M, Kohlbacher O, Zell A. 2009. Modeling metabolic networks in *C. glutamicum*: a comparison of rate laws in combination with various parameter optimization strategies. *BMC Syst Biol* 3:5.
- Graham JWA, Williams TCR, Morgan M, Fernie AR, Ratcliffe RG, Sweetlove LJ. 2007. Glycolytic Enzymes Associate Dynamically with Mitochondria in Response to Respiratory Demand and Support Substrate Channeling. *Plant Cell* 19(11):3723-3738.
- Hadlich F, Noack S, Wiechert W. 2009. Translating biochemical network models between different kinetic formats. *Metabolic Engineering* 11(2):87-100.
- Heijnen JJ. 2005. Approximative kinetic formats used in metabolic network modeling. *Biotechnol Bioeng* 91(5):534-45.
- Heinzle E, Matsuda F, Miyagawa H, Wakasa K, Nishioka T. 2007. Estimation of metabolic fluxes, expression levels and metabolite dynamics of a secondary metabolic pathway in potato using label pulse-feeding experiments combined with kinetic network modelling and simulation. *Plant Journal* 50(1):176-187.
- Ishii N, Suga Y, Hagiya A, Watanabe H, Mori H, Yoshino M, Tomita M. 2007. Dynamic simulation of an *in vitro* multi-enzyme system. *FEBS Letters* 581(3):413-420.
- Jonges GN, Van Noorden CJ, Lamers WH. 1992. *In situ* kinetic parameters of glucose-6-phosphatase in the rat liver lobulus. *J Biol Chem* 267(7):4878-81.
- Kim HM, Heinzle E, Wittmann C. 2006. Deregulation of aspartokinase by single nucleotide exchange leads to global flux rearrangement in the central metabolism of *Corynebacterium glutamicum*. *Journal of Microbiology and Biotechnology* 16(8):1174-1179.
- Minton AP. 2006. How can biochemical reactions within cells differ from those in test tubes? *J Cell Sci* 119(14):2863-2869.
- Resat H, Petzold L, Pettigrew MF. 2009. Kinetic modeling of biological systems. *Methods Mol Biol* 541:311-35.
- Rizzi M, Baltes M, Theobald U, Reuss M. 1997. *In vivo* analysis of metabolic dynamics in *Saccharomyces cerevisiae*: II. Mathematical model. *Biotechnol Bioeng* 55(4):592-608.

- Shearer G, Lee JC, Koo J, Kohl DH. 2005. Quantitative estimation of channeling from early glycolytic intermediates to CO<sub>2</sub> in intact *Escherichia coli*. *Febs Journal* 272(13):3260-3269.
- Theobald U, Mailinger W, Baltes M, Rizzi M, Reuss M. 1997. In vivo analysis of metabolic dynamics in *Saccharomyces cerevisiae* : I. Experimental observations. *Biotechnol Bioeng* 55(2):305-16.
- Visser D, van Zuylen GA, van Dam JC, Eman MR, Proll A, Ras C, Wu L, van Gulik WM, Heijnen JJ; 2004 Oct 20. Analysis of in vivo kinetics of glycolysis in aerobic *Saccharomyces cerevisiae* by application of glucose and ethanol pulses.
- Yuan YB, Yang TH, Heinzle E. 2010. C-13 metabolic flux analysis for larger scale cultivation using gas chromatography-combustion-isotope ratio mass spectrometry. *Metabolic Engineering* 12(4):392-400.
- Zhou H-X, Rivas G, Minton AP. 2008. Macromolecular Crowding and Confinement: Biochemical, Biophysical, and Potential Physiological Consequences\*. *Annual Review of Biophysics* 37(1):375-397.

## Appendix

### Berkeley Madonna Program for Intracellular Metabolite Concentration Simulation

Berkeley Madonna program for simulation of metabolite concentration in glycolysis and pentose phosphate pathway

METHOD RK4

STARTTIME = 0  
STOPTIME=7200  
DT = 0.001

#Initial concentration definition#

INIT G6P=3;           mM  
INIT F6P=0;           mM  
INIT P5P=0;           mM  
INIT S7P=0;           mM  
INIT ATP=0.5;         mM  
INIT ADP=1.5;         mM  
INIT NADP=2;          mM  
INIT NAD=2;           mM  
INIT NADPH=0;         mM  
INIT NADH=0;          mM  
INIT F16BP=0;         mM  
INIT PEP=0;           mM  
INIT DHAP=0;          mM  
INIT C6PG=0;          mM  
INIT C3PG=0;          mM  
INIT E4P=0;           mM

Rate constant pre-evaluation

k1=1e-3;     Rate constant  
k1r=1e-3;    Rate constant  
k2=1e-3;     Rate constant  
k3=1e-3;     Rate constant  
k4=1e-3;     Rate constant  
k5=1e-3;     Rate constant  
k6=1e-3;     Rate constant  
k7=1e-3;     Rate constant  
k8=1e-3;     Rate constant  
k9=1e-3;     Rate constant  
k10=1e-3;    Rate constant  
k11=1e-3 ;   Rate constant

Mass balance

$G6P' = -k2 * G6P * NADP - k1 * G6P + k1r * F6P$

## Kinetic modeling of *in-situ* enzymatic system

---

$$C6PG' = k_2 * G6P * NADP - k_3 * C6PG * NADP$$

$$F6P' = k_1 * G6P - k_{1r} * F6P - k_7 * F6P * ATP + k_6 * P5P * E4P + k_5 * S7P * DHAP$$

$$E4P' = -k_6 * P5P * E4P + k_5 * S7P * DHAP$$

$$S7P' = -k_5 * S7P * DHAP + k_4 * P5P^2$$

$$P5P' = -2 * k_4 * P5P^2 + k_3 * C6PG * NADP$$

$$F16BP' = k_7 * F6P * ATP - k_8 * F16BP$$

$$DHAP' = +2 * k_8 * FBP + k_6 * P5P * E4P - k_9 * NAD * DHAP * ADP + k_4 * P5P^2$$

$$C3PG' = k_9 * NAD * DHAP * ADP - k_{10} * C3PG$$

$$PEP' = k_{10} * C3PG - k_{11} * PEP * ADP$$

$$ATP' = -k_7 * F6P * ATP + k_9 * NAD * DHAP * ADP + k_{11} * PEP * ADP$$

$$ADP' = -ATP'$$

$$NADP' = -k_2 * G6P * NADP - k_2 * G6P * NADP$$

$$NADPH' = -NADP'$$

$$NAD' = -k_9 * NAD * DHAP * ADP$$

$$NADH' = -NAD'$$

$$H6P = F6P + G6P$$

$$\text{limit } G6P \geq 0$$

$$\text{limit } F6P \geq 0$$

$$\text{limit } P5P \geq 0$$

$$\text{limit } S7P \geq 0$$

$$\text{limit } ATP \geq 0$$

$$\text{limit } ADP \geq 0$$

$$\text{limit } NADP \geq 0$$

$$\text{limit } NAD \geq 0$$

$$\text{limit } NADPH \geq 0$$

$$\text{limit } NADH \geq 0$$

$$\text{limit } FBP \geq 0$$

$$\text{limit } PEP \geq 0$$

$$\text{limit } DHAP \geq 0$$

$$\text{limit } C6PG \geq 0$$

$$\text{limit } C3PG \geq 0$$

$$\text{limit } E4P \geq 0$$

# Chapter 7

## Concluding Remarks

There is a large expectation that biotechnology particularly involving genetically engineered organisms will contribute to solve many of the problems of this world in food supply, supply of fuels and pharmaceuticals (Tyo et al. 2007). The complexity of organism metabolic systems makes it extremely difficult to understand them deeply and improve them (Bailey 1991). Metabolic engineering, which can provide useful tools for this study of metabolic network, plays an important role to improve these cellular properties for a further application in industry and biomedical field. The works in this thesis characterizes metabolic network activity by describing two novel strategies for *in-vivo* metabolic flux analysis and *in-situ* enzymatic network kinetic study. However, many other efforts subject to above two strategies, both in experimental and kinetic modeling aspects, need to be further investigated in the future.

### **Application of GC-C-IRMS for metabolic flux analysis at large scale**

GC-C-IRMS allows only the average carbon labeling but not mass isotopomer distribution for each analyte. Therefore, fluxes of reversible reactions cannot be determined. Consequently, only the net fluxes were determined using GC-C-IRMS data in this study. This limitation can be overcome, e.g., by a parallel experimental design using more tracer substrates with different positional labeling to increase information content, similar to reports (Yang et al. 2006d; Yang et al. 2006e) which measured labeling in produced CO<sub>2</sub>. Proteinogenic amino acids have been employed for metabolic fluxes determination at steady state owing to their high stability and high concentration in cells (Wittmann 2007). The analysis of other intracellular metabolites, e.g. F16BP and DHAP in PPP and glycolysis, is also promising for obtaining more labeling information content. However, the measurements of the intermediates were limited by their low concentrations in samples obtained from cell extracts. These are close to or below detection limits. Additionally, quenching of reactions is often difficult. This problem might be eliminated by using GC-C-IRMS measurement because of the high precision of labeling measurements and ability for application in large-scale fermentations. A relative large scale tracer fermentation can be carried out and followed by a quenching sampling step. Partial leakage of metabolites

## Concluding Remarks

---

from frozen cells can be ignored because the absolute amounts of these metabolites are not taken into account in this case but only their degree of labeling. Intracellular metabolites in the sample will be later concentrated to required concentration levels. For IRMS analysis, there are two possibilities: (i) develop derivatization methods for these metabolites and then later measure isotope enrichment by GC-C-IRMS. (ii) measure directly by LC-IRMS which was started in 1990's (Godin et al. 2007c). The finally obtained labeling enrichment of each metabolite can be then introduced into flux estimation program.

### **Permeabilization of microorganism (*In-situ*)**

Several chemicals were tested in this work and Triton X-100 was found best for the permeabilization of *Corynebacterium glutamicum*, *E.coli* (tested by Weyler Christian in his diploma work) and mammalian CHO cell (tested by Melnyk Armin in his diploma work). Enzymes of interest after permeabilization are still kept inside the bacteria cells, but leak out of mammalian cells. Microscope pictures of the permeabilized mammalian cells indicate that cells still keep their spherical shape, but the created pores in cell membranes are too large to retain enzymes. Enzyme activities can be still measured directly from the permeabilized mammalian cells suspension. However, it is hard to make a kinetic experiment in these permeabilized mammalian cells due to the impossibility to wash away originally present low molecular mass metabolites. The treatment with lower concentration of chemicals have been shown not useful. Another possibility to control the degree of permeabilization is to treat cells with electric pulse which recently has been successfully applied on *Corynebacterium glutamicum* (Tryfona and Bustard 2008b). This physical method might be controllable to permeabilized mammalian cells and later applied for metabolic network kinetic studies.

### **MALDI-TOF MS quantification of intracellular metabolites**

A new approach for quantitative measurement of intracellular metabolites with MALDI-TOF MS was established in this study. Compared to conventional methods, e.g., enzymatic assay and LC-MS method, it is a simple, rapid and permits the analysis of a large number of samples in short time, hence, it is very suitable for analyzing samples from kinetic experiments. 9-aminoacridine has been proven in this study as a useful matrix for low molecular mass metabolites of PPP and glycolysis. However, the peaks of 9AA matrix itself and its derivatives are at a range of 50-400 m/z, which is also the region of the spectrum for most of intracellular metabolites. Although peaks of matrix can be

## Concluding Remarks

---

successfully separated from peaks of metabolites owing to the high resolution of the MALDI spectrum (a difference smaller than 0.02 can be well separated), a better matrix with much less or no noisy peaks is highly desirable. One possible matrix called DMAN (1,8-bis(dimethylamino)naphthalene) has been investigated as matrix for metabolites in negative mode (Rohit and Alescaron 2009; Shroff et al. 2009) and no noisy peaks were found in the low mass spectra area. Besides the matrix, internal standard is critical for quantification of metabolites by MALDI. It can compensate the competitive ionization / ion suppression and improve the shot-to-shot reproducibility as well. [U-<sup>13</sup>C] glucose-6-phosphate was proven a good internal standard for the metabolites, which not only contain phosphate group(s) but also have masses similar to the internal standard. Compared to the large number of metabolites in a living cells, only a small part of them can be quantified with this developed method, unfortunately, some very important cofactors such as ATP, ADP, NADP, NAD, are not included. For a deep understanding of the whole network it could be necessary to quantify as many metabolites and cofactors as possible. An isotopomer of each analyte would be the ideal internal standard. [U-<sup>13</sup>C] aspartate was also investigated as internal standard and proven applicable for metabolites in TCA cycle and methionine biosynthetic pathway. By the combination of different internal standard, the quantifiable metabolites can be largely expanded. On the other hand, these internal standards should not be limited only to stable labeled isotopomers, some other natural labeled compounds were also proven applicable for some groups of metabolites (Mims and Hercules 2003; Mims and Hercules 2004). Unlike chemically synthesized stable labeled isotopomer, which are difficult to obtain, natural compounds are more reachable. Therefore, it is promising to explore some new internal standards, which can greatly benefit MALDI-TOF MS quantification.

## Concluding Remarks

---

### Reference:

- Bailey JE. 1991. Toward a Science of Metabolic Engineering. *Science* 252(5013):1668-1675.
- Godin JP, Fay LB, Hopfgartner G. 2007. Liquid chromatography combined with mass spectrometry for <sup>13</sup>C isotopic analysis in life science research. *Mass Spectrom Rev* 26(6):751-74.
- Mims D, Hercules D. 2003. Quantification of bile acids directly from urine by MALDI-TOF-MS. *Analytical and Bioanalytical Chemistry* 375(5):609-616.
- Mims D, Hercules D. 2004. Quantification of bile acids directly from plasma by MALDI-TOF-MS. *Analytical and Bioanalytical Chemistry* 378(5):1322-1326.
- Rohit S, Alescaron S. 2009. 1,8-Bis(dimethylamino)naphthalene: a novel superbasic matrix for matrix-assisted laser desorption/ionization time-of-flight mass spectrometric analysis of fatty acids. *Rapid Communications in Mass Spectrometry* 23(15):2380-2382.
- Shroff R, Rulisek L, Doubsky J, Svatos A. 2009. Acid-base-driven matrix-assisted mass spectrometry for targeted metabolomics. *Proceedings of the National Academy of Sciences of the United States of America* 106(25):10092-10096.
- Tryfona T, Bustard MT. 2008. Impact of Pulsed Electric Fields on *Corynebacterium glutamicum* Cell Membrane Permeabilization. *The Society for Biotechnology, Japan* 105(4):375-382.
- Tyo KE, Alper HS, Stephanopoulos GN. 2007. Expanding the metabolic engineering toolbox: more options to engineer cells. *Trends in Biotechnology* 25(3):132-137.
- van der Werf MJ, Takors R, Smedsgaard J, Nielsen J, Ferenci T, Portais JC, Wittmann C, Hooks M, Tomassini A, Oldiges M and others. 2007. Standard reporting requirements for biological samples in metabolomics experiments: microbial and in vitro biology experiments. *Metabolomics* 3(3):189-194.
- Yang TH, Wittmann C, Heinzle E. 2006a. Respiriometric C-13 flux analysis - Part II: In vivo flux estimation of lysine-producing *Corynebacterium glutamicum*. *Metabolic Engineering* 8(5):432-446.
- Yang TH, Wittmann C, Heinzle E. 2006b. Respiriometric C-13 flux analysis, Part 1: Design, construction and validation of a novel multiple reactor system using on-line membrane inlet mass spectrometry. *Metabolic Engineering* 8(5):417-431.

# Summary of this thesis

The works in this thesis consist of two parts, Chapter 2 and Chapter 3 focus on developing a novel strategy for *in-vivo* metabolic flux analysis using GC-C-IRMS, Chapter 4, Chapter 5 and Chapter 6 focus on *in-situ* enzymatic network kinetic study.

Chapter 2 shows a GC-C-IRMS based analysis that allows the detection of low enrichment of  $^{13}\text{C}$  in proteinogenic amino acids owing to its high reliability and precision. Significant kinetic isotope effects in metabolic flux studies at low degree of labeling were found but can be corrected by using two parallel experiments applying substrate with natural abundance and  $^{13}\text{C}$  enriched tracer substrate, respectively. The fractional enrichment obtained in natural substrate is subtracted from that of the enriched one. The new approach provides a strong basis for  $^{13}\text{C}$  metabolic flux analysis using a low degree of labeling, e.g., an application of about 0.5 % [1- $^{13}\text{C}$ ] glucose in the cultivation of *Corynebacterium glutamicum*. Compared to conventional GC-MS method, the new method allows detecting enrichments that are 200-300 times lower without affecting the high precision. Therefore, the amount of expensive tracer substrate can be dramatically decreased. The developed methodology provides the possibility to reliably study metabolic fluxes of industrially relevant organisms directly at larger scale that is normally very empirical and hard to be extrapolated to other scales. Except various amino acids, other important carbohydrates can be analyzed employing different derivatization procedures and respective gas chromatography parameters. In addition, this technique can be potentially applied in fed-batch fermentations.

Chapter 3 introduces a novel strategy to estimate metabolic fluxes using GC-C-IRMS at low degree of labeling. Four different low labeling fractions in [1- $^{13}\text{C}$ ] labeled and non-labeled glucose mixture from 0.5 to 10% were employed for the estimation of fluxes in the central metabolism of *C. glutamicum*. The reliability of the final results was found to greatly depend on the reproducibility of experimental procedure and measurement accuracy. Parallel experiments using conventional GC-MS method applying 99% [1- $^{13}\text{C}$ ] glucose were carried out at the same time. The results are very similar to these from GC-C-IRMS. The flux values obtained from the labeling measurements using GC-C-IRMS were found to be also well consistent with a previous report using the GC-MS method under the same condition (Kim et al. 2006a).

## Summary of this thesis

---

The method described in Chapter 2 and Chapter 3 is promising for the investigation of metabolic fluxes in industrially relevant organisms on larger scales. It promises also potential to be successfully applied for dynamic metabolic flux analysis to determine very initial changes after a carbon-isotope perturbation of previously naturally labeled substrate and for the protein synthesis investigation using isotope tracers.

Chapter 4 describes NAD(P)H-dependent intracellular enzyme assays in permeabilized cell suspension. Several variables such as agent type, cell density, agent concentration and the incubation condition were optimized for the permeabilization of *C. glutamicum*. Triton X-100 was found the most suitable agent for this procedure, and the optimized permeabilization condition in *C. glutamicum* obtained were CDW concentration of 10 mg/ml and treatment with 0.05 % Triton X-100 at room temperature for only 5 minutes. TE was also found a good candidate but needed a concentration of 10 % and a much longer incubation time of more than 40 min to obtain the highest enzyme activity. Kinetic parameters of several enzymes, including the dehydrogenases G6PDH, 6PGDH and ME, PGI were determined in permeabilized cells. As conclusion, permeabilization, so called *in-situ* condition, is a rapid, simple and mild technique and provides intracellular enzymes whose properties are assumed to be more similar to those of *in-vivo* conditions.

In Chapter 5 a novel strategy for enzyme network kinetic study combining permeabilization technique and MALDI-TOF MS quantitative measurement is developed. A reliable quantitative measurement of 13 low molecular mass phosphorylated metabolites was successfully done using MALDI-TOF MS analysis and [U-<sup>13</sup>C<sub>6</sub>] G6P as internal standard. Signal suppression exists during MALDI ionization but could be largely compensated by the use of this internal standard. This quantification method is also applicable for determination of enzyme activities or the entries to pentose-phosphate pathway and glycolysis of other organisms.

Permeabilization was introduced in details in Chapter 4. All enzymes of interest in permeabilized cells are assumed to be at their *in-situ* conditions but reachable, furthermore, these *in-situ* enzymes were more stable than those of *in-vitro* purified enzymes were. This specialty of the permeabilized cell makes it a good material for network kinetic studies. No inactivation needed to be considered in experiment owing to its good stability. The adding

## Summary of this thesis

---

of designed substrates and cofactors into permeabilized cell suspension starts reactions and the samples were collected subsequently. It is a big advantage that no quenching step is needed in this approach, and all reactions can be stopped by the isolation of enzymes from suspension by a simple centrifugation since all the metabolites of interest are contained in the supernatant but not inside the cells. Metabolites in samples are then quantified by the developed MALDI quantification method and kinetics curves can be drawn subsequently. In Chapter 6, kinetics of six metabolite were drawn and simulated using developed quantification method and constructed mathematical model.

## List of publications:

### Journal articles:

Heinzle E\*, **Yuan Y**, Kumar S, Wittmann C, Gehre M, Richnow HH, Wehrung P, Adam P, Albrecht P. **2008**. Analysis of C-13 labeling enrichment in microbial culture applying metabolic tracer experiments using gas chromatography-combustion-isotope ratio mass spectrometry. **Analytical Biochemistry** 380(2):202-210.

**Yuan Y**, Yang TH, Heinzle E. 2010. C-13 metabolic flux analysis for larger scale cultivation using gas chromatography-combustion-isotope ratio mass spectrometry. **Metabolic Engineering** 12(4):392-400.

**Yuan Y**, Heinzle E. **2009**. Permeabilization of *Corynebacterium glutamicum* for NAD(P)H-dependent intracellular enzyme activity measurement. **Comptes Rendus Chimie** 12(10-11):1154-1162.

**Yuan Y**, Heinzle E. **2010**. in-situ multi-enzyme network kinetics study using MALDI-TOF MS. submitted to **Analytical Biochemistry**.

**Yuan Y**, Heinzle E. **2010**. Kinetic modeling of in-situ enzymatic system. In preparation.

### Oral presentations:

Application of Gas Chromatography-Combustion-Isotope Ratio Mass Spectrometry for in vivo estimation of metabolic fluxes in *Corynebacterium glutamicum*. ProcessNet & DECHEMA, Aachen. September 2010

Application of Gas Chromatography-Combustion-Isotope Ratio Mass Spectrometry for in vivo estimation of metabolic fluxes in *Corynebacterium glutamicum*. GRK 532, Wallerfangen. June 2009

Permeabilization of *Corynebacterium glutamicum* for NAD(P)H-dependent intracellular enzyme activity measurement. GRK 532, uberrherrn. September 2009

### Poster presentations:

Application of gas chromatography-combustion-isotope ratio mass spectrometry for in vivo estimation of <sup>13</sup>C metabolic fluxes in *Corynebacterium glutamicum*. DECHEMA Gesellschaft für Chemische Technik und Biotechnologie e.V., Mannheim. September 2009

## List of publications

---

Application of Isotope Ratio Monitoring Gas Chromatography-Mass Spectrometry to the Analysis of  $^{13}\text{C}$  Labeling Enrichment in Metabolic Tracer Experiments. International research training group-Graduiertenekolleg 532 seminar, Strassburg. December 2007

Analysis of  $^{13}\text{C}$  Labeling Enrichment in Microbial Culture Applying Metabolic Tracer Experiments Using Gas Chromatography-Combustion-Isotope Ratio Mass Spectrometry. GRK 532, Perl-Nennig. June 2008

Study of Permeabilization in *Corynebacterium glutamicum* for Intracellular Enzyme Activity Measurement. GRK 532, Losheim. November 2008

## Curriculum Vitae

### Personal Data

Name: **Yongbo Yuan**  
Date of Birth: May 12, 1977  
Place of Birth: Shandong Province, P. R. China  
Citizenship: P. R. China

### Education

Jul. 1995 - Jul. 1999      Northeastern University (China)  
Degree:                      BS degree  
Major:                        Mineral processing engineering

Sep. 2004 – Apr. 2007      University of Science and Technology Beijing (USTB)  
   Institute of Microbiology, Chinese Academy of Sciences (CAS)  
Degree:                        Master degree  
Major:                         Biochemical engineering  
Supervisor:                  **Prof. Ning Jiang (CAS) and Prof. Song Cunyi (USTB)**

May 2007 - Present         Saarland University (Germany)  
Degree:                        PhD degree expected in Sep. 2010  
Major:                         Biotechnology  
Supervisor:                  **Prof. Elmar Heinzle (e.heinzle@mx.uni-saarland.de)**